

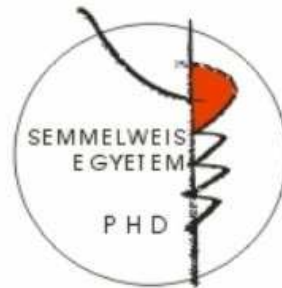
METABOLIC PATHWAYS AFFECTING MITOCHONDRIAL SUBSTRATE-LEVEL PHOSPHORYLATION

PhD thesis

Dóra Ravasz

János Szentágothai Doctoral School of Neurosciences

Semmelweis University



Supervisor: Christos Chinopoulos, MD, Ph.D

Official reviewers: Krisztián Tárnok, Ph.D
Csaba Sóti, MD, D.Sc

Head of the Final Examination Committee:
Péter Enyedi, MD, D.Sc

Members of the Final Examination Committee:
Krisztina Káldi, MD, Ph.D
Kitti Linda Pázmándi, Ph.D

Budapest
2018

TABLE OF CONTENTS

THE LIST OF ABBREVIATIONS.....	4
1. INTRODUCTION.....	7
1.1. Oxidative phosphorylation and mitochondrial respiration	8
1.2. Reversibility of the F ₀ -F ₁ ATP synthase and the ANT.....	10
1.3. The B space of mitochondrial phosphorylation.....	12
1.4. Mitochondrial substrate-level phosphorylation	14
1.5. Metabolic pathways affecting mitochondrial substrate-level phosphorylation ...	16
1.6. γ -Aminobutyrate (GABA).....	18
1.7. The GABA shunt	19
1.8. γ -Hydroxybutyrate (GHB).....	23
1.9. Diaphorases.....	24
1.10. NAD(P)H quinone oxidoreductase 1 (NQO1).....	25
2. OBJECTIVES.....	27
3. METHODS.....	29
3.1. Animals.....	29
3.2. Isolation of mitochondria.....	29
3.3. Determination of membrane potential ($\Delta\Psi_m$) in isolated brain and liver mitochondria	30
3.4. Mitochondrial respiration	31
3.5. Determination of NADH autofluorescence in permeabilized or intact mitochondria	31
3.6. Determination of diaphorase activity.....	32
3.7. Cell culturing	32

3.8. Mitochondrial membrane potential determination of in situ mitochondria of permeabilized HepG2 cells	32
3.9. siRNA and transfection of cells	33
3.10. Western blotting.....	33
3.11. Statistics	33
3.12. Reagents.....	34
4. RESULTS	35
4.1. Catabolism of GABA, succinic semialdehyde or γ -hydroxybutyrate through the GABA shunt impairs mitochondrial substrate-level phosphorylation.....	35
4.1.1. GABA as a bioenergetic substrate	35
4.1.2. Succinic semialdehyde as a bioenergetic substrate	37
4.1.3. γ -Hydroxybutyrate as a bioenergetic substrate	41
4.1.4. Investigation of mitochondrial substrate-level phosphorylation.....	43
4.1.5. GABA abolishes mitochondrial SLP in anoxia	44
4.1.6. Succinic semialdehyde abolishes mitochondrial SLP in anoxia	46
4.1.7. γ -Hydroxybutyrate abolishes mitochondrial SLP in anoxia	48
4.2. Contribution of Nqo1 to NAD ⁺ provision and mitochondrial SLP using endogenous or exogenous quinones	50
4.2.1. Determination of NAD(P)H oxidation and quinone reduction capacity in cytosolic extracts and permeabilized mitochondria from the livers of WT and Nqo1 ^{-/-} mice	50
4.2.2. Effect of quinones on NADH oxidation capacity of permeabilized liver mitochondria from WT and Nqo1 ^{-/-} mice.....	55
4.2.3. Effect of quinones on respiratory capacity of intact mitochondria from WT and Nqo1 ^{-/-} mice	55
4.2.4. Effect of targeted ETC inhibition on quinone-assisted respiration in intact mitochondria of WT and Nqo1 ^{-/-} mice	57

4.2.5. The contribution of mitochondrial Nqo1 to quinone-induced gain in $\Delta\Psi_m$ in rotenone-treated mitochondria	60
4.2.6. Substrate-level phosphorylation supported by non-Nqo1 dicoumarol-sensitive mitochondrial diaphorases using endogenous quinones	61
4.2.7. MNQ supports mitochondrial SLP preferably through Nqo1	63
4.2.8. Investigating the contribution of diaphorases including NQO1 to mitochondrial SLP in HepG2 cells	66
5. DISCUSSION.....	70
6. CONCLUSION	79
7. SUMMARY	80
8. ÖSSZEFOGLALÁS	81
9. BIBLIOGRAPHY	82
10. BIBLIOGRAPHY OF THE CANDIDATE’S PUBLICATIONS.....	106
10.1. Publications related to the PhD thesis.....	106
10.2. Publications not related to the PhD thesis	107
11. ACKNOWLEDGEMENTS	108

THE LIST OF ABBREVIATIONS

ADP	adenosine 5'-diphosphate
ANT	adenine nucleotide translocase
AOAA	aminooxyacetic acid (GABA-T inhibitor)
A-SUCL	ADP-forming succinate-CoA ligase (human)
ATP	adenosine 5'-triphosphate
ATP _{in} /ADP _{in}	intramitochondrial ATP/ADP ratio
atpn	atpenin A5 (succinate dehydrogenase inhibitor)
cATR	carboxyatractyloside (ANT inhibitor)
CHR	chrysin (diaphorase inhibitor)
CN	potassium cyanide
CoASH	coenzyme A
CoQ1	coenzyme Q1 = ubiquinone 5
CoQ10	coenzyme Q10 = ubiquinone = ubiquinone 50
CoQ9	coenzyme Q9 = ubiquinone 45
D2HGDH	D-2-hydroxyglutarate dehydrogenase
DCPIP	2,6-dichlorophenol-indophenol
DHODH	dihydroorotate dehydrogenase
DIC	dicoumarol (diaphorase inhibitor)
DLD	dihydrolipoil dehydrogenase
dOH-F	dihydroxyflavone (diaphorase inhibitor)
DQ	duroquinone = 2,3,5,6-Tetramethyl-1,4-benzoquinone
e ⁻ D	electron donor
e ⁻ D(red) or e ⁻ D(ox)	electron donor in the reduced or oxidized state, respectively
E _{rev_ANT}	reversal potential of the adenine nucleotide translocase
E _{rev_ATPase}	reversal potential of the F _o -F ₁ ATP synthase
ETC	electron transport chain
ETF	electron-transferring flavoprotein
ETF _{FDH}	electron-transferring flavoprotein dehydrogenase
FAD	flavin adenine dinucleotide (oxidized form)
FADH ₂	flavin adenine dinucleotide (reduced form)
GABA	γ-aminobutyrate

GABA-T	γ -aminobutyrate aminotransferase = GABA transaminase
GAD	glutamate decarboxylase
GAD(65 or 67)	glutamate decarboxylase, 65 or 67 kDa isoform
GDP	guanosine 5'-diphosphate
GHB	γ -hydroxybutyrate
glu	glutamate
GLUD	glutamate dehydrogenase
GOT2	mitochondrial aspartate aminotransferase = glutamate-oxaloacetate transaminase 2
GPDH	glycerol-3-phosphate dehydrogenase
G-SUCL	GDP-forming succinate-CoA ligase (human)
GTP	guanosine 5'-triphosphate
HOT	hydroxyacid-oxoacid transhydrogenase
IDB	idebenone = 2-(10-hydroxydecyl)-5,6-dimethoxy-3-methylcyclohexa-2,5-diene-1,4-dione
IDH	isocitrate dehydrogenase
KGDHC	α -ketoglutarate dehydrogenase complex
mal	malate
MCT	monocarboxylate transporter
MCT(2 or 4)	monocarboxylate transporter, isoform 2 or 4, respectively
mito	mitochondria
mitoQ	mitoquinone = [10-(4,5-Dimethoxy-2-methyl-3,6-dioxo-1,4-cyclohexadien-1-yl)decyl](triphenyl)phosphonium
mln	malonate (succinate dehydrogenase inhibitor)
MND	menadione = vitamin K3 = 2-methyl-1,4-naphtoquinone
MNQ	2-methoxy-1,4-naphtoquinone
mtDNA	mitochondrial DNA
NAD(P) ⁺	nicotinamide adenine dinucleotide (phosphate), oxidized form
NAD(P)H	nicotinamide adenine dinucleotide (phosphate), reduced form
NQO1 or Nqo1	NAD(P)H quinone oxidoreductase 1 (human or mouse)
Nqo2	NAD(P)H quinone oxidoreductase 1 (mouse)
olgm	oligomycin (F ₀ -F ₁ ATP synthase inhibitor)

PEPCK	phosphoenolpyruvate carboxykinase
PHND	phenindione (diaphorase inhibitor)
P _i	inorganic phosphate
Q	lipophilic quinone
Q'	hydrophilic quinone
QH ₂	lipophilic quinol
QH ₂ '	hydrophilic quinol
RCR	respiratory control ratio
RET	reverse electron transport
ROS	reactive oxygen species
rot	rotenone (complex I inhibitor)
SDH	succinate dehydrogenase
SF	SF6847 = 3,5-di-tert-butyl-4-hydroxybenzylidenemalononitrile (uncoupler)
shRNA	short hairpin RNA
siRNA	small interfering RNA
SLP	substrate-level phosphorylation
SSA	succinic semialdehyde
SSADH	succinic semialdehyde dehydrogenase
SSAR	succinic semialdehyde reductase
stigm	stigmatellin (complex III inhibitor)
succ	succinate
SUCL	succinate-CoA ligase = succinyl-CoA synthetase = succinate thiokinase (human)
SUCLA2 or Sucla2	ADP-forming succinate-CoA ligase β subunit (human or mouse)
Suclg2	GDP-forming succinate-CoA ligase β subunit (mouse)
VGBT	vigabatrin = γ -vinyl-GABA (GABA-T inhibitor)
WT	wild type
α -KG	α -ketoglutarate
β -OH	β -hydroxybutyrate
$\Delta\Psi_m$	mitochondrial membrane potential

1. INTRODUCTION

Mitochondria, double-membrane-bound organelles found in the most eukaryotic cells, form a dynamic network with frequent changes in their number and morphology. Their ubiquitous presence was first described by Altmann in 1890 and since then extensive literature has accumulated regarding their structure and operation [1]. Mitochondria are usually brought in context as the sites of cellular respiration since they consume oxygen for the aerobic metabolism of nutrients. Beside energy provision, mitochondria exhibit an important role in several other cell functions, such as heat production, regulation of Ca^{2+} homeostasis, or production of intracellular reactive oxygen species (ROS) as signaling molecules. They are also involved in the synthesis of steroid hormones, heme, Fe-S clusters, lipids and pyrimidine nucleotides. In addition to their role of maintaining these vital processes, it has turned out that they are key components in cell death. Another unique feature of these organelles is that they possess their own DNA (mtDNA). This encodes however 13 proteins only, all of which are components of the oxidative phosphorylation. The majority of mitochondrial proteins is thus nuclear-encoded and has to be actively imported into the mitochondrial compartments, followed by assembly into functional macromolecular complexes.

Mindful of their diverse roles, it is not surprising that the dysfunction of mitochondria has been described to participate in a number of pathological conditions. Mutations in mtDNA or in genes of nuclear-encoded mitochondrial proteins lead to a heterogeneous group of – usually severe and incurable – diseases. The contribution of mitochondria to the pathomechanism of neurodegenerative diseases, cancer, ischaemia-reperfusion injury, obesity, metabolic syndrome, and aging rendered these organelles an important subject of research [2; 3].

ATP generation by mitochondria is a key component in determining the outcome of the above mentioned diseases. In case the condition is associated with an impaired respiration of these organelles, oxygen-independent energy-producing pathways such as mitochondrial substrate-level phosphorylation (SLP) become of particular importance. The topic of the present thesis concerns the bioenergetic aspects of mitochondrial metabolism when the respiratory chain is dysfunctional, focusing on the metabolic pathways influencing SLP.

1.1. Oxidative phosphorylation and mitochondrial respiration

Catabolic pathways converge at mitochondria, where the final phase of fuel degradation, the oxidative phosphorylation takes place. Carbohydrates, amino acids and fatty acids are eventually oxidized in the citric acid cycle in the mitochondrial matrix. Electrons arising from the action of dehydrogenases are transferred to the complexes of the inner mitochondrial membrane by universal electron carriers, NAD^+ or FAD. The membrane-embedded four complexes of the respiratory chain allow the flow of electrons to their final electron acceptor, molecular oxygen. Electrons carried in the form of NADH enter the respiratory chain at the level of complex I, whereas those coming from succinate oxidation are transferred to the FAD prosthetic group of complex II (succinate dehydrogenase, SDH). Both complexes reduce a mobile electron carrier, ubiquinone to ubiquinol. Ubiquinol can also be produced by the electron-transferring flavoprotein (ETF) system, or by glycerol-3-phosphate dehydrogenase (GPDH) [4], or in the reaction catalyzed by dihydroorotate dehydrogenase (DHODH) [5]. The first one represents a pathway in fatty acid oxidation, in which electrons from fatty acyl-CoA are transferred to ETF and from there they are passed to ubiquinone via electron-transferring flavoprotein dehydrogenase (ETFHDH). GPDH converts glycerol-3-phosphate to dihydroxyacetone phosphate, and DHODH is involved in de novo pyrimidine biosynthesis, oxidizing dihydroorotate into orotate – both reactions are coupled to the reduction of ubiquinone [4; 5]. Ubiquinol coming from either source donates electrons to complex III, which is then reoxidized by an intermembrane space protein, cytochrome c. This moves to complex IV, where electrons are ultimately passed to molecular oxygen. The utilization of substrates is connected to oxygen consumption this way, which is the basis of cellular respiration [4].

After years of searching for the mechanism by which mitochondria link nutrient oxidation to ATP production, the chemiosmotic theory was introduced by Mitchell in 1961 [6] and later confirmed experimentally by several laboratories [1]. The key aspect of this theory is that the respiratory chain complexes possess proton pump activity, and the free energy change arising from the electron transfer allows the translocation of protons from the matrix into the intermembrane space. Due to the proton impermeability of the inner membrane this creates an electrochemical gradient, termed the proton-motive force. This gradient, composed of a chemical (ΔpH) and an electrical

potential energy (mitochondrial membrane potential, $\Delta\Psi_m$), drives the synthesis of ATP as protons flow back into the matrix through the F_o - F_1 ATP synthase complex [4].

The F_o - F_1 ATP synthase consists of a membrane-embedded F_o part, through which protons can flow back into the matrix, and an extramembraneous F_1 sector, which is responsible for ATP production. The enzyme establishes ATP synthesis through a rotational catalysis, with the c-ring of the F_o moiety rotating in a clockwise direction (as viewed from the membrane) at about 100 times per second. The structure of the mammalian c-ring has been determined recently and lead to the recognition, that the translocation of 2.7 protons is required to generate one ATP molecule [7].

ATP synthesized in the matrix is transported to the cytosol by an integral protein of the inner membrane, the adenine nucleotide translocase (ANT). The enzyme exports ATP in exchange for ADP with a 1:1 stoichiometry. Since ATP has one more negative charge than ADP, the transport is electrogenic and is driven by the membrane potential [8; 9]. ANT is the most abundant protein in the inner mitochondrial membrane, representing approximately 10% of the total protein content. Until now four ANT isoforms have been identified in mammals, with a sequence homology between 80 and 90% and with a different tissue-specific expression pattern. Beside the exchange of ATP and ADP, the role of the different isoforms in apoptosis and cancer progression has been described as well [10]. ANT is known to be a modulatory element of the mitochondrial permeability transition pore [11] – a pore in the inner mitochondrial membrane the opening of which is triggered by Ca^{2+} and possibly leads to cell death –, and ANT1 has been recently identified as the voltage sensor of this phenomenon [12]. Unlike the F_o - F_1 ATP synthase which utilizes Mg^{2+} -complexes, the substrates of ANT are the free adenine nucleotides only [9; 13].

In intact mitochondria, ATP synthesis and oxygen consumption are obligatory coupled: in the absence of ADP respiration is impaired, and vice versa, the lack of oxygen prevents phosphorylation. Respiratory steady states in experiments using isolated mitochondria were defined by Chance and Williams in 1955 [14]. According to this terminology, state 1 refers to the presence of mitochondria in a phosphate-containing medium which lacks substrate and phosphate acceptor. State 2 is achieved by the addition of ADP, under these conditions the rate limiting component of respiration is the concentration of endogenous substrates. Provision of exogenous substrates results

in the acceleration of oxygen consumption, this is the state of oxidative phosphorylation termed state 3. After the exhaustion of ADP respiration slows down and state 4 is reached, and the consumption of all the dissolved oxygen (in a closed chamber) leads to state 5, the state of anoxia. This nomenclature has been modified later, based on a different sequence of additions in the experimental protocol [15; 16]. In the new system state 2 indicates the condition after the addition of respiratory substrates, followed by state 3 where ADP is present as well. The definition of state 1, 3, 4 and 5 remained basically unchanged. Oxygen consumption in state 2 - when exogenous substrates are provided but the phosphate acceptor is absent - reflects the proton conductance of the inner membrane (proton leak): some protons can return to the matrix through alternative pathways compared to the F_o-F_1 ATP synthase. ANT was shown to be the main contributor to this basal proton leak [17].

These well-defined respiratory states cannot be applied directly for mitochondria under physiological conditions. Little is known about the rate of oxygen consumption of mitochondria *in vivo*, but it is thought that due to the physiological ATP turnover, mitochondria in the cell exist in an intermediate state between state 3 and 4 [18].

1.2. Reversibility of the F_o-F_1 ATP synthase and the ANT

The F_o-F_1 ATP synthase can not only synthesize ATP but is also capable of hydrolyzing it [19]. Since in the presence of high concentrations of inorganic phosphate (P_i) ΔpH across the mitochondrial membrane is small [20], the direction of the enzyme complex is mainly regulated by the $\Delta\Psi_m$ component of the proton-motive force. When this parameter moves towards more positive values, the F_o-F_1 ATP synthase can reverse and pump protons out of the mitochondrial matrix in order to maintain a suboptimal membrane potential. The $\Delta\Psi_m$ value where the enzyme complex switches from ATP producing to ATP hydrolyzing mode is termed reversal potential (E_{rev_ATPase}). The reversal potential of the F_o-F_1 ATP synthase complex can be calculated using the following equation [21]:

$$E_{\text{rev_ATPase}} = -\frac{316}{n} - \frac{2.3RT}{n} \times \log \frac{[\text{ATP}^{4-}]_{\text{free_in}} \times K_{\text{M(ADP)}}}{[\text{ADP}^{3-}]_{\text{free_in}} \times K_{\text{M(ATP)}} \times [\text{P}_i]_{\text{in}}} \\ - \frac{2.3 RT}{F} \times (\text{pH}_{\text{out}} - \text{pH}_{\text{in}})$$

and

$$[\text{P}_i]_{\text{in}} = \frac{[\text{P}_i]_{\text{total}}_{\text{in}}}{1 + 10^{\text{pH}_{\text{in}} - \text{pK}_{\text{a2}}}}$$

where in and out signify inside and outside of the mitochondrial matrix, n is the H^+ /ATP coupling ratio [7], R is the universal gas constant ($8.31 \text{ J} \cdot \text{mol}^{-1} \cdot \text{K}^{-1}$), F is the Faraday constant ($9.64 \times 10^4 \text{ C} \cdot \text{mol}^{-1}$), T is temperature (in degrees Kelvin), $K_{\text{M(ADP)}}$ and $K_{\text{M(ATP)}}$ are the true affinity constants of Mg^{2+} for ADP and ATP valued $10^{-3.198}$ and $10^{-4.06}$, respectively [22], and $[\text{P}_i]$ is the free phosphate concentration (in molar) given by the second equation, where pK_{a2} is 7.2 for phosphoric acid.

During the reverse operation of the enzyme, the ATP that is hydrolyzed can originate either from intramitochondrial resources or from the cytosol. The latter requires the reversal of the ANT, so that the transporter will import extramitochondrial ATP and export ADP generated in the matrix. The reversal potential of the ANT ($E_{\text{rev_ANT}}$) can be defined according to the following equation [21]:

$$E_{\text{rev_ANT}} = \frac{2.3 RT}{F} \times \log \frac{[\text{ADP}^{3-}]_{\text{free_out}} \times [\text{ATP}^{4-}]_{\text{free_in}}}{[\text{ADP}^{3-}]_{\text{free_in}} \times [\text{ATP}^{4-}]_{\text{free_out}}}$$

where the same symbols are used as in the case of $E_{\text{rev_ATPase}}$.

In summary, when the oxidative phosphorylation is impaired, mitochondrial membrane potential can decrease below the reversal potential values, which leads to a reverse operating ANT and $\text{F}_0\text{-F}_1$ ATP synthase. The reversal of the two enzymes serves the purpose of preventing further depolarization and a subsequent opening of the permeability transition pore. The glycolytic ATP being imported by the ANT will be hydrolyzed by the $\text{F}_0\text{-F}_1$ ATP synthase while protons are translocated to the intermembrane space. In reverse mode, also the electrogenic nature of the ANT contributes to the maintenance of the potential difference across the inner membrane [23].

1.3. The B space of mitochondrial phosphorylation

As the intramitochondrial ATP/ADP ratio ($\text{ATP}_{\text{in}}/\text{ADP}_{\text{in}}$) is a common parameter in the two equations above, $E_{\text{rev_ATPase}}$ and $E_{\text{rev_ANT}}$ can be represented in one figure as a function of $\text{ATP}_{\text{in}}/\text{ADP}_{\text{in}}$. Based on this, Fig. 1 from reference [21] shows a computational estimation for the reversal potential values of the two enzymes.

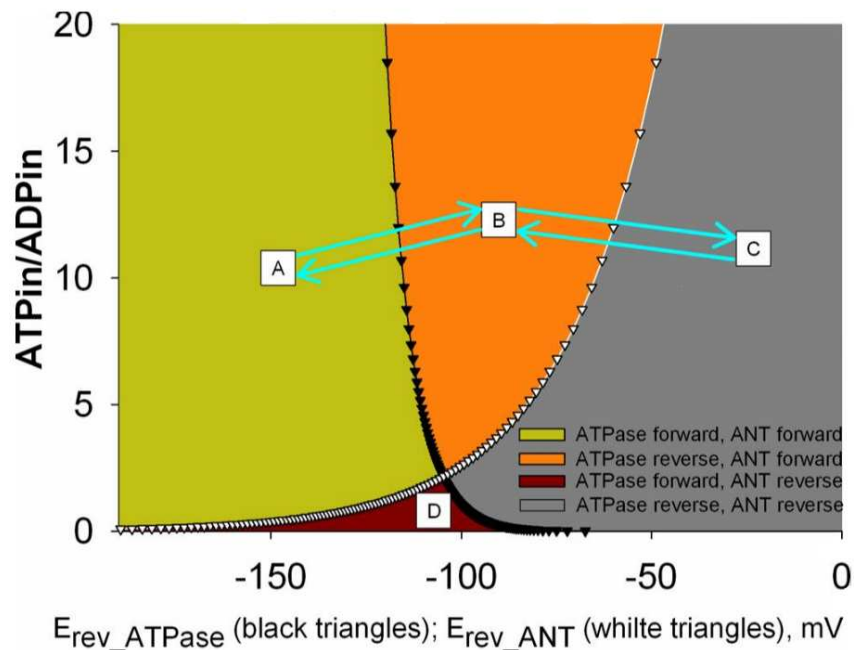


Figure 1. Computational estimation of $E_{\text{rev_ANT}}$ and $E_{\text{rev_ATPase}}$ at different free $[\text{ATP}]_{\text{in}}/[\text{ADP}]_{\text{in}}$ ratios. A: ATPase forward, ANT forward; B: ATPase reverse, ANT forward; C: ATPase reverse, ANT reverse; D: ATPase forward, ANT reverse. Black triangles represent $E_{\text{rev_ATPase}}$; white triangles represent $E_{\text{rev_ANT}}$. Values were computed for $[\text{ATP}]_{\text{out}} = 1.2 \text{ mM}$, $[\text{ADP}]_{\text{out}} = 10 \text{ }\mu\text{M}$, $[\text{P}_i]_{\text{in}} = 0.02 \text{ M}$, $n = 3.9$, $\text{pH}_{\text{in}} = 7.38$, and $\text{pH}_{\text{out}} = 7.25$. (Adapted from reference [21])

The two curves define four areas in the graph: mitochondria with a $\Delta\Psi_{\text{m}}$ value and an $\text{ATP}_{\text{in}}/\text{ADP}_{\text{in}}$ which places them in the A space have the $F_0\text{-}F_1$ ATP synthase and the ANT working in forward mode, which implies that they produce and export ATP. Mitochondria with low membrane potential are found in the C space, with reversed $F_0\text{-}F_1$ ATP synthase and ANT. In this case the organelles import and hydrolyze cytosolic ATP. However, the directionality of the $F_0\text{-}F_1$ ATP synthase and ANT do not necessarily change simultaneously. In the B space, mitochondria have a membrane potential value more positive than the $E_{\text{rev_ATPase}}$ but more negative than the $E_{\text{rev_ANT}}$, indicating that the $F_0\text{-}F_1$ ATP synthase hydrolyzes ATP but the ANT still operates in ATP-exporting direction. Finally, in the D space the $F_0\text{-}F_1$ ATP synthase produces ATP, but the ANT also increases $\text{ATP}_{\text{in}}/\text{ADP}_{\text{in}}$ by importing ATP from outside. Nevertheless,

this region is characterized by a high membrane potential and a low matrical ATP/ADP ratio, which is very unlikely to occur under natural conditions, thus probably this area has no biological relevance. This also implies that in living cells, the $E_{\text{rev_ATPase}}$ is more negative than the $E_{\text{rev_ANT}}$ [23].

It is important to stress that from the reversal potential values only the directionality of the two enzymes can be concluded, the figure provides no information of the actual enzyme activities. Experiments on isolated [24; 25] and in situ [26] mitochondria showed that during depolarization, the ADP-ATP exchange rate of the ANT decreases as the membrane potential is approaching $E_{\text{rev_ANT}}$. At the reversal potential there is no net transport of adenine nucleotides across the inner mitochondrial membrane, whereas after passing this value, the transport of substrates in the opposite direction will start. The same scenario is assumed for the F_0 - F_1 ATP synthase [23].

The B space of the figure is of special interest, since in such case, despite a substantial depolarization, mitochondria do not consume cytosolic ATP for the maintenance of their membrane potential. This phenomenon could have significance under many pathological conditions, where generation of the proton-motive force is damaged. Neurodegenerative diseases are usually associated with different respiratory complex deficiencies, for example a defect in complex I activity is reported in patients with Parkinson's disease [27]. In Alzheimer's disease primarily complex IV was shown to have diminished activity [28]. In addition, many rare mitochondrial diseases are known where due to mtDNA or mitochondrial protein encoding nuclear gene abnormalities the assembly of the respiratory complexes is damaged [29], thus a loss of membrane potential and reversal of the F_0 - F_1 ATP synthase is expected. Another relevant pathological condition is ischaemic-reperfusion injury where mitochondrial membrane potential is diminished due to limited oxygen availability [30]. In either case, mitochondrial $\Delta\Psi_m$ generation is compromised, and if the organelles get into the C space, they will start consuming cytosolic ATP. A decrease in the cellular energy pool can lead to a damage of essential cell functions, like to the hampered operation of ATP-dependent pumps such as the Na^+/K^+ -ATPase and Ca^{2+} -ATPase. Therefore it can be critical for mitochondria to stay within the boundaries of the B space, so that cytosolic ATP pools will be preserved and the chances of the cell for survival will be improved [23; 31].

1.4. Mitochondrial substrate-level phosphorylation

Mitochondria with parameters located in the B space do not cease to export ATP despite a reverse working F_0 - F_1 ATP synthase. This implies that the ATP, which is hydrolyzed and exported simultaneously, comes from intramitochondrial sources other than the oxidative phosphorylation. Reactions capable of producing high energy phosphates independent of the respiratory chain are termed substrate-level phosphorylation. ATP originating from mitochondrial SLP can be crucial to keep mitochondria in the B space when their respiratory chain is dysfunctional [21]. Sufficient ATP production by SLP can prevent mitochondria from entering the C space in three ways: i) by providing ATP for the reverse operating F_0 - F_1 ATP synthase thereby maintaining a moderate $\Delta\Psi_m$ ii) an increase in ATP_{in}/ADP_{in} will translocate mitochondria upwards along the y axis in Fig. 1 making them more likely to stay in the B space, iii) it will affect the reversal potential values of both the F_0 - F_1 ATP synthase and the ANT. Based on equations 1 and 2, E_{rev_ATPase} will be shifted towards more negative and E_{rev_ANT} towards more positive values, leading to a broadening of the B space [23]. Thus a functional SLP can prevent mitochondria from ANT reversal and a subsequent consumption of cytosolic ATP.

In mitochondria, phosphoenolpyruvate carboxykinase (PEPCK) and the succinate-CoA ligase (SUCL, or succinate thiokinase or succinate-CoA ligase) are able to perform SLP. Mitochondrial PEPCK participates in the transfer of the phosphorylation potential from the matrix to the cytosol and vice versa [32]. SUCL catalyzes a reversible reaction in the citric acid cycle, it converts succinyl-CoA, ADP (or GDP) and P_i to succinate, ATP (or GTP) and CoASH [33]. The enzyme is a heterodimer, being composed of an invariant α subunit encoded by *SUCLG1* and a substrate-specific β subunit encoded by either *SUCLA2* or *SUCLG2*. This dimer combination results in either an ATP-forming succinate-CoA ligase (A-SUCL; EC 6.2.1.5) or a GTP-forming succinate-CoA ligase (G-SUCL; EC 6.2.1.4). The GTP-forming enzyme occurs mainly in anabolic tissues like liver and kidney, whereas A-SUCL can be found first of all in brain, heart and muscle [32; 33]. It was shown in human brain samples, that the ATP-forming β subunit is expressed exclusively in neurons of the cerebral cortex [34]. Moreover, in glial cells none of the two enzyme forms was found, suggesting that in these cells an alternative pathway bypasses this step of the citric acid cycle [35]. SUCL exists in the matrix in

association with a mitochondrial nucleoside diphosphate kinase known as NM23-H4 (NDPK-D, EC 2.7.4.6), an enzyme capable of the interconversion of nucleoside triphosphates, thus GTP produced by G-SUCL is also able to contribute to the matrix ATP pool [36; 37].

Growing evidence confirms that the adequate operation of SUCL is necessary to prevent ANT reversal when mitochondrial respiration is inhibited. It is known that the citric acid cycle is operational in anoxia, with succinate as an end product [38]. Also, the fact that anaerobic mitochondrial metabolism can generate ATP via SLP and maintain mitochondrial energization this way has been substantiated extensively [38]. The α -ketoglutarate dehydrogenase complex (KGDHC) provides succinyl-CoA for SUCL, and this is considered to be the rate-limiting step among the sequential reactions [39]. Experiments performed on mitochondria isolated from mice heterozygote for different subunits of KGDHC showed that the enzyme complex is essential for the operation of SUCL, and that impaired function of KGDHC results in ANT reversal during respiratory failure. This was supported by measurements performed on in situ neuronal somal mitochondria as well [40]. The role of SUCL itself was investigated in [41], in which *Sucla2*^{+/-}, *Suclg2*^{+/-}, or *Sucla2*^{+/-}/*Suclg2*^{+/-} mice were generated and characterized extensively from a bioenergetic point of view. Mitochondrial respiration and electron transport chain (ETC) activities showed no alterations in the transgenic animals (except for a significant elevation of complex II activity in the double heterozygote samples). Decreased mtDNA content and alterations in the concentration of blood carnitine esters were found in *Sucla2*^{+/-} and in *Sucla2*^{+/-}/*Suclg2*^{+/-} mice. Regarding mitochondrial SLP, no difference was observed in the heterozygote models compared to wild type (WT) littermates. This is either due to i) a rebound increase in *Suclg2* expression and associated GTP-forming activity as it was found in *Sucla2*^{+/-} and *Sucla2*^{+/-}/*Suclg2*^{+/-} mice; or ii) the small flux control coefficient of SUCL (compared to that of the KGDHC) which makes it possible that even a decreased enzyme activity is able to maintain sufficient ATP production for the ANT to work in forward mode. Nevertheless, submaximal pharmacological inhibition of SUCL in the heterozygote samples lead to an abolition of SLP. The importance of SUCL in preventing ANT reversal has been strengthened in fibroblasts from patients suffering from SUCLA2 deficiency as well. These cells are unable to perform sufficient SLP, and start to import

cytosolic ATP when their respiratory chain is inhibited [41]. Another finding which confirms the significance of this reaction is that inorganic phosphate activates SUCL [42]. The P_i produced by a reverse working F_0 - F_1 ATP synthase in anoxia results in a greater activity of this rescue mechanism.

Mindful of these findings, enhancing SUCL function by succinyl-CoA provision could be helpful in diseases mentioned in the previous chapter. The practical relevance of this notion is confirmed by publications where substrates supporting mitochondrial SLP improved the outcome of anoxic or ischaemic conditions (as summarized in [38]). In addition, recently methylene blue, a drug which shows beneficial effects in stroke and neurodegenerative disease models, was found to enhance mitochondrial SLP [43].

1.5. Metabolic pathways affecting mitochondrial substrate-level phosphorylation

Regarding the role of SLP in preventing ANT reversal during respiratory arrest, it is worth considering the factors that could influence its operation. The succinyl-CoA – succinate interconversion mediated by SUCL is reversible, ($\Delta G=0.07$ kJ/mol) [44]. Therefore the availability of the substrates will largely determine the direction of the reaction, and any metabolic pathway influencing the concentration of the participants will predictably impact SLP.

First of all, provision of succinyl-CoA is crucial for keeping the reaction in ATP-producing direction [40]. A possible source of succinyl-CoA is the reaction mediated by KGDHC, which catalyzes the irreversible conversion of α -ketoglutarate, CoASH, and NAD^+ to succinyl-CoA, NADH, and CO_2 in the citric acid cycle. In experiments using isolated mitochondria, α -ketoglutarate and glutamate are the two substrates that support SLP to the greatest extent, especially when provided together with malate, which assists in their entry into mitochondria. It is obvious though, that for the operation of KGDHC oxidized NAD^+ is needed, the availability of which is expected to be markedly decreased in anoxia or during complex I inhibition. Despite this, experiments showing that there is substantial SLP under these conditions indicate that sufficient NAD^+ is generated for KGDHC [21; 40; 45]. The origin of this NAD^+ in anoxia is assumed to be the mitochondrial diaphorases [45].

Other sources for succinyl-CoA can be the catabolism of certain biomolecules (methionine, threonine, isoleucine, valine, propionate, odd chain fatty acids and

cholesterol), the degradation of which converges to succinyl-CoA as an entry point into the citric acid cycle [46].

By the same token, any metabolic pathway which consumes succinyl-CoA can hamper SLP. When SUCL proceeds in the direction towards succinyl-CoA formation, this can take part in δ -aminolevulinate generation, a step of heme synthesis [47]. Ketone body catabolism requires succinyl-CoA as a CoASH donor for acetoacetyl-CoA formation, with succinate staying behind, bypassing the reaction by SUCL this way [48]. These reactions possibly steal succinyl-CoA away from the high-energy phosphate producing step.

In addition, succinate accumulation can shift the reaction mediated by SUCL into the ATP (GTP) hydrolyzing direction. Addition of succinate resulted in ANT reversal in isolated mitochondria when the electron transport chain was inhibited distal from complex II, reflecting an impairment of SLP [21]. It has been recently shown, that itaconate, an antimicrobial compound produced by macrophages upon lipopolysaccharide stimulation, abolishes mitochondrial SLP [49]. This was attributed to three different effects: i) itaconate is metabolized through thioesterification by SUCL, and this step requires ATP (or GTP); ii) the product of its metabolism, itaconyl-CoA traps CoASH from the KGDHC; iii) itaconate inhibits SDH, leading to a buildup of succinate. Another possible metabolic pathway which can lead to succinate accumulation in respiratory-inhibited mitochondria is the catabolism of the neurotransmitter γ -aminobutyrate (GABA) through the so-called GABA shunt [50; 51]. Inhibitory effect of GABA on SLP has been reported in a study [52], where incubation with GABA appreciably reduced ATP and GTP production in uncoupled rat brain mitochondria. However, the mechanism of inhibition was not established. γ -Hydroxybutyrate (GHB), a neurotransmitter and a psychoactive drug is also converted to succinate during its degradation [53], and possibly exerts similar effects on SLP.

The present thesis focuses on i) the effect of GABA and GHB metabolism on mitochondrial SLP; ii) the contribution of a diaphorase enzyme, NAD(P)H quinone oxidoreductase 1 (Nqo1) to SLP. Therefore, in the next chapters I will give a brief overview about mitochondrial diaphorases, GABA, the GABA shunt, and GHB.

1.6. γ -Aminobutyrate (GABA)

4-Aminobutyrate, also known as 4-aminobutanoate, γ -aminobutyrate or more frequently, GABA, is most widely known as the predominant inhibitory neurotransmitter in the adult brain [54]. Since its discovery in the central nervous system [55-57], GABA has been increasingly recognized to participate in processes other than neurotransmission as it is present in many organs other than the brain, such as pancreas, testes, gastrointestinal tract, ovaries, placenta, uterus and adrenal medulla [58; 59]. Most notably though, very high concentrations of GABA have been found in the livers of all animal species reported, particularly humans [60].

GABA exerts an inhibitory effect on synaptic transmission by interacting with ionotropic receptors on the postsynaptic membrane, resulting in an increased chloride conductance, thus an inward chloride current and a consequent hyperpolarization [61]. These channels are termed GABA_A receptors. Based on different pharmacological properties previously another GABA-sensitive anion channel type was distinguished, designated as GABA_C receptors, but later these were classified rather as a subfamily of GABA_A receptors and the use of the term GABA_C receptor is not recommended any more [62]. GABA can cause hyperpolarization of neurons and a diminished neurotransmitter release by acting on metabotropic GABA_B receptors as well [63]. However, in neonatal hippocampal neurons the electrochemical gradient of chloride is outward directed, therefore, opening the receptor channels is associated with depolarization; hence, at this developmental stage, GABA is an excitatory neurotransmitter [64]. It is also worth mentioning that in the brain GABA has been further branded as a gliotransmitter [65; 66]. However, the concept of GABA as gliotransmitter has been met with skepticism from those asserting that many of the phenomena attributed to release of transmitters by the glia can be explained by changes in the activity or expression of astrocytic membrane transporters, reviewed in [67].

GABA can be found in numerous tissues outside the central nervous system. Regarding the liver, it was hypothesized that this organ is responsible for clearing GABA from the systemic circulation. GABA is only catabolized but very little synthesized in the liver, and it originates from the intestinal flora [60] finding its way through the portal system; however, hepatic lobular GABA synthesis increases >300%

following partial hepatectomy [60]. Relevant to this, the high GABA concentration in liver has been implicated in the pathophysiology of hepatic encephalopathy [68].

In pancreas, GABA acts as an intra-islet transmitter regulating hormone release. In α -cells, GABA induces membrane hyperpolarization and suppresses glucagon secretion, whereas in islet β -cells it induces membrane depolarization and increases insulin secretion [69]. This difference in the effect of GABA on membrane polarization is due to the different expression of cation-Cl⁻-cotransporters in islet α and β -cells [70], which leads to an opposite electrochemical driving force of chloride ion in the two cell types. In the gastrointestinal tract, GABA is involved in the regulation of gut motility [71], in the adrenal medulla it is thought to play a role in modulating the release of catecholamines [72], and it may have an important role in reproductive function [73; 74]. Furthermore, GABA is released by immune cells and has a number of immunomodulatory effect [75], acts as a developmental signal during brain organogenesis [76], and even inhibits mitophagy and pexophagy in mammalian cells of various tissues, in an mTOR-sensitive manner [77]. Finally, GABA's realm has been recently recognized to extent to plantae, playing a vital role as a plant-signaling molecule [78].

Altered GABA concentration and signaling plays a role in a number of pathological conditions such as epilepsy, Parkinson's and Alzheimer's disease, depression, anxiety, schizophrenia and panic disorders [79; 80]. It is not surprising therefore, that the GABAergic system is a center of interest as a pharmacological target [80].

1.7. The GABA shunt

Despite that the participation of GABA in diverse biological processes implies different downstream effectors responsive to this molecule, its metabolism is rather uniform among all tissues: GABA is metabolized through the 'GABA shunt' (represented in Fig. 2), a pathway representing an alternative route for converting α -ketoglutarate to succinate in the citric acid cycle circumventing succinate-CoA ligase [50; 51]. Enzymes of the GABA shunt are expressed not only in the brain but also in a variety of nonneural tissues [81; 82].

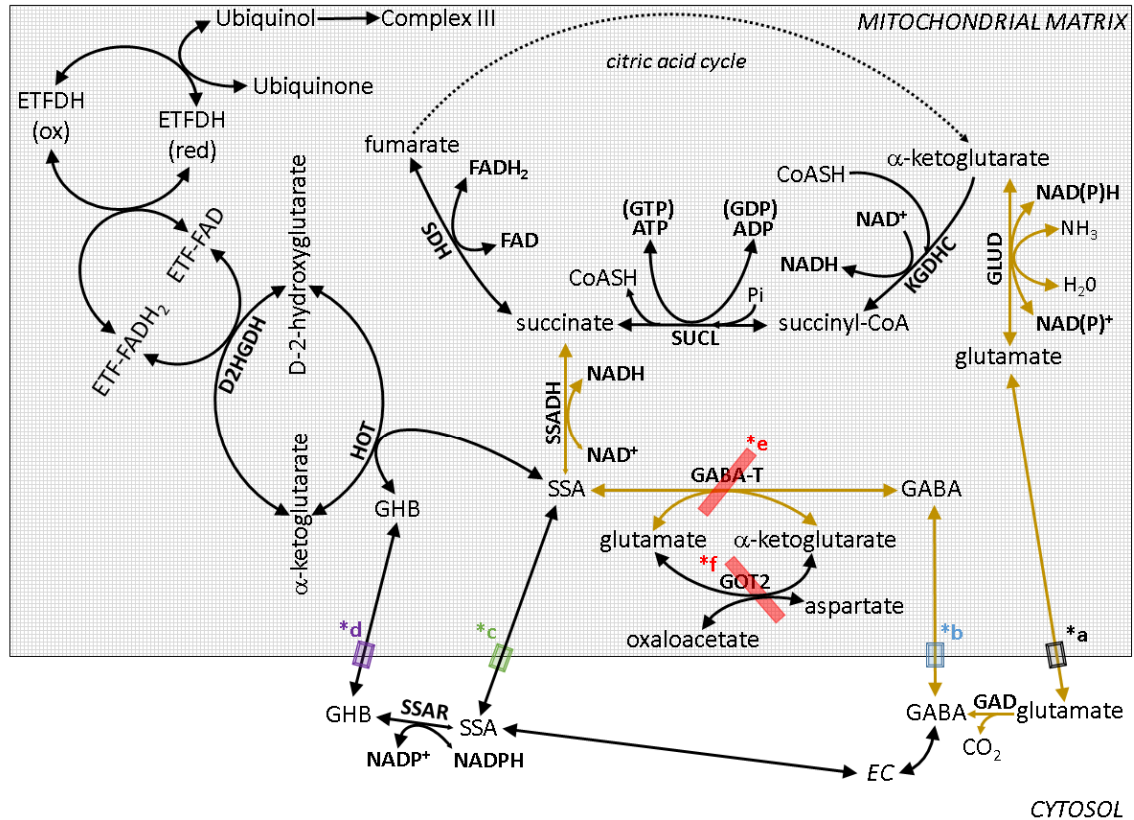


Figure 2. The GABA shunt (outlined by arrows in gold color) and pertinent reactions. SUCL: succinate-CoA ligase; KGDHC: α -ketoglutarate dehydrogenase complex; GLUD: glutamate dehydrogenase; GAD: glutamate decarboxylase; GABA: γ -aminobutyrate; GABA-T: γ -aminobutyrate aminotransferase; GOT2: mitochondrial aspartate aminotransferase; SSAR: succinic semialdehyde reductase; GHB: γ -hydroxybutyrate; SSA: succinic semialdehyde; SSADH: succinic semialdehyde dehydrogenase; HOT: hydroxyacid-oxoacid transhydrogenase; D2HGDH: D-2-hydroxyglutarate dehydrogenase; ETF: electron-transferring flavoprotein; ETFDH: electron-transferring flavoprotein dehydrogenase; SDH: succinate dehydrogenase. *a: glutamate transporters; *b: putative mitochondrial GABA transporter; *c: putative mitochondrial SSA transporter; *d: putative mitochondrial GHB transporter; *e: inhibitors for GABA-T used in this study: vigabatrin and f; *f: inhibitor for GOT2 in this study: AOAA.

As shown in Fig. 2, GABA can be derived from glutamate by glutamate decarboxylase (GAD), encoded by either *GAD65* or *GAD67*. The two isoforms have different molecular weights (65 and 67 kDa) and different subcellular localization, with *GAD65* found primarily in axon terminals and *GAD67* more widely distributed in neurons [83]. Since GAD is a cytosolic enzyme, glutamate needs to be exported from mitochondria; this may occur through well-characterized transporters (depicted as a black semi-transparent box *a), as an electroneutral transport driven by Δ pH [84; 85].

GABA may also arise by metabolism of putrescine [86] or homocarnosine [87] (not shown), or enter the cytoplasm from the extracellular space. In any case, in order for GABA to undergo further transamination it must first enter the mitochondrial matrix. The transport of GABA across the inner mitochondrial membrane (depicted by a blue semi-transparent box *b) has been proposed to occur by “diffusion of a species with no net charge, at rates which are able to maintain maximum activity of the GABA shunt” [88]. However, in plants, a mitochondrial GABA permease has been recently identified, termed AtGABP [89]. No such protein has been identified in animals, but a BLASTp homology search yielded a highly homologous (94%) predicted protein termed ‘amino acid permease BAT1 (partial)’ with a sequence ID: XP_019577258.1 expressed in *Rhinolophus sinicus* (Chinese rufous horseshoe bat), as well as some other proteins from other species but with low homology (below 35%). In mice and humans there is 23–31% homology of AtGABP to an ‘epithelial-stromal interaction protein 1’, and no homologous proteins were identified in tissues from rats and guinea pigs. Thus, although several isoforms of plasmalemmal GABA transporters have been identified [90], their reversibility documented [91–94], and GABA is known to permeate murine mitochondria [88] and become intramitochondrially metabolized [95], the means of GABA entry to mitochondria remains speculative.

Once in the matrix, GABA transaminates with α -ketoglutarate to form glutamate and succinic semialdehyde (SSA) by the mitochondrial GABA transaminase (GABA-T). Succinic semialdehyde will get dehydrogenated by succinic semialdehyde dehydrogenase (SSADH) yielding succinate and NADH, and thus enter the citric acid cycle. SSADH is also the enzyme responsible for further metabolism of aldehyde 4-hydroxy-2-nonenal, an intermediate known to induce oxidant stress [96]. Glutamate and α -ketoglutarate are in equilibrium with oxaloacetate and aspartate through a mitochondrial aspartate aminotransferase (GOT2). GABA-T is inhibited by vigabatrin and aminoxyacetic acid (AOAA) [88; 97]. The latter compound is also known to inhibit GOT2 as well as other pyridoxal phosphate-dependent enzymes [98; 99].

Regarding SSA, there are three possible scenarios for its appearance in the matrix: i) from the cytosol, transported through the inner mitochondrial membrane by a protein (depicted by a green semi-transparent box *c) that is yet to be characterized [100]; ii) by the action of hydroxyacid-oxoacid transhydrogenase (HOT), encoded by *ADHFE1*,

transhydrogenating γ -hydroxybutyrate (GHB) and α -ketoglutarate to D-2-hydroxyglutarate and SSA; or iii) by succinic semialdehyde reductase (SSAR, encoded by *AKR7A2*), converting GHB to SSA in the cytosol [101-104] and the latter getting transported into the matrix; however, the equilibrium of the SSAR reaction is strongly favored towards GHB formation.

The first evidence regarding the existence of HOT came from experiments investigating GHB catabolism in rat brain and kidney samples [105]. The enzyme was isolated and further characterized from rat tissues [106] and later on, its gene was identified [107]. The existence of human HOT has been demonstrated in homogenates of human liver and fibroblasts as well [108; 109]. HOT is not the only enzyme interconverting D-2-hydroxyglutarate and α -ketoglutarate; D-2-hydroxyglutarate dehydrogenase (D2HGDH) localized in mitochondria [110; 111] also performs such an interconversion, but this is coupled to the ETF system, eventually donating electrons to complex III through ubiquinone. D-2-Hydroxyglutarate is formed as a degradation product of L-hydroxylysine [112] and possibly also from δ -aminolevulinate [113]. Interestingly, isocitrate dehydrogenase (IDH) 1 and 2 mutations confer a novel enzymatic activity that facilitates reduction of α -ketoglutarate to D-2-hydroxyglutarate impeding oxidative decarboxylation of isocitrate [114; 115]. The accumulation of D-2-hydroxyglutarate due to IDH mutations has been implicated in tumorigenesis [116]; however, accumulation of D-2-hydroxyglutarate in glutaric acidurias is associated with encephalopathy and cardiomyopathy, but not tumors [117]. This metabolite is known to permeate the cell membrane through a sodium-dicarboxylate cotransporter (NaDC3) and an organic anion transporter (OAT1) [118] but a mitochondrial transport mechanism is yet to be described.

The reaction catalyzed by HOT is reversible, therefore SSA produced by GABA-T in mitochondria could be converted to succinate or GHB as well, but the predominant pathway of SSA metabolism is probably oxidation by SSADH because of the significant lower K_m of the enzyme for SSA, compared to HOT [81]. The rate limiting step of GABA catabolism is the reaction catalyzed by GABA-T, therefore SSA coming from GABA is rapidly oxidized by SSADH and its concentration is kept low [119; 120]. In SSADH deficiency though – a rare disease with nonprogressive encephalopathy,

hypotonia and delay in mental and motor development –, SSA accumulates, leading to elevated GABA and GHB levels [100].

1.8. γ -Hydroxybutyrate (GHB)

GHB is a neurotransmitter and neuromodulator in the human brain, but is also synthesized outside the central nervous system [121], however, its physiological role is not completely understood. As a therapeutical agent, GHB was originally developed for an anesthetic [122], today it is a drug for the treatment of narcolepsy with cataplexy and alcohol withdrawal [123; 124]. In the industry it is used in the production of polymers. It is also used illegally as a recreational drug and a drug of abuse [125], and FDA placed it in Schedule I of the Controlled Substances Act, since 2000 [126].

The molecule acts with high affinity on GHB receptors [127], which probably belong to the G-protein family [128]. In higher concentrations, it binds to GABA_B receptors as well, causing hyperpolarization [129; 130], and the majority of the reported pharmacological and behavioral effects of exogenous GHB are mediated via GABA_B receptors [131]. GHB was shown to modulate neurotransmitter release [132; 133], alter the release of opioids [134], increase growth hormone and prolactin secretion [135], reduce blood cholesterol levels [122] and to induce slow-wave sleep [136].

The major precursor for the synthesis of GHB in neurons is GABA: it is converted to SSA by GABA-T, subsequently, SSA can be oxidized to succinate and enter the citric acid cycle, or it can be reduced to GHB by cytosolic SSAR. Nonetheless, studies have shown that only 0.05-0.16% of the metabolic flux coming from GABA takes the reductive pathway. Alternative routes for GHB synthesis are hydrolysis of γ -butyrolactone or reduction of 1,4-butanediol [53], these are administered illegally as GHB precursors.

GHB permeates the plasma membrane through monocarboxylate transporters (MCTs) [137; 138] Although it is still controversial whether mitochondrial and plasma membranes share at least some MCT isoforms [139; 140] – though MCT2 and MCT4 were recently reported to localize in mitochondria in addition to the plasma membrane [141] – it is very likely that GHB crosses the inner mitochondrial membrane through one or more mitochondrial MCT (purple semi-transparent box *d).

GHB is predominantly degraded through the conversion to SSA by a cytosolic NADP-dependent aldehyde reductase encoded by *AKR1A1* [142]. Alternatively, in peripheral tissues GHB can be converted to SSA by HOT after being transported into mitochondria [105]. The reduction is followed by metabolism to GABA by GABA-T or conversion to succinate by SSADH, the latter providing energy through oxidation in the citric acid cycle [53].

1.9. Diaphorases

Diaphorases are flavoenzymes catalyzing the oxidation of reduced pyridine nucleotides by endogenous or artificial electron acceptors. The first diaphorase enzyme was purified in 1939 [143]), and was shown later to be identical to the DLD subunit of KGDHC [144]. Since then, several other mammalian proteins were found to exhibit diaphorase activity. NAD^+ originating from diaphorases can be utilized by KGDHC to form succinyl-CoA, which is in turn converted to succinate by succinate-CoA ligase yielding ATP or GTP depending on the subunit composition of the enzyme. As recently shown in our laboratory, under respiratory chain inhibition when NADH cannot be oxidized by complex I, NAD^+ supply by mitochondrial diaphorases is sufficient to maintain mitochondrial SLP [45]. In isolated mouse liver mitochondria supported by glutamate and malate, up to 81% of the NAD^+ pool could be regenerated by intramitochondrial diaphorases. Applying different diaphorase inhibitors – dicoumarol, chrysin, dihydroxyflavone and phenindione – lead to the abolition of SLP under these conditions, pointing out the indispensable role of diaphorases for the adequate operation of KGDHC. In the reaction catalyzed by diaphorases, the electrons of NADH have to be passed on to a suitable electron acceptor. The effect of 14 quinone compounds as possible diaphorase substrates was tested, from which three – menadione (MND), mitoquinone (mitoQ) and duroquinone (DQ) – were shown to boost mitochondrial SLP when complex I was inhibited by rotenone. In anoxia, when the operation of the entire respiratory chain is hindered, only duroquinone was effective in improving SLP. From these experiments it was concluded that in freshly isolated, rotenone-treated mitochondria respiring on glutamate and malate, provision of exogenous quinones for NADH oxidation by diaphorases is not critical due to the presence of sufficient amounts of endogenous quinones. However, mitochondrial diaphorases are not saturated by

endogenous quinones, and the addition of exogenous reducible diaphorase substrates can boost SLP by providing NAD^+ for KGDHC. A scheme for the pathway of electrons during respiratory arrest was proposed: diaphorases transfer electrons from NADH to suitable quinones, from where electrons are taken over by complex III, which is then oxidized by cytochrome c [45].

1.10. NAD(P)H quinone oxidoreductase 1 (NQO1)

The identity of the diaphorase enzymes participating in NAD^+ regeneration for SLP is not known. NAD(P)H quinone oxidoreductase 1 (NQO1, EC 1.6.99.2.), a ubiquitously expressed flavoprotein was proposed as a potential candidate [45]. The enzyme was identified by Lars Ernster and colleagues and was originally named 'DT-diaphorase' because of its ability to react with $\underline{\text{D}}$ PNH (reduced diphosphopyridine nucleotide, i.e. NADH) and TPNH (reduced triphosphopyridine nucleotide, i.e. NADPH) as well [145-147]. Although NQO1 is mostly considered a cytosolic enzyme, it – as well as DT-diaphorase activity with signatures similar to those of NQO1 – has been shown to localize also in the mitochondrial matrix [148-157] (except in [158]). All reports showed that mitochondrial diaphorase activity accounted for <15% of the total. The reaction catalyzed by NQO1 is irreversible [152] and follows a ping-pong mechanism [159]. As electron acceptor, the enzyme can use a variety of quinones, from which naphtho- and benzoquinones without a long side-chain are the most active [149; 152].

Regarding its physiological role, the enzyme was found to exhibit vitamin K reductase activity [152], thereby it was suggested to play a role in the vitamin K cycle, but the *in vivo* significance of this has been questioned lately [160-162]. In a detailed study examining the *in vivo* role of Nqo1 it was demonstrated that $\text{Nqo1}^{-/-}$ mice exhibit lower levels of abdominal adipose tissue, and altered carbohydrate, lipid and nucleotide metabolism, due to an altered intracellular NAD(P)H/NAD(P) ratio [163].

NQO1 was also shown to be involved in carcinogenesis through multiple processes, but with opposing outcomes: the enzyme can protect against cancer development by: i) catalyzing a two-electron reduction of quinones and this way avoiding the production of highly reactive semiquinone intermediates [164] ii) preventing oxidative stress through superoxide scavenging [165; 166] and maintaining

endogenous antioxidants [167; 168] iii) inhibiting proteasomal degradation of p53 and p33ING1b [169; 170], proteins that are critical for tumor repression. Relevant to this, disruption of the *Nqo1* gene in mice leads to increased susceptibility to menadione- and benzene-induced toxicity [171; 172], to increased risk of skin cancer induced by polycyclic aromatic hydrocarbons [173; 174], and to hyperplasia of bone marrow [175]. A polymorphism of the human *NQO1* gene encodes a protein which has negligible enzyme activity. Individuals who are homozygous for the variant allele have greater risk for benzene-induced bone marrow toxicity and the resulting hematological malignancies [176], and the polymorphism has been associated with several types of cancer [177]. Even though these facts indicate that cancer development is associated with lower or absent NQO1 activity, a variety of solid tumors are known to overexpress the enzyme [177; 178], probably due to its ability to reduce oxidative stress. The contribution of NQO1 to carcinogenesis is supported by that NQO1 expression is induced by Nrf2 [179], a transcription factor that is being increasingly recognized to favor survival of malignant cells [180; 181]. Also, NQO1 may induce tumor formation through the bioactivation of environmental procarcinogens [182].

2. OBJECTIVES

The catabolism of GABA and GHB leads to SSA, an intermediate of the GABA shunt, which is finally converted to succinate, an entry point of the citric acid cycle. Therefore it is assumable that in anoxia – when SDH is inhibited –, to a certain extent, succinate will accumulate in mitochondria. An elevation of succinate concentration shifts the reaction mediated by SUCL into succinyl-CoA producing direction, abolishing ATP (GTP) production this way. Mindful of the importance of SLP in preserving high energy phosphate levels in the matrix of respiration-impaired mitochondria [21; 23; 31; 40], it is hypothesized in the present thesis that the metabolism of GABA through the GABA shunt results in an inhibition of mitochondrial SLP and causes reverse operation of ANT in anoxia. The same conception is postulated for the metabolism of SSA and GHB. Therefore, **the first aim of the present work is to test the effects of exogenous GABA, SSA and GHB addition on bioenergetic parameters and SLP of isolated mouse brain and liver mitochondria.**

The second major issue of my thesis is to get closer to the identity of the diaphorase(s) which provide NAD^+ for the KGHDC when the respiratory chain is inhibited, as this is critical for the uninterrupted operation of SLP and the prevention of ANT reversal. Because of its ubiquitous expression in numerous tissues, its localization in mitochondria, and its ability to reduce a great variety of quinone substrates, Nqo1 is a possible candidate for performing this. **The second aim of my thesis is to address the contribution of Nqo1 to NAD^+ provision and SLP under conditions of impaired mitochondrial respiration**, by investigating bioenergetic parameters and ANT reversal in samples from wild type and Nqo1^{-/-} mice.

Finally, in the previous work of our laboratory the effect of diaphorase substrates on SLP was tested [45], from which menadione, mitoquinone and duroquinone had a beneficial impact on ATP generation via SUCL. Thus, the question was raised whether these compounds exert their effect through being reduced by Nqo1. Two additional quinones, idebenone (IDB) and 2-methoxy-1,4-naphthoquinone (MNQ) are known to transfer electrons from cytosolic NADH to the mitochondrial respiratory chain, bypassing complex I [183; 184]. For idebenone this effect was proposed to be mediated by cytosolic NQO1 – in the reaction idebenol is generated, which is able to donate electrons to the respiratory chain at the level of complex III [185]. Hence it is

reasonable to hypothesize that these two substrates could assist in maintaining the mitochondrial NAD^+ pool as well and consequently SLP when NADH oxidation through complex I is limited. **My third aim in this thesis to examine the effect of the aforementioned five substrates on mitochondrial SLP and to scrutinize whether this effect is Nqo1-dependent or not.**

3. METHODS

3.1. Animals

Mice were of mixed 129Sv and C57Bl/6 background. *Nqo1*^{-/-} mice were a kind gift of Dr. Frank J. Gonzalez. The animals used in our study were of either sex and between 2 and 6 months of age. Mice were housed in a room maintained at 20-22 °C on a 12-h light-dark cycle with food and water available ad libitum. All experiments were approved by the Animal Care and Use Committee of the Semmelweis University and the EU Directive 2010/63/EU for animal experiments.

3.2. Isolation of mitochondria

Isolation of mitochondria from mouse liver and brain: liver mitochondria from all animals were isolated as described in [186], with minor modifications. Mice were killed by cervical dislocation. The liver was removed and immediately placed in ice-cold isolation buffer containing 225 mM mannitol, 75 mM sucrose, 5 mM HEPES (free acid), 1 mM EGTA and 1 mg/ml bovine serum albumin (fatty acid-free), with the pH adjusted to 7.4 with Trizma® (Sigma-Aldrich, St. Louis, MO, USA). The organs were chopped, washed, homogenized and the homogenate was centrifuged at 1,250 g for 10 min. The upper fatty layer of the centrifuged homogenate was aspirated and the pellet was discarded. The supernatant was transferred into clean centrifuge tubes and centrifuged at 10,000 g for 10 min. After this step the supernatant was discarded and the pellet was resuspended in isolation buffer and centrifuged again in clean tubes at 10,000 g for 10 min. At the end of the third centrifugation the pellet was resuspended in 0.2 ml of a buffer with the same composition as described above but containing only 0.1 mM EGTA.

Non-synaptic mouse brain mitochondria were isolated on a Percoll gradient as described previously [187; 188], with minor modifications. After cervical dislocation brains were removed, chopped and homogenized in ice-cold isolation buffer. For the preparation of brain mitochondria the same isolation buffer was used as for liver mitochondria but without BSA. The homogenate was centrifuged at 1,250 g for 10 min; the pellet was discarded, and the supernatant was centrifuged at 10,000 g for 10 min. The pellet was resuspended in 15% Percoll (Sigma) and layered on a preformed Percoll gradient (40 and 23%). The tubes were centrifuged at 40,000 g for 6 min, and non-

synaptic brain mitochondria were collected from the interface between the 23% and 40% Percoll layers. After the dilution of mitochondria with isolation buffer they were centrifuged at 25,000 g for 10 min; the pellet was resuspended in isolation buffer and centrifuged again at 10,000 g for 10 min. Finally, the pellet was resuspended in 0.1 ml of the same medium as for the last step in the isolation of liver mitochondria.

Protein concentration was determined using the bicinchoninic acid assay, and calibrated using bovine serum standards using a Tecan Infinite® 200 PRO series plate reader (Tecan Deutschland GmbH, Crailsheim, Germany). Yields were typically 0.2 ml of ~20 mg/ml per two brains; for liver yields were typically 0.7 ml of ~70 mg/ml per two livers.

3.3. Determination of membrane potential ($\Delta\Psi_m$) in isolated brain and liver mitochondria

$\Delta\Psi_m$ of isolated mitochondria (0.25-1 mg – depending on the tissue of origin and machine used – per two ml of medium containing, in mM: KCl 8, K-gluconate 110, NaCl 10, Hepes 10, KH_2PO_4 10, EGTA 0.005, mannitol 10, MgCl_2 1, substrates as indicated in the figure legends, 0.5 mg/ml bovine serum albumin [fatty acid-free], pH 7.25, and 5 μM safranin O) was estimated fluorimetrically with the cationic dye safranin O due to its accumulation inside energized mitochondria [189]. Traces obtained from mitochondria were calibrated to millivolts as described in [21], by constructing a voltage-fluorescence calibration curve. Fluorescence was recorded in a Hitachi F-7000 spectrofluorimeter (Hitachi High Technologies, Maidenhead, UK) at a 5-Hz acquisition rate, using 495- and 585-nm excitation and emission wavelengths, respectively, or at a 1-Hz rate using the O2k- Fluorescence LED2-Module of the Oxygraph-2k (Oroboros Instruments, Innsbruck, Austria) equipped with a LED exhibiting a wavelength maximum of 465 ± 25 nm (current for light intensity adjusted to 2 mA, i.e., level '4') and an <505 nm shortpass excitation filter (dye-based, filter set "Safranin"). Emitted light was detected by a photodiode (range of sensitivity: 350-700 nm), through an >560 nm longpass emission filter (dye-based). Experiments were performed at 37 °C. Safranin O is known to exert adverse effects on mitochondria if used at sufficiently high concentrations (i.e. above 5 μM , discussed in [45]). However, for optimal conversion of the fluorescence signal to $\Delta\Psi_m$, a concentration of 5 μM

safranin O is required, even if it leads to diminishment of the respiratory control ratio (RCR) by approximately one unit (not shown). Furthermore, the non-specific binding component of safranin O to mitochondria (dictated by the mitochondria/safranin O ratio) was within 10% of the total safranin O fluorescence signal, estimated by the increase in fluorescence caused by the addition of a detergent to completely depolarized mitochondria (not shown). As such, it was accounted for, during the calibration of the fluorescence signal to $\Delta\Psi_m$.

3.4. Mitochondrial respiration

Oxygen consumption was estimated polarographically using an Oxygraph-2k (Oroboros Instruments, Innsbruck, Austria). 0.5-1 mg – depending on the tissue of origin – mitochondria was suspended in 2 ml incubation medium, the composition of which was identical to that as for $\Delta\Psi_m$ determination. Substrate combinations were used as indicated in the figure legends. Experiments were performed at 37 °C. Oxygen concentration and oxygen flux ($\text{pmol}\cdot\text{s}^{-1}\cdot\text{mg}^{-1}$; negative time derivative of oxygen concentration, divided by mitochondrial mass per volume and corrected for instrumental background oxygen flux arising from oxygen consumption of the oxygen sensor and back-diffusion into the chamber) were recorded using DatLab software (Oroboros Instruments).

3.5. Determination of NADH autofluorescence in permeabilized or intact mitochondria

NADH autofluorescence was measured using 340 and 435 nm excitation and emission wavelengths. Measurements were performed in a Hitachi F-7000 fluorescence spectrophotometer at a 5 Hz acquisition rate. 0.5 mg of mouse liver or 0.25 mg of brain mitochondria were suspended in 2 ml incubation medium, the composition of which was identical to that as for $\Delta\Psi_m$ determination. Mitochondria were permeabilized by 20 μg alamethicin. For measurement of the NADH oxidation rate (chapter 4.2.2.), the medium also contained NADH, MNQ or duroquinone, and rotenone as indicated in the respective figure legend. Experiments were performed at 37 °C. NADH autofluorescence was calibrated by adding known amounts of NADH to the suspension.

3.6. Determination of diaphorase activity

NADH and NADPH, dicoumarol-sensitive diaphorase activity was measured by two different methods, one relying on 2,6-dichlorophenol-indophenol (DCPIP) reduction [190] with the modifications detailed in [191], and the other on cytochrome c reduction [192]. Activities were determined by either method from the cytosolic and mitochondrial fractions from WT and Nqo1^{-/-} mouse livers. Cytosolic fractions were obtained by ultracentrifugation of the liver homogenate as detailed in [163].

For the first method the assay system contained 25 mM TRIS/HCl (pH=7.4), 0.18 mg/ml BSA, 5 μ M FAD, 0.01% Tween 20, 40 μ M DCPIP, 200 μ M NADH or NADPH and 20 μ g mitochondrial or 100 μ g cytosolic protein. Reduction of DCPIP was followed at 600 nm ($\epsilon=21 \text{ mM}^{-1} \cdot \text{cm}^{-1}$). For the second method, the reaction mixture contained 50 mM TRIS/HCl buffer (pH=7.5), 330 μ M NaCN, 200 μ M NADH, 20 μ g mitochondrial or 100 μ g cytosolic protein, 10 μ M of the respective quinone (MNQ, menadione or duroquinone) as primary electron acceptor, and 80 μ M cytochrome c in order to reoxidize the quinol formed. Reduction of cytochrome c was monitored at 550 nm ($\epsilon=18.5 \text{ mM}^{-1} \cdot \text{cm}^{-1}$). Measurements on mitochondrial fractions were performed in the presence of 2 μ M rotenone in both methods. All experiments were repeated in the presence of 10 μ M dicoumarol. Both assays were performed at 30 °C.

3.7. Cell culturing

HepG2 cells were cultured in Dulbecco's modified Eagle's medium (DMEM) containing 10% fetal bovine serum and antibiotic solution (containing penicillin and streptomycin) at 37 °C in 5% CO₂. 300-350,000 cells were plated in 75 cm² culture flasks.

3.8. Mitochondrial membrane potential determination of in situ mitochondria of permeabilized HepG2 cells

Mitochondrial membrane potential was estimated using fluorescence quenching of safranin O [189]. Cells were harvested by scraping, permeabilized as detailed previously [26] and suspended in a medium identical to that as for $\Delta\Psi_m$ measurements in isolated mitochondria. Substrates were 5 mM glutamate, 5 mM α -ketoglutarate and 5 mM malate. Fluorescence was recorded in a Tecan Infinite® 200 PRO series plate

reader using 495 and 585 nm excitation and emission wavelengths, respectively. Experiments were performed at 37 °C.

3.9. siRNA and transfection of cells

The On-TARGETplus SMARTpool containing 4 different siRNA sequences, all specific to human NQO1 and the corresponding non-targeting control (scrambled siRNA), were designed and synthesized by Thermo Scientific Dharmacon. HepG2 cells were transfected with 100 nM of either siRNA or scrambled siRNA using lipofectamine 2000 (Invitrogen, Carlsbad, CA, USA) according to the manufacturer's instructions. Cells were probed for mitochondrial SLP after 56 hours, and immediately afterwards harvested for Western blotting.

3.10. Western blotting

Cells were solubilized in RIPA buffer containing a cocktail of protease inhibitors (Protease Inhibitor Cocktail Set I, Merck Millipore, Billerica, MA, USA) and frozen at -80°C for further analysis. Frozen pellets were thawed on ice, and their protein concentration was determined using the bicinchoninic acid assay as detailed above, loaded at a concentration of 20 µg per well on the gels and separated by sodium dodecyl sulfate-polyacrylamide gel electrophoresis (SDS-PAGE). Separated proteins were transferred onto a methanol-activated polyvinylidene difluoride membrane. Immunoblotting was performed as recommended by the manufacturers of the antibodies. Rabbit polyclonal anti-NQO1 (Abcam) and mouse monoclonal anti-β-actin (Abcam) primary antibodies were used at titers of 1:1,000 and 1:5,000, respectively. Immunoreactivity was detected using the appropriate peroxidase-linked secondary antibody (1:5000, donkey anti-rabbit or donkey anti-mouse Jackson Immunochemicals Europe Ltd, Cambridgeshire, UK) and enhanced chemiluminescence detection reagent (ECL system; Amersham Biosciences GE Healthcare Europe GmbH, Vienna, Austria).

3.11. Statistics

Data are presented as averages ± SEM. Significant differences between two groups were evaluated by Student's t-test; significant differences between three or more groups were evaluated by one-way analysis of variance followed by Tukey's post-hoc

analysis. $p < 0.05$ was considered statistically significant. If normality test failed, ANOVA on Ranks was performed. * implies $p < 0.05$. ** implies $p < 0.001$. Wherever single graphs are presented, they are representative of at least 3 independent experiments.

3.12. Reagents

Standard laboratory chemicals, GABA, aminooxyacetic acid, vigabatrin, stigmatellin, 4-hydroxybenzaldehyde, disulfiram, 2-methoxy-1,4-naphthoquinone (cat no #189162) and safranin O were from Sigma. Carboxyatractyloside (cATR) was from Merck (Merck KGaA, Darmstadt, Germany). SF 6847 and atpenin A5 were from Enzo Life Sciences (ELS AG, Lausen, Switzerland). Succinic semialdehyde was from Santa Cruz Biotechnology Inc, (Dallas, TX, 75 220, U.S.A). γ -Hydroxybutyrate was manufactured by Lipomed AG (Arlesheim, Switzerland), and imported by permission (093012/ 2016/KAB) from the National Healthcare Service Center, Narcotics Division (<http://www.enkk.hu>). Mitochondrial substrate stock solutions were dissolved in bi-distilled water and titrated to pH 7.0 with KOH. ADP was purchased as K^+ salt of the highest purity available (Merck) and titrated to pH 6.9.

4. RESULTS

4.1. Catabolism of GABA, succinic semialdehyde or γ -hydroxybutyrate through the GABA shunt impairs mitochondrial substrate-level phosphorylation

Succinate, ensuing from catabolism of GABA through the GABA shunt might be of sufficient flux to force the reaction of succinate-CoA ligase toward ATP (or GTP) hydrolysis. In this chapter the hypothesis is tested that exogenous addition of GABA or its immediate catabolite, succinic semialdehyde, or GHB which is a precursor of SSA, abolish mitochondrial SLP. To address this, first it was verified that GABA, SSA and GHB energize mouse liver and brain mitochondria in aerobic conditions. Then SLP was investigated by interrogating the directionality of the ANT during anoxia using a biosensor test devised by us.

4.1.1. GABA as a bioenergetic substrate

The use of GABA and SSA as bioenergetic substrates has been addressed in a limited type of tissues, almost exclusively rat brain mitochondria [193-196]. From these studies it was inferred that the “free” mitochondria (a mixture from neuronal and astrocytic origin) exhibit a higher rate of GABA metabolism than synaptic mitochondria [193]. This is in agreement with later studies showing that GABA is mostly metabolized in astrocytes, not neurons [197], reviewed in [198]. In order to verify that in our hands and for the type of mitochondria that we prepared (Percoll-purified mouse brain and crude liver), GABA and SSA can be metabolized, we investigated the effect of exogenously adding these compounds on mitochondrial membrane potential and compared it to that obtained from ‘classical’ substrates.

As shown in Fig. 3A for brain and 3B for liver, mitochondria (mito) were added in the suspension without exogenously added substrates, and safranin O fluorescence was recorded. Safranin O is a positively charged dye, the distribution of which between mitochondria and the external medium is dependent on $\Delta\Psi_m$, therefore a decrease in the fluorescence signal reflects $\Delta\Psi_m$ generation [189]. Brain mitochondria do not exhibit a significant pool of endogenous substrates, thus, they develop only a minor $\Delta\Psi_m$. On the other hand, liver mitochondria contain endogenous substrates to a higher extent and this is reflected by a more significant polarization, which however, gradually subsides as these endogenous substrates are consumed.

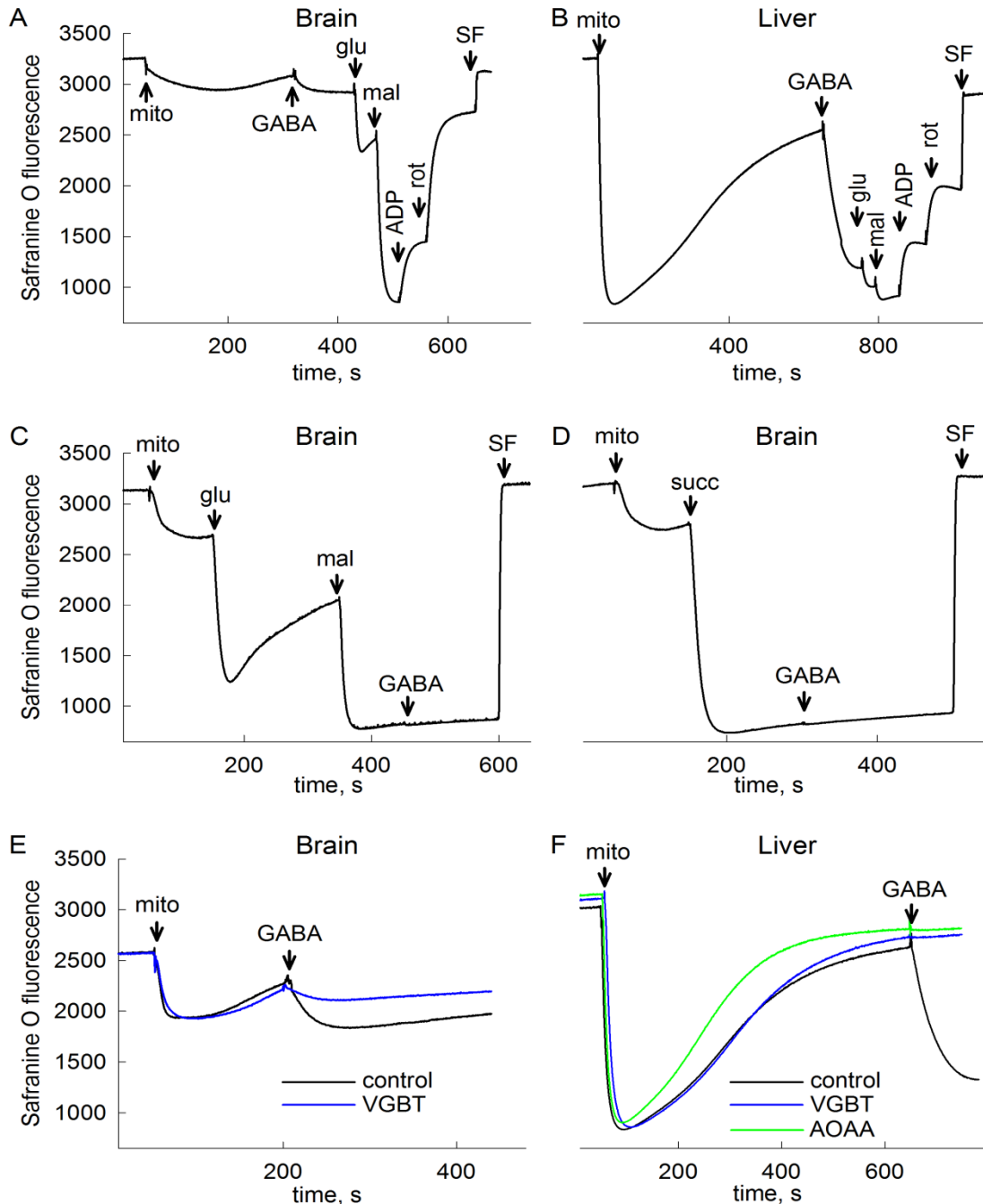


Figure 3. The effect of GABA on the membrane potential of isolated brain (A, C, D, E) and liver (B, F) mitochondria. Reconstructed time-courses of safranine O fluorescence (arbitrary fluorescence) indicating $\Delta\Psi_m$. Mitochondria (mito) were added where indicated; 0.25 mg for brain, 0.5 mg for liver. GABA (1 mM), glutamate (glu, 5 mM), malate (mal, 5 mM), succinate (succ, 5 mM), ADP (2 mM), rotenone (rot, 1 μ M), SF6847 (SF, 1 μ M) was added where indicated. In the experiments depicted by the blue traces in panels E and F vigabatrin (VGBT, 0.3 mM) was present in the medium prior to addition of mitochondria. In the experiment depicted by the green trace in panel F aminooxyacetic acid (AOAA, 0.1 mM) was present in the medium prior to addition of mitochondria. Panels to the right share the same y-axis with panels to the left. Each trace is representative of at least four independent experiments.

Addition of GABA to both types of mitochondria leads to further polarization, which is quantitatively higher in liver. Further addition of glutamate (5 mM) and malate (5 mM) leads to an even further polarization, implying that addition of GABA did not lead to achievement of maximum $\Delta\Psi_m$. Subsequent addition of ADP, rotenone and an uncoupler, SF6847 yielded the expected rise in safranin O fluorescence, implying anticipated responses in decreasing $\Delta\Psi_m$.

By adding GABA after the sequential addition of glutamate and malate (panel 3C) or succinate (panel 3D) to isolated brain mitochondria, no further polarization was recorded implying that the electron transport chain generating $\Delta\Psi_m$ has been saturated with reducing equivalents, NADH (through complex I) and/or FADH₂ (through SDH). Similar traces were obtained from liver mitochondria (not shown).

Next, we questioned if the GABA-induced polarization is genuinely due to the GABA shunt, eventually entering the citric acid cycle as succinate (see Fig. 2). To check this we used vigabatrin, a specific inhibitor of GABA-T. Vigabatrin (VGBT, 0.3 mM), abolished the GABA-induced $\Delta\Psi_m$ generation in both brain (panel 3E, blue trace) and liver (panel 3F, blue trace) mitochondria. Likewise, by adding the alternative GABA-T inhibitor, aminooxyacetic acid (AOAA, 0.1 mM, panel 3F, green trace), GABA-induced $\Delta\Psi_m$ generation was prevented.

4.1.2. Succinic semialdehyde as a bioenergetic substrate

To address the possibility that the GABA-induced polarization does not stem from supporting α -ketoglutarate to glutamate conversion by GABA-T, in turn leading to NAD(P)H formation from glutamate to α -ketoglutarate conversion by glutamate dehydrogenase (GLUD, see Fig. 2), we tested the effect of SSA on the membrane potential of isolated mitochondria. The results of these experiments are shown in Fig. 4. As shown in panel 4A for brain, and panel 4B for liver mitochondria, addition of SSA (1 mM) in the absence of exogenously added substrates lead to generation of $\Delta\Psi_m$. Because the subsequent addition of glutamate and malate did not lead to any further polarization, we concluded that SSA conferred the maximum $\Delta\Psi_m$ achievable. Thus, GABA generates $\Delta\Psi_m$ by transamination to SSA, which is subsequently dehydrogenated by SSADH, entering the citric acid cycle as succinate. As expected, the SSA-mediated $\Delta\Psi_m$ generation was insensitive to GABA-T inhibitors, shown in Fig. 4C

and D, for brain and liver mitochondria, respectively. We attempted to inhibit SSADH using 4-hydroxybenzaldehyde [199] or disulfiram [200], however both compounds were strongly uncoupling mitochondria (not shown).

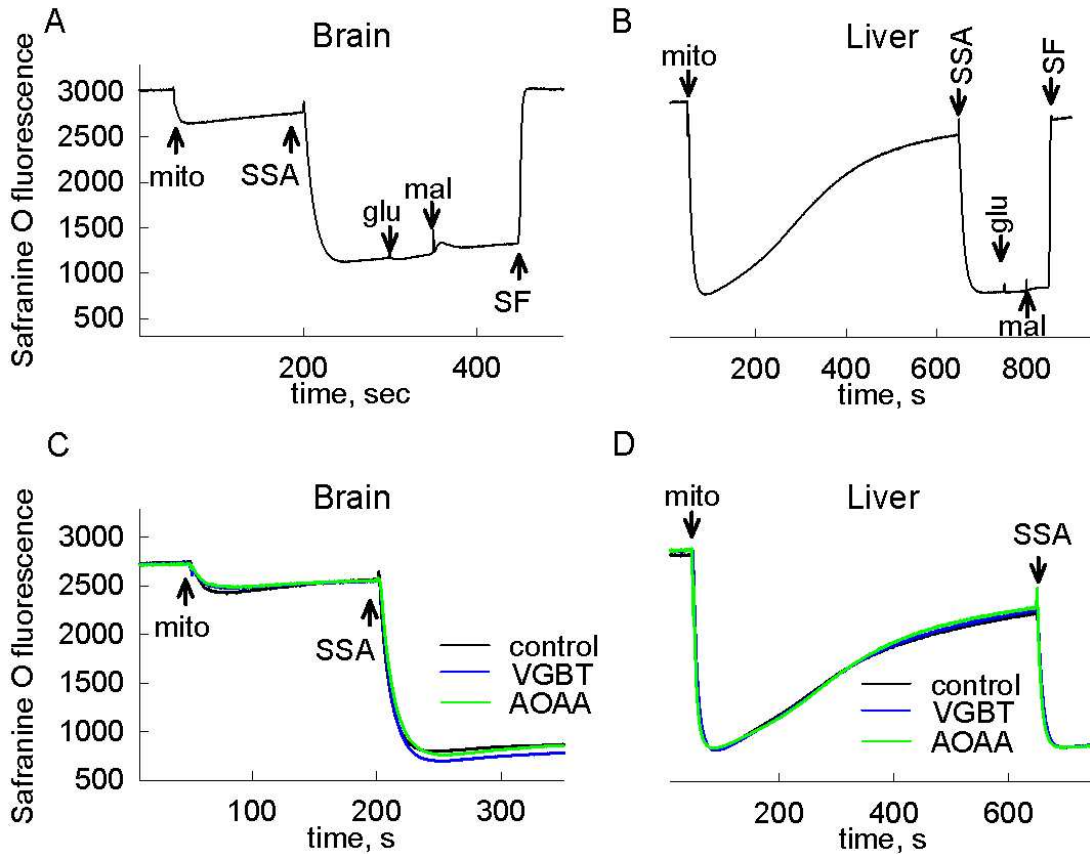


Figure 4. The effect of SSA on membrane potential of isolated brain (A, C) and liver (B, D) mitochondria. Reconstructed time-courses of safranine O fluorescence (arbitrary fluorescence) indicating $\Delta\Psi_m$. Mitochondria (mito) were added where indicated; 0.25 mg for brain, 0.5 mg for liver. SSA (1 mM), glutamate (glu, 1 mM), malate (mal, 1 mM), SF6847 (SF, 1 μ M) was added where indicated. In the experiments depicted by the blue traces in panels C and D, vigabatrin (VGBT, 0.3 mM), and in those depicted by green traces, aminooxyacetic acid (AOOA, 0.1 mM) was present in the medium prior to addition of mitochondria. Panels to the right share the same y-axis with panels to the left. Each trace is representative of at least four independent experiments.

At this junction, the question arose if $\Delta\Psi_m$ generation was due to NADH production by SSADH, or $FADH_2$ production supported by succinate, or both. To address this, we added either rotenone (Fig. 5A) or atpenin A5 (Fig. 5B) or both (Fig. 5C) after SSA and recorded the changes in $\Delta\Psi_m$ of liver mitochondria. When rotenone or atpenin A5 were added alone, there were no changes in safranine O fluorescence, implying that in the first case $FADH_2$ production from SDH was supporting $\Delta\Psi_m$, and

in the latter case, NADH production from SSADH was responsible for the generation of reducing equivalents. When both complex I and II inhibitors were present, $\Delta\Psi_m$ collapsed, and the same effect was observed by inhibiting complex III with stigmatellin (Fig. 5D). This implies that $\Delta\Psi_m$ generated by SSA is supported by both FADH_2 production through SDH, and NADH formation through SSADH.

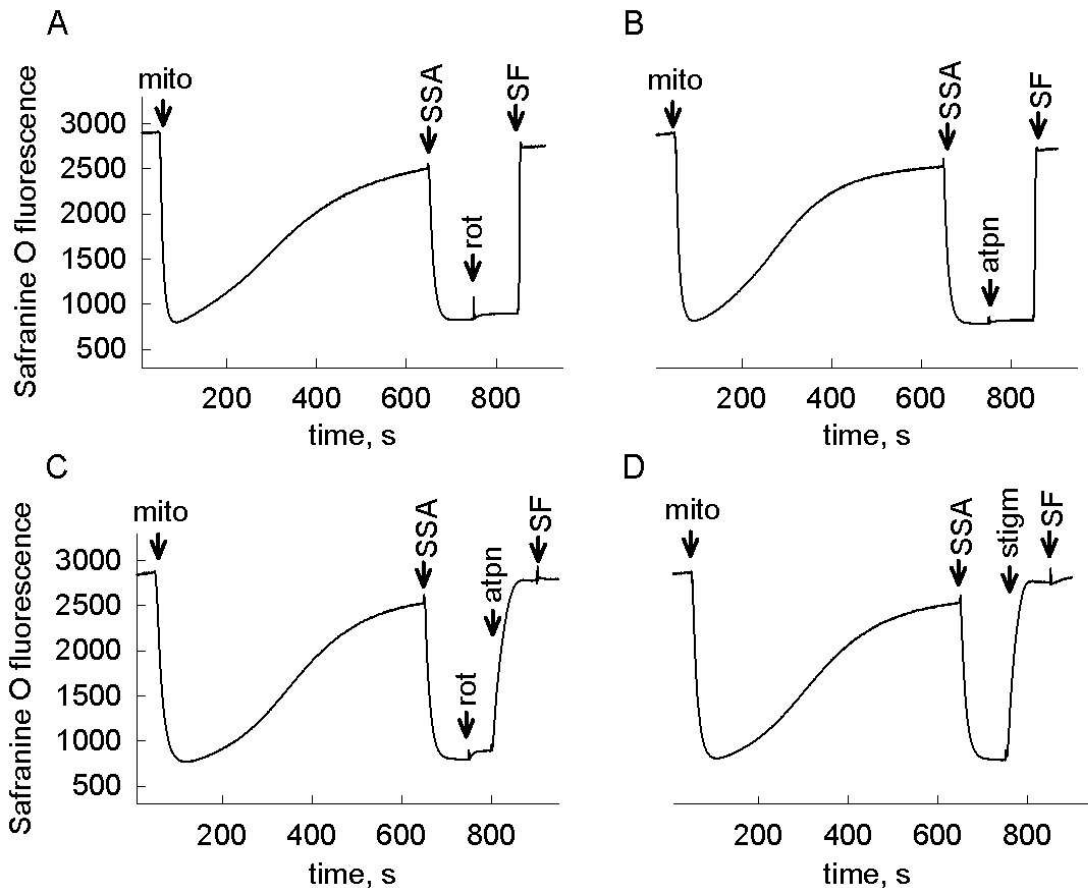


Figure 5. The effect of respiratory complex inhibitors on membrane potential of isolated liver mitochondria energized by SSA. Reconstructed time-courses of safranine O fluorescence (arbitrary fluorescence) indicating $\Delta\Psi_m$. Mitochondria (mito) were added where indicated; 0.25 mg for brain, 0.5 mg for liver. SSA (1 mM), rotenone (rot, 1 μM), atpenin A5 (atpn, 2 μM), stigmatellin (stigm, 1 μM) SF6847 (SF, 1 μM). Panels to the right share the same y-axis with panels to the left. Each trace is representative of at least four independent experiments.

To further address the contribution of SSA in yielding NADH through SSADH, we recorded the effect of the substrate on NADH autofluorescence in permeabilized or intact mitochondria. The results of these experiments are shown in Fig. 6. As shown in Fig. 6A for brain, and 6B for liver, mitochondria were added when indicated, and NADH autofluorescence was recorded. After approximately 100 s mitochondria were

permeabilized by alamethicin, yielding a minor decrease in the signal. Further addition of NAD^+ did not lead to any appreciable changes. Subsequent addition of 10 mM malonate ensures that SDH was fully inhibited. Then, addition of 1 mM SSA yielded a strong increase in NADH concentration. Despite the fact that atpenin A5 has been branded as a specific inhibitor of SDH, we wished to verify that it does not affect SSADH activity either. Indeed, by including 2 μM atpenin A5 and repeating the experiments (red traces, panels A and B), traces were nearly identical to those obtained in the absence of this SDH inhibitor (black traces, Fig. 6A and B). What is also evident by comparing Fig. 6A and 6B is that the extent of NADH production by SSA is nearly 10 times higher in liver than in brain mitochondria. Since liver mitochondria were double the amount of brain mitochondria for these experiments, it is inferred that SSADH activity in liver is approximately 5 times higher than that in brain mitochondria. As expected, addition of succinate after SSA did not yield any further increase in NADH autofluorescence.

In order to demonstrate that NADH can be generated by SSA in intact mitochondria, the following experiment was performed: as shown in Fig. 6C, liver mitochondria were added when indicated, and NADH autofluorescence was recorded. A small amount of the uncoupler (40 nM SF6847) was subsequently added in order to reach the maximum oxidized state of NADH/NAD^+ pools and this was reflected by a decrease in the signal. Subsequent addition of rotenone blocked complex I, thus regenerating some amount of the NADH pool. Then, addition of either SSA (Fig. 6C, black trace) or succinate (Fig. 6C, orange trace) yielded an increase in intramitochondrial NADH fluorescence, but with different kinetics. In the case of SSA, the increase in NADH is due to SSADH activity, while in the case of succinate is probably due to downstream dehydrogenases of the citric acid cycle, thus the timing of NADH increase is more gradual. The pool of NAD^+ for the dehydrogenases in the absence of a functional complex I due to rotenone could be mitochondrial diaphorases, as described previously [45].

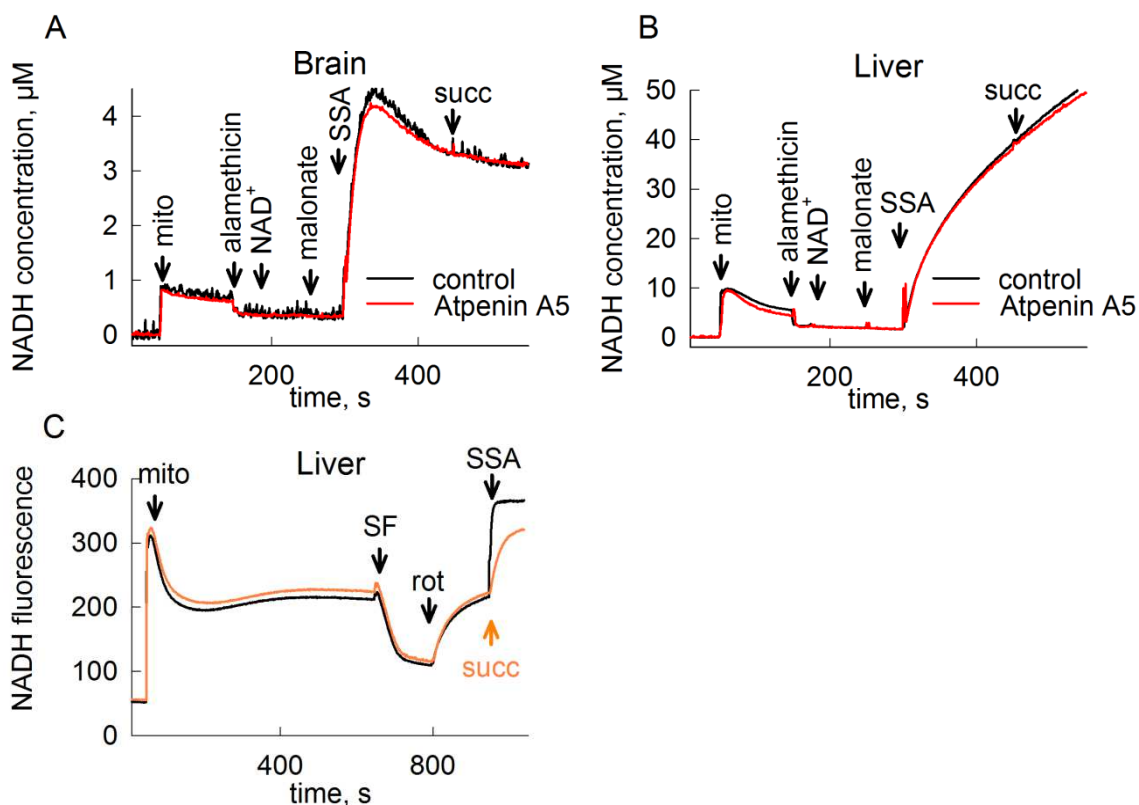


Figure 6. The effect of SSA on NADH autofluorescence in permeabilized brain (A) and liver (B) and intact liver (C) mitochondria. Reconstructed time-courses of calibrated (A, B) and uncalibrated (C) NADH autofluorescence. Mitochondria (mito) were added where indicated; 0.25 mg for brain, 0.5 mg for liver. Alamethicin (20 µg), NAD⁺ (1 mM), malonate (10 mM) SSA (1 mM), rotenone (rot, 1 µM), succinate (succ, 1 mM), SF6847 (SF, 40 nM) was added where indicated. In the experiments depicted by the red traces in panels A and B, 2 µM atpenin A5 was present in the medium prior to addition of mitochondria. Panel B shares the same y-axis with panel A. Each trace is representative of at least four independent experiments.

4.1.3. γ -Hydroxybutyrate as a bioenergetic substrate

Regarding GHB, the catabolism of this molecule by mitochondria was also addressed mainly in rat tissues [105; 201]. As mentioned under section 1.8 and shown in Fig. 2, GHB transhydrogenates with α -ketoglutarate to SSA and D-2-hydroxyglutarate by HOT. However, HOT exhibits a very strong tissue-specific expression; most notably, HOT is scarcely expressed in the brain [105; 202], a phenomenon that may contribute to the lingering neurologically-related effects of GHB acting on specific receptors [203], as it is catabolized very slowly. On the other hand, HOT is abundantly expressed in the liver [105]. Thus, exogenously added GHB to mitochondria isolated from brain should not lead to any appreciable bioenergetic

effects; such effects should be observed if liver mitochondria are used instead. Indeed, as shown in Fig. 7A, addition of 5 mM GHB before addition of 5 μ M α -ketoglutarate (red trace) or addition of 50 μ M α -ketoglutarate before GHB (black trace, because freshly purified brain mitochondria are devoid of endogenous substrates and H₂O₂ requires both GHB and α -ketoglutarate to generate D-2-hydroxyglutarate and SSA) did not lead to a significant gain of $\Delta\Psi_m$ in Percoll-purified brain mitochondria. Further addition of malate (1 mM) led to full polarization which was abolished by rotenone (1 μ M), implying that these mitochondria were entirely competent to generate $\Delta\Psi_m$ by substrates other than GHB. In contrast, addition of GHB to isolated liver mitochondria (Fig. 7B) before endogenous substrates were fully consumed (thus, minor amounts of α -ketoglutarate were expected to exist in the mitochondrial matrix) led to a considerable polarization compared to vehicle; further addition of a minute amount of α -ketoglutarate (5 μ M) led to a further gain of $\Delta\Psi_m$. As expected, the concomitant presence of GABA-T inhibitors (Fig. 7B) vigabatrin (VGBT, blue trace) or aminooxyacetic acid (AOAA, green trace) did not affect the GHB-induced polarization in liver mitochondria, compared to control (black trace).

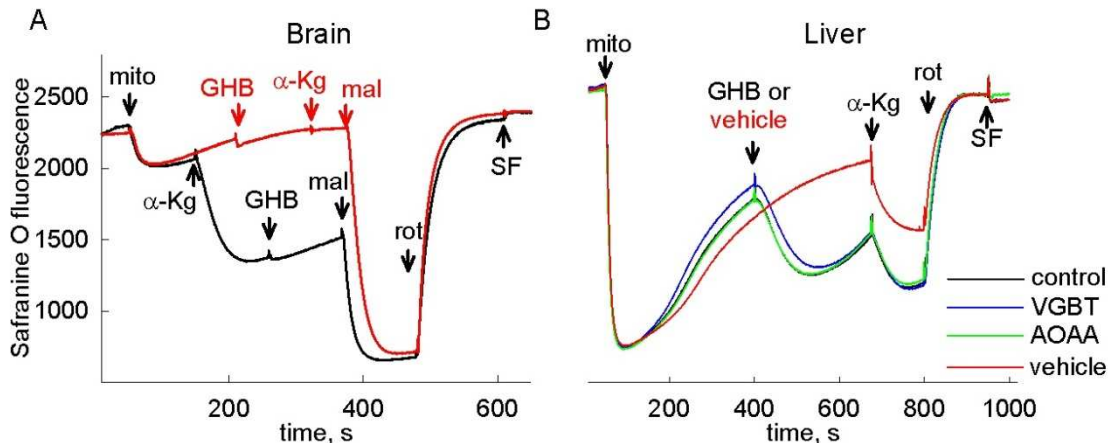


Figure 7. The effect of GHB on membrane potential of isolated brain (A) and liver (B) mitochondria. Reconstructed time-courses of safranin O fluorescence (arbitrary fluorescence) indicating $\Delta\Psi_m$. Mitochondria (mito) were added where indicated; 0.25 mg for brain, 0.5 mg for liver. GHB (5 mM), α -ketoglutarate (α -Kg, 50 or 5 μ M), malate (mal, 1 mM), rotenone (rot, 1 μ M), SF6847 (SF, 1 μ M) was added where indicated. In the experiments depicted by the blue traces in panel B, vigabatrin (VGBT, 0.3 mM), and in those depicted by green trace, aminooxyacetic acid (AOAA, 0.1 mM) was present in the medium prior to addition of mitochondria. Red trace is a vehicle control for GHB. Panel B shares the same y-axis with panel A. Each trace is representative of at least four independent experiments.

It is presumable that degradation of GHB by HOT contributes to membrane potential generation with producing D-2-hydroxyglutarate, for this can donate electrons to complex III through the ETF system. However, in our hands, addition of D-2-hydroxyglutarate to isolated mitochondria did not yield any appreciable $\Delta\Psi_m$ (not shown).

4.1.4. Investigation of mitochondrial substrate-level phosphorylation

In order to interrogate the effects of GABA, SSA and GHB on SLP in intact mitochondria, we employed a biosensor test developed by our laboratory [21], where the effect of the ANT inhibitor carboxyatractyloside is investigated on safranin O fluorescence reflecting $\Delta\Psi_m$. The principle of the test is shown in Fig. 8. In the experiments, mitochondria are polarized by different substrates present in the medium, then oxidative phosphorylation is induced by 2 mM ADP, resulting in a loss of membrane potential as ATP generation is coupled to utilization of the proton-motive force. Respiratory chain is inhibited either by 1 μ M rotenone or by reaching anoxia, which lead to a further depolarization. At this membrane potential, F₀-F₁ ATP synthase operates in reverse mode, i.e. it is pumping protons out of the matrix at the expense of matrix ATP hydrolysis. Next, the effect of cATR is examined: the adenine nucleotide exchange through the ANT is electrogenic, since one molecule of ATP⁴⁻ is exchanged for one molecule of ADP³⁻ [8]. Thus, in sufficiently energized mitochondria the export of ATP in exchange for ADP decreases $\Delta\Psi_m$ [204]. Therefore, during the forward mode of ANT, abolition of its operation by the ANT inhibitor cATR leads to a gain of $\Delta\Psi_m$ (Fig. 8, black line), whereas during the reverse mode of ANT, abolition of its operation by the inhibitor leads to a loss of $\Delta\Psi_m$ (Fig. 8, red line). If ANT was still working in forward mode, mitochondria could remain in the B space despite their inhibited respiratory chain, and this is due to the adequate operation of mitochondrial SLP. If ANT was working in reverse mode, mitochondria could not prevent entering the C space because of an insufficient ATP production through mitochondrial SLP. Finally, an uncoupler (SF6847) is added to reach complete depolarization.

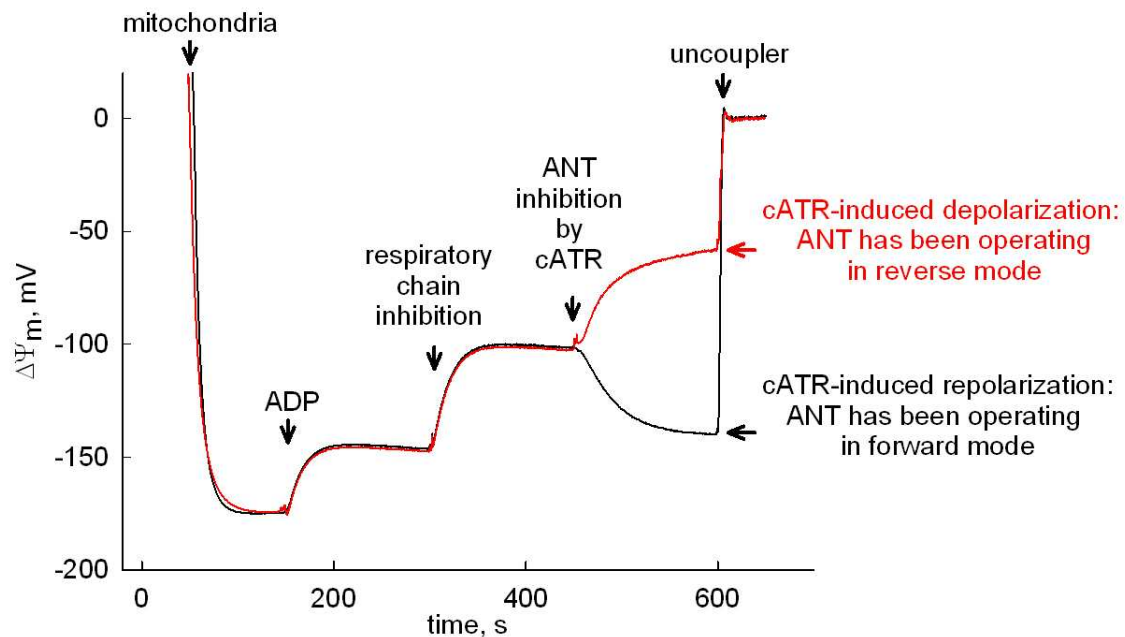


Figure 8. The biosensor test used for determining ANT directionality under respiratory inhibition. Substrates are present in the experimental medium. Addition of ADP initiates oxidative phosphorylation in mitochondria which is reflected in a decrease in membrane potential. Then the respiratory chain is inhibited pharmacologically or by the depletion of oxygen in the chamber. The change in membrane potential after the addition of cATR depends on the directionality of adenine nucleotide translocase. If ANT has been operating in forward mode (exporting ATP and importing ADP, therefore exporting one negative charge), its inhibition by cATR results in a gain of membrane potential. If ANT has been operating in reverse mode, the addition of cATR lowers the membrane potential. Finally, an uncoupler is added to reach complete depolarization.

4.1.5. GABA abolishes mitochondrial SLP in anoxia

The results of such experiments for GABA are shown in Fig. 9, where membrane potential values are indicated by solid traces and parallel measurements of oxygen concentration by dotted traces. As it can be seen in Fig. 9A for brain and 9B for liver, mitochondria respired on glutamate and malate (black trace), or glutamate and malate plus GABA (red trace) and allowed to fully polarize. State 3 respiration was initiated by 2 mM ADP. The presence of GABA did not increase the rates of respiration, consistent with the findings of Fig. 3C showing no further polarization by GABA, in the presence of glutamate and malate.

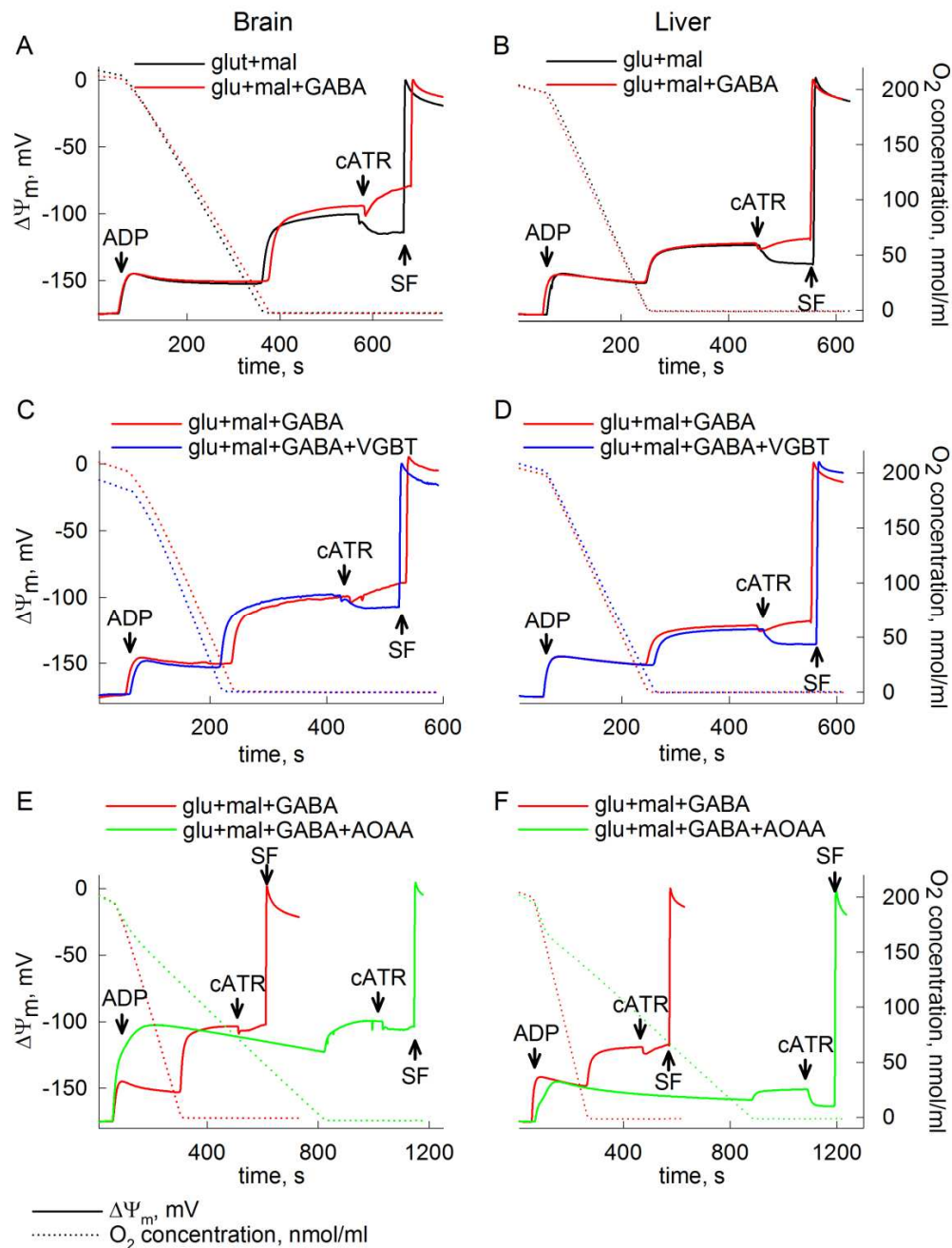


Figure 9. The effect of GABA on mitochondrial SLP during anoxia. Reconstructed time courses of safranin O signal calibrated to $\Delta\Psi_m$ (solid traces), and parallel measurements of oxygen concentration in the medium (dotted traces) in isolated brain (0.5 mg, A, C, E) and liver (1 mg, B, D, F) mitochondria in the presence of either GABA (5 mM, red traces) or GABA + vigabatrin (VGBT, 0.3 mM, blue traces), or GABA + aminooxyacetic acid (AOAA, 0.1 mM green traces). ADP: 2 mM; carboxyatractyloside (cATR), 1 μ M. Substrate concentrations were: glutamate (5 mM) and malate (5 mM). At the end of each experiment 1 μ M SF 6847 was added to achieve complete depolarization. Each trace is representative of at least four independent experiments.

In an air-tight chamber, mitochondria consume the entire amount of oxygen and this is verified by recording 'zero' levels of dissolved oxygen. Anoxia also coincided with the onset of an additional depolarization leading to a clamp of $\Delta\Psi_m$ at around -100 mV. In mitochondria respiring on substrates supporting SLP, as in these experiments, i.e. glutamate and malate [21], inhibition of the ANT by cATR conferred a moderate repolarization, implying that the translocase was still operating in the forward mode. In contrast, mitochondria fueled by glutamate and malate plus GABA, reacted to cATR with a depolarization during the anoxic period. The effect of GABA, reverting the cATR induced changes from repolarization to depolarization implying abolition of SLP was antagonized by the GABA-T inhibitors vigabatrin (VGBT, 0.3 mM, blue traces in Fig. 9C for brain and 9D for liver) and aminooxyacetic acid (AOAA, 0.1 mM green traces in Fig. 9E for brain and 9F for liver). It is also notable that AOAA diminished state 3 respiration, which is expected because it is an inhibitor of pyridoxal phosphate-dependent enzymes [98; 99; 205], most participating in several bioenergetic pathways.

From the above experiments we concluded that GABA metabolism through the GABA shunt led to an increase in succinate formation, which favored the reversible reaction catalyzed by succinate-CoA ligase towards ATP (or GTP) hydrolysis, thus abolishing SLP.

4.1.6. Succinic semialdehyde abolishes mitochondrial SLP in anoxia

Regarding the effect of SSA on SLP, the results of these experiments are shown in Fig. 10. As shown in Fig. 10A for brain and 10B for liver, mitochondria respired on glutamate and malate (black trace), or glutamate and malate plus SSA (red trace) and allowed to fully polarize (solid traces). State 3 respiration was initiated by 2 mM ADP. The presence of SSA affected very minorly the rates of respiration. However, during the anoxic period the presence of SSA reverted the cATR induced changes from repolarization to depolarization implying abolition of SLP, but unlike in the case of GABA, the GABA-T inhibitors vigabatrin (VGBT, 0.3 mM, blue traces in Fig. 10C for brain and 10D for liver) and aminooxyacetic acid (AOAA, 0.1 mM green traces in Fig. 10E for brain and 10F for liver) did not ameliorate the effect of SSA. This is expected, because SSA entry to the GABA shunt is after the GABA-T step (see Fig. 2).

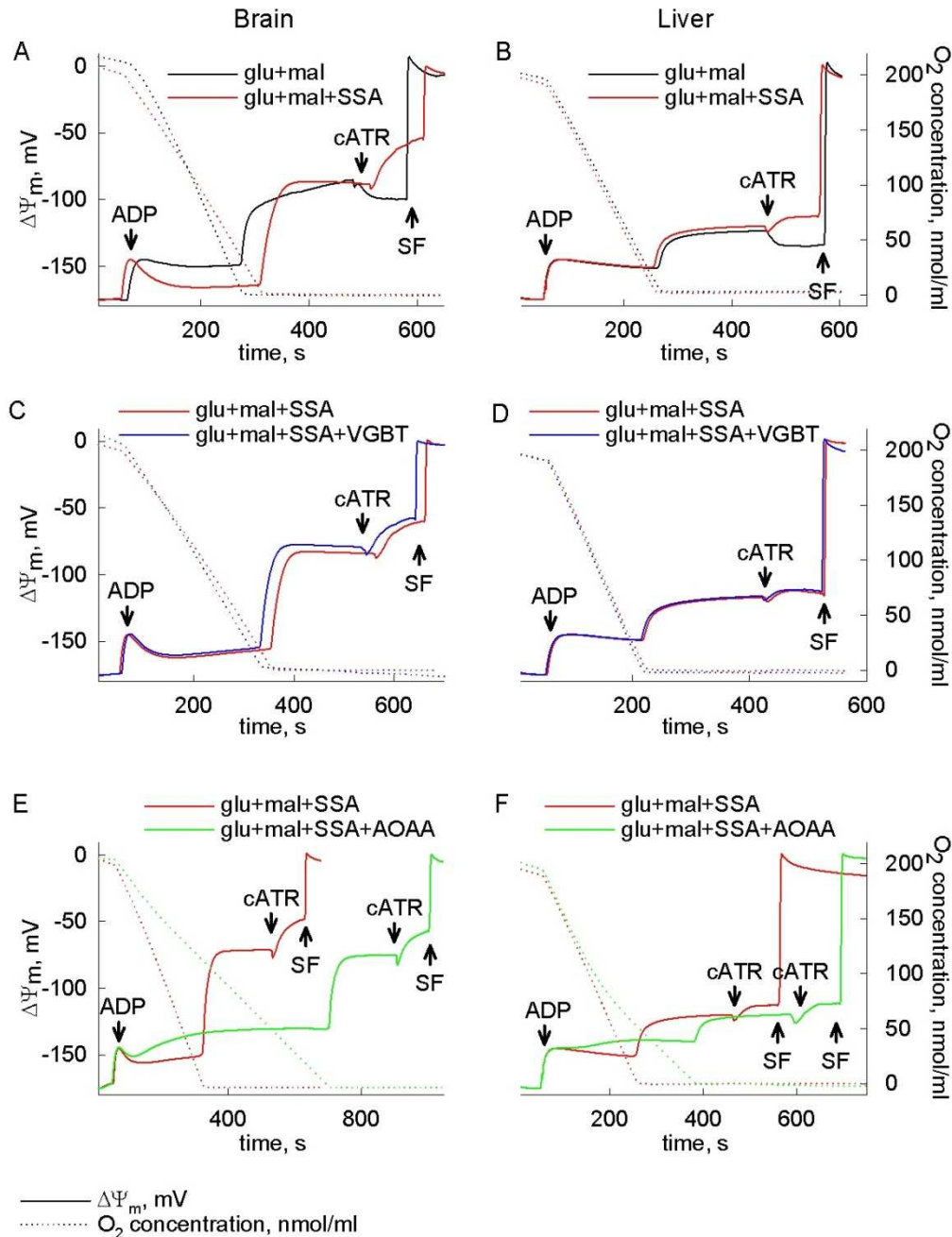


Figure 10. The effect of SSA on mitochondrial SLP during anoxia. Reconstructed time courses of safranin O signal calibrated to $\Delta\Psi_m$ (solid traces), and parallel measurements of oxygen concentration in the medium (dotted traces) in isolated brain (0.5 mg, A, C, E) and liver (1 mg, B, D, F) mitochondria in the presence of either SSA (1 mM, red traces) or SSA + vigabatrin (VGBT, 0.3 mM, blue traces), or SSA + aminooxyacetic acid (AOAA, 0.1 mM green traces). ADP: 2 mM; carboxyatractyloside (cATR), 1 μ M. Substrate concentrations were: glutamate (5 mM) and malate (5 mM). At the end of each experiment 1 μ M SF 6847 was added to achieve complete depolarization. Each trace is representative of at least four independent experiments.

4.1.7. γ -Hydroxybutyrate abolishes mitochondrial SLP in anoxia

Regarding the effect of GHB on SLP, the results of these experiments are shown in Fig. 11. As shown in Fig. 11A for brain and 11B for liver, mitochondria respired on α -ketoglutarate and malate (black trace), or α -ketoglutarate and malate plus GHB (red trace) and allowed to fully polarize (solid traces). State 3 respiration was initiated by 2 mM ADP. The presence of GHB minorly affected the rates of liver but not brain mitochondrial respiration. In liver mitochondria, during the anoxic period the presence of GHB reverted the cATR induced changes from repolarization to depolarization implying abolition of SLP, but unlike in the case of GABA, vigabatrin (VGBT, 0.3 mM, Fig. 11C blue trace) or aminooxyacetic acid (AOAA, 0.1 mM Fig. 11D, green trace) did not ameliorate the effect of GHB. This is expected, because GHB entry to the GABA shunt does not involve the GABA-T step (see Fig. 2). Unlike liver mitochondria, GHB did not inhibit SLP in brain mitochondria (Fig. 11A) consistent with the fact that HOT is scarcely expressed in the brain, precluding the formation of an appreciable amount of SSA.

From the above experiments we concluded that during anoxia, the beneficial effect of SLP preventing mitochondria from becoming extramitochondrial ATP consumers is abolished by GABA, SSA and GHB.

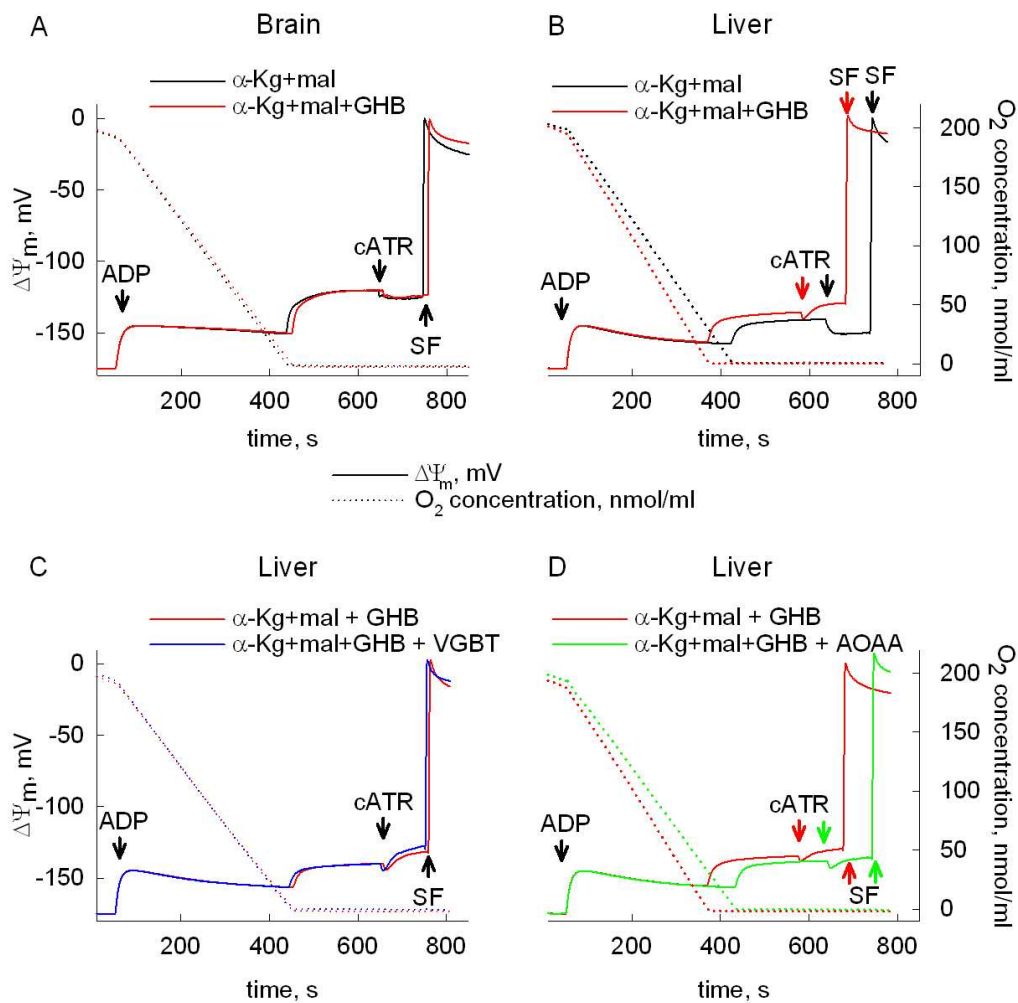


Figure 11. The effect of GHB on mitochondrial SLP during anoxia. Reconstructed time courses of safranin O signal calibrated to $\Delta\Psi_m$ (solid traces), and parallel measurements of oxygen concentration in the medium (dotted traces) in isolated brain (0.5 mg, A) and liver (1 mg, B, C, D) mitochondria in the presence of either GHB (5 mM, red traces) or GHB + vigabatrin (VGBT, 0.3 mM, blue traces), or GHB + aminooxyacetic acid (AOAA, 0.1 mM green traces). ADP: 2 mM; carboxyatractyloside (cATR), 1 μ M. Substrate concentrations were: glutamate (5 mM) and malate (5 mM). At the end of each experiment 1 μ M SF 6847 was added to achieve complete depolarization. Each trace is representative of at least four independent experiments.

4.2. Contribution of Nqo1 to NAD⁺ provision and mitochondrial SLP using endogenous or exogenous quinones

Mindful that Nqo1 localizes to mitochondria (even though accounting for <15% of total cellular diaphorase activity), we were interested in the extent of contribution of this protein yielding NAD⁺ in the matrix when complex I is inhibited. The experiments demonstrated in this chapter examine NADH-oxidizing activity, oxygen consumption rate and SLP in Nqo1^{-/-} mitochondria compared to WT. To characterize further the ability of mitochondrial Nqo1 oxidizing reducing equivalents, we tested the effect of a host of redox-active quinones on the above mentioned parameters.

4.2.1. Determination of NAD(P)H oxidation and quinone reduction capacity in cytosolic extracts and permeabilized mitochondria from the livers of WT and Nqo1^{-/-} mice

The extent of contribution of Nqo1 to overall diaphorase activity in mouse liver was measured using two different methods (as described in chapter 3.6.): i) by determining the dicoumarol-sensitive rates of DCPIP reduction during NADH and NADPH oxidation and ii) by determining the dicoumarol-sensitive rates of cytochrome c reduction using various quinones in the presence of NADH. The principles of these two methodologies are depicted in Fig. 12.

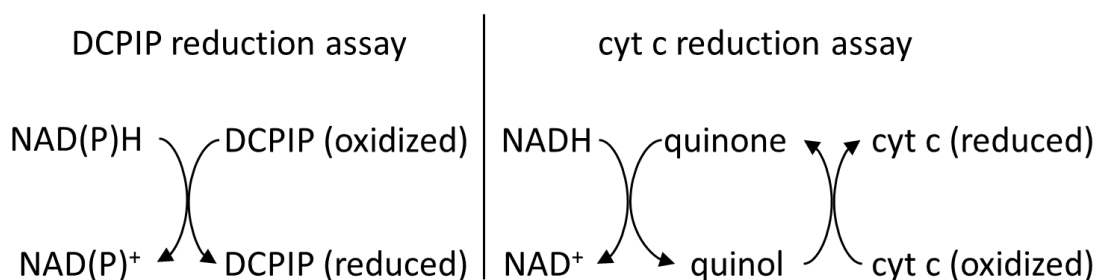


Figure 12. Principle of the diaphorase activity assays. The electrons of NAD(P)H are either transferred to DCPIP and the reduction of the dye is monitored; or they are passed to a quinone and then to a secondary electron acceptor, cytochrome c (cyt c), the absorbance of which is measured.

Data obtained from WT and Nqo1^{-/-} mice were pooled and compared. Nqo1^{-/-} mice have been developed by the group of Jaiswal [171]. As shown in Fig. 13A, the presence of 10 μ M dicoumarol decreased DCPIP reduction to nearly zero when using NADH in cytosolic extracts from the livers of WT mice. When NADPH was used instead of NADH, DCPIP reduction was 100% eliminated by dicoumarol (Fig. 13B, white bars). These two results confirm that the cytosolic NAD(P)H-dependent diaphorase activity is almost 100% sensitive to dicoumarol. By repeating these experiments but using cytosolic extracts from the livers of Nqo1^{-/-} mice (grey hatched bars) it is obvious that diaphorase activity is largely – but not exclusively – due to Nqo1. This methodology relies on the ability of diaphorases (including Nqo1) to reduce DCPIP; however, different diaphorases exhibit different affinities for electron acceptors, thus we measured cytochrome c oxidation rates in the presence of various quinones (as electron acceptors), which were later used for further experiments. As shown in Fig. 13C, D and E, the rates of cytochrome c reduction and their sensitivities to dicoumarol varied in the presence of MND, DQ or MNQ, using cytosolic extracts from the livers of WT mice. With this methodology, a statistically significant decrease in diaphorase activity was demonstrated only by using MND and MNQ. On the other hand, dicoumarol failed to decrease diaphorase activity in cytosolic extracts obtained from the livers of Nqo1^{-/-} mice. The finding that in the hepatic cytosols of Nqo1^{-/-} mice higher diaphorase activities were observed using the cytochrome c reduction method vs the DCPIP reduction method reflects the fact that other diaphorases are present in this compartment, which are not dicoumarol-sensitive and exhibit higher affinities for redox-active compounds other than DCPIP.

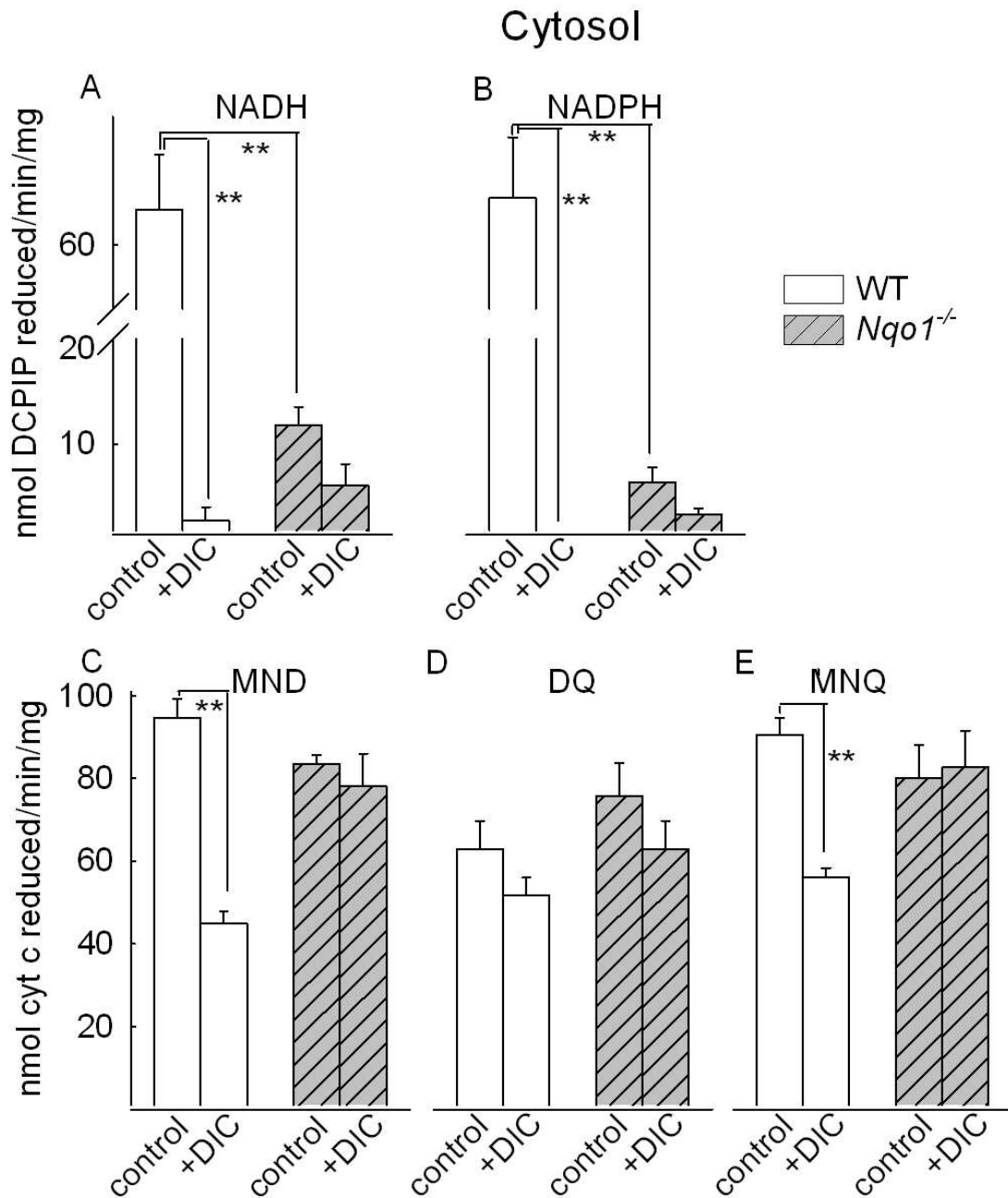


Figure 13. Determination of diaphorase activity in cytosolic extracts from the livers of WT and *Nqo1*^{-/-} mice. White bars signify data from WT mice, grey-hatched bars from *Nqo1*^{-/-} mice. Panels A and B depict data obtained by the DCPIP reduction method using NADH or NADPH as indicated in the panels. Panels C, D and E depict data obtained by the cytochrome c reduction method using menadione (MND, 10 μ M), duroquinone (DQ, 10 μ M) or 2-methoxy-1,4-napthoquinone (MNQ, 10 μ M) as indicated in the panels, in the presence of NADH. All samples were measured in the absence (control) or presence of 10 μ M dicoumarol (DIC).

To investigate the extent of contribution of mitochondrial Nqo1 to overall diaphorase activity, the same experiments were performed using freeze-thawed isolated mitochondria from the livers of WT and Nqo1^{-/-} mice, in the presence of 2 μ M rotenone. As shown in Fig. 14A, the presence of 10 μ M DIC decreased DCPIP reduction to a small and not significant level, despite the extremely high DCPIP reduction rate in the presence of NADH, in both types of mitochondria isolated from the livers of WT and Nqo1^{-/-} mice. When NADPH was used in lieu of NADH, a ~20 times lower rate of DCPIP reduction was recorded, which was also minorly sensitive to DIC (Fig. 14B). These findings reflect the presence of DCPIP reduction mechanisms dependent on NADH but not NADPH in mitochondria, a concept which is not at odds with the very rich redox matrix environment and its dependence on NADH/NAD⁺ ratio. Exclusive mitochondrial Nqo1 activity can be calculated by subtracting the [control minus DIC-insensitive] rate obtained from Nqo1^{-/-} mice from the [control minus DIC-insensitive] DCPIP reduction rate obtained from WT mice, for either NADH or NADPH. This calculation yielded evanescently small amounts (<1 nmol) of DCPIP reduced per minute per mg protein in mitochondria, which is in agreement with an average estimation of <15% of total [148-157]. By using the cytochrome c reduction method with various quinones in freeze-thawed isolated mitochondria, a very high reduction rate was recorded for all quinones tested (Fig. 14C, D and E). Notably, if MNQ was the used quinone, there a statistically significant difference in diaphorase activity was observed by comparing WT with Nqo1^{-/-} mice (Fig. 14E). When quinones other than MNQ were used, mitochondria from Nqo1^{-/-} mice also showed diminished rates of cytochrome c reduction compared to those obtained from WT mice, albeit these differences did not reach statistical significance. As for the results obtained from cytosolic extracts, it can be concluded that the mitochondrial matrix also harbors other than Nqo1 diaphorases which are also not dicoumarol-sensitive and exhibit higher affinities for redox-active compounds other than DCPIP.

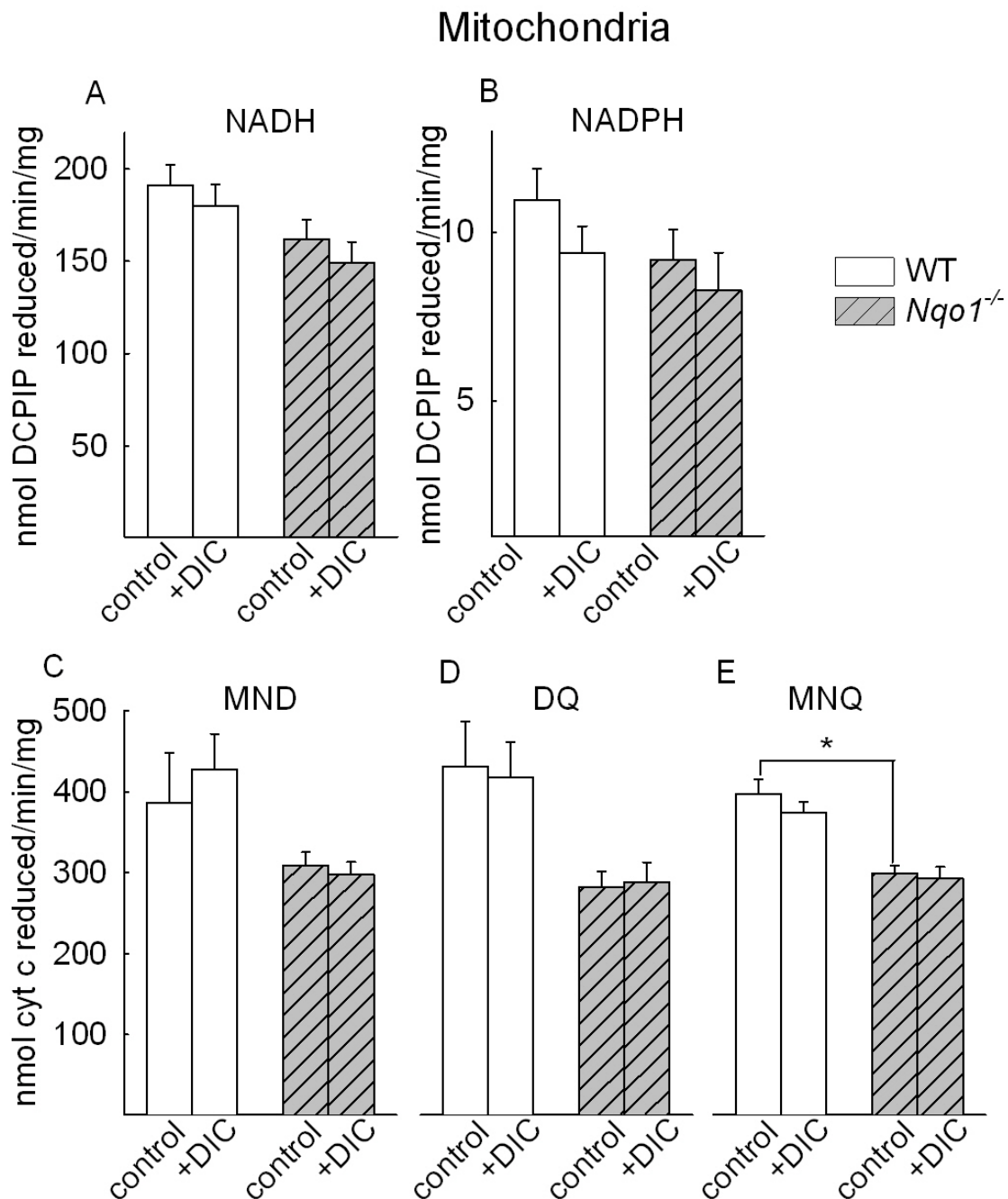


Figure 14. Determination of diaphorase activity in permeabilized mitochondria from the livers of WT and *Nqo1*^{-/-} mice. White bars signify data from WT mice, grey-hatched bars from *Nqo1*^{-/-} mice. Panels A and B depict data obtained by the DCPIP reduction method using NADH or NADPH as indicated in the panels. Panels C, D and E depict data obtained by the cytochrome c reduction method using menadione (MND, 10 μ M), duroquinone (DQ, 10 μ M) or 2-methoxy-1,4-naphtoquinone (MNQ, 10 μ M) as indicated in the panels, in the presence of NADH. All samples were measured in the absence (control) or presence of 10 μ M dicoumarol (DIC).

4.2.2. Effect of quinones on NADH oxidation capacity of permeabilized liver mitochondria from WT and *Nqo1*^{-/-} mice

To examine the extent of contribution of mitochondrial *Nqo1* to mitochondrial NADH oxidation capacity, the impacts of MNQ and DQ on NADH oxidation in permeabilized mitochondria from the livers of WT and *Nqo1*^{-/-} mice was investigated. As shown in Fig. 15A and 15B, addition of either MNQ or DQ caused NADH oxidation in mitochondria from WT (white bars) and *Nqo1*^{-/-} (grey hatched bars) mice. The rates of NADH oxidation of mitochondria from *Nqo1*^{-/-} mice were, however, lower than those from WT mice, and statistical significance was reached only in the case of DQ. These results imply that mitochondrial diaphorases other than *Nqo1* can contribute to NADH oxidation supported by exogenous quinones, and DQ is largely reduced by *Nqo1*.

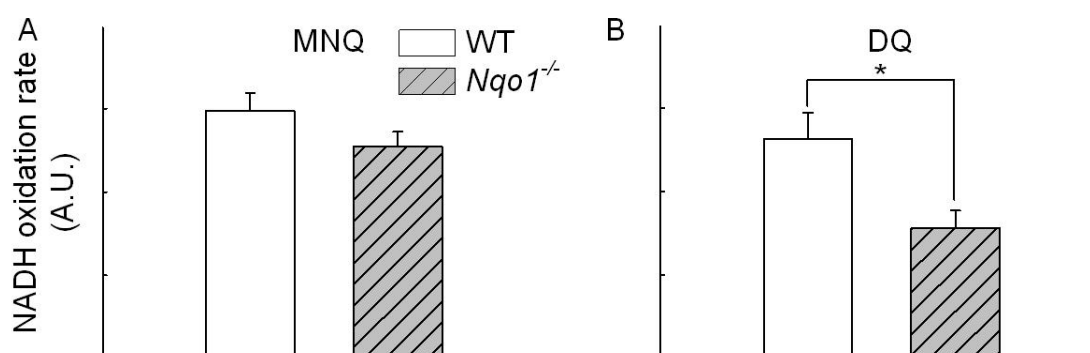


Figure 15. Effect of quinones on NADH oxidation of permeabilized liver mitochondria from WT and *Nqo1*^{-/-} mice. White bars signify data from WT mice, grey hatched bars from *Nqo1*^{-/-} mice. Mitochondria were permeabilized by alamethicin (20 μ g), and NADH-oxidation was followed in the presence of the respective quinone and 1 μ M rotenone. The concentrations of quinones used for panels A and B were: 2-methoxy-1,4-naphthoquinone (MNQ): 100 μ M; duroquinone (DQ): 0.2 mM.

4.2.3. Effect of quinones on respiratory capacity of intact mitochondria from WT and *Nqo1*^{-/-} mice

Nqo1^{-/-} mice are known to exhibit lower levels of nicotinamide nucleotides in their tissues [163; 206] which could affect the function of several NAD⁺-dependent proteins [207] and as an extension of this, the overall process of mitochondrial respiration. However, as shown in Fig. 16A and 16B, by using four different substrate combinations (glutamate and malate, glutamate and malate and β -hydroxybutyrate, α -

ketoglutarate and malate, α -ketoglutarate) all being NADH-linked substrates, no differences in either state 2 or state 3 respiration was observed in intact liver mitochondria from WT vs $Nqo1^{-/-}$ mice.

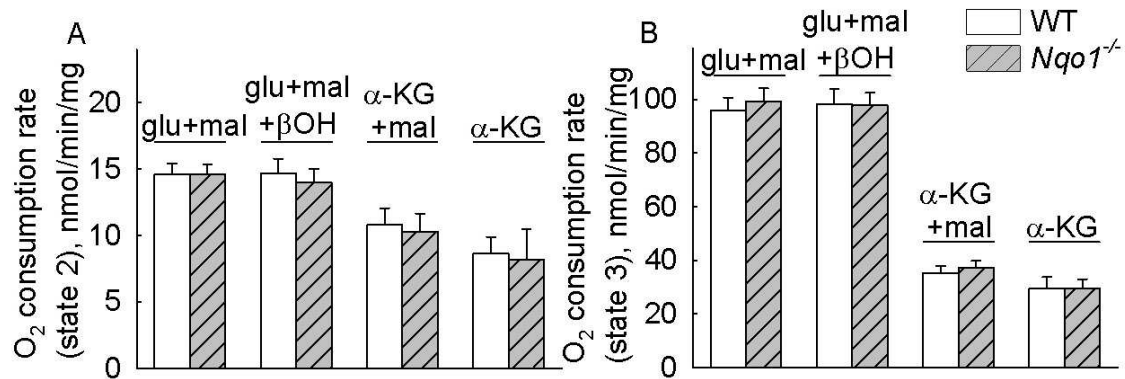


Figure 16. Respiratory capacity of intact WT and $Nqo1^{-/-}$ mouse liver mitochondria supplied with different substrate combinations. White bars signify data from WT mice, grey hatched bars from $Nqo1^{-/-}$ mice. State 2 respiration is depicted in panel A and state 3 in panel B. The concentrations of substrates were as follows: glutamate (glu): 5 mM; malate (mal): 5 mM; β -hydroxybutyrate (β -OH): 2 mM, α -ketoglutarate (α -Kg): 5 mM.

To examine the extent of contribution of mitochondrial $Nqo1$ to mitochondrial respiration as a function of exogenous quinones, the impact of various quinones on oxygen consumption rates was investigated (in the presence of glutamate and malate and β -hydroxybutyrate). As shown in Fig. 17A and 17B, some quinones led to a statistically significant increase vs decrease in state 2 and state 3 respiration, respectively, consistent with previous reports that some exhibit mitochondrial toxicities on recognized targets other than $Nqo1$ [208; 209]. What is also apparent from Fig. 16 and 17 is that the RCR of ~ 8.5 (for glutamate and malate and β -hydroxybutyrate) for liver mitochondria obtained from both WT and $Nqo1^{-/-}$ mice affords the assurance that the lack of statistically significant difference in RCR between them is not due to poor mitochondrial quality that could potentially obliterate any variances.

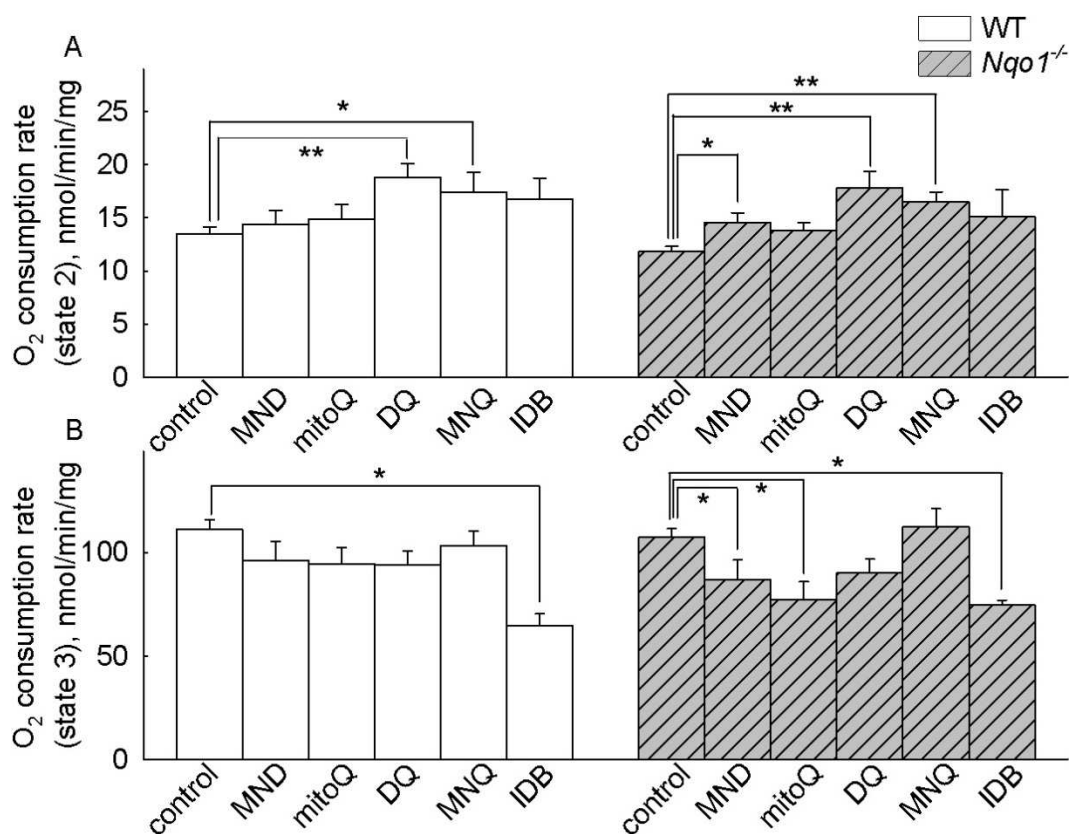


Figure 17. Respiratory capacity of intact liver mitochondria from WT and *Nqo1*^{-/-} mice in the presence of exogenous quinones. White bars signify data from WT mice, grey hatched bars from *Nqo1*^{-/-} mice. The effect of quinones on state 2 (panel A) and state 3 (panel B) was tested in mitochondria respiring on glutamate (5 mM), malate (5 mM) and β -hydroxybutyrate (2 mM). The concentrations of quinones used were: menadione (MND): 10 μ M; mitoquinone (mitoQ): 0.5 μ M; duroquinone (DQ): 0.1 mM; 2-methoxy-1,4-napthoquinone (MNQ): 10 μ M; idebenone (IDB): 10 μ M.

4.2.4. Effect of targeted ETC inhibition on quinone-assisted respiration in intact mitochondria of WT and *Nqo1*^{-/-} mice

When complex I is fully inhibited, respiration supported by quinones implies that they were reduced to the corresponding hydroquinone derivative which was later used by complexes III and IV. Quinone reduction may occur by complex II, *Nqo1* or other mitochondrial diaphorases. To interrogate the molecular entity reducing the quinones, we performed the following experiments: as shown in Fig. 18A, oxygen consumption rate of intact mitochondria was recorded, while ADP, rotenone, a quinone and inhibitors were sequentially added. Substrates (glutamate and malate) were already present in the medium. Dotted lines indicate oxygen concentration in the medium, and solid lines indicate oxygen consumption rate (flux) calculated as detailed in section 3.4. Black line

is a representative trace using liver mitochondria from WT mice, while red line represents a trace obtained by using *Nqo1*^{-/-} mice. Briefly, state 2 respiration was recorded for 50 sec and then ADP (2 mM) was added leading to >8-fold increase in respiration rates. Subsequently, respiration was halted by the addition of rotenone (1 μ M); the complete cessation of respiration is expected since, glutamate and malate are NADH-linked substrates, thus relying on NADH oxidation by complex I. Subsequently, a quinone was added (in panel A MNQ was added) which led to a small, but statistically significant increase in respiration. Then, the complex II inhibitor atpenin A5 was added that abolished this increase in respiration. Subsequently, the complex III and IV inhibitors stigmatellin and KCN (CN), respectively, were added that led to no further decrease in respiration. The 'dip' in respiration rate upon addition of stigmatellin is artifactual, and it is due to brief introduction of oxygen in the air-tight chamber upon addition of the inhibitor through the syringe. Results from using menadione, mitoQ, duroquinone, MNQ (10 μ M), idebenone and MNQ (50 μ M) are shown in Fig. 18B, 18C, 18D, 18E, 18F, and 18G, respectively. Those obtained from WT mice are depicted in white bars, and those from *Nqo1*^{-/-} mice in grey hatched bars. As shown in Fig. 18B-G, addition of any quinone led to a statistically significant increase in respiration which was subsequently abolished by atpenin A5. The increase in respiration by MNQ in rotenone-treated mitochondria was also sensitive to inhibition by malonate, a competitive inhibitor of complex II, shown in Fig. 18I. To examine the contribution of dicoumarol-sensitive diaphorases in producing quinols for complex III supporting respiration, the effect of dicoumarol prior to addition of MNQ was tested. As shown in Fig. panel 18H, addition of dicoumarol after rotenone led to a protracted increase in respiration upon further addition of MNQ (comparing Fig. 18H with 18E and 18I), albeit a statistically significant increase was recorded. Due to very low values of respiration after the addition of rotenone, statistical analysis comparing three groups (MNQ, MNQ+DIC, and MNQ+atpn) would require a very large number of experiments in order to reveal a statistical significance, and that was not performed. What is also apparent from all panels shown in Fig. 18 is that the absence of *Nqo1* does not impact on mitochondrial respiration supported by quinones in the presence of rotenone, and this was largely due to reduction of the quinones by complex II forming quinols, in turn supporting complexes III and IV.

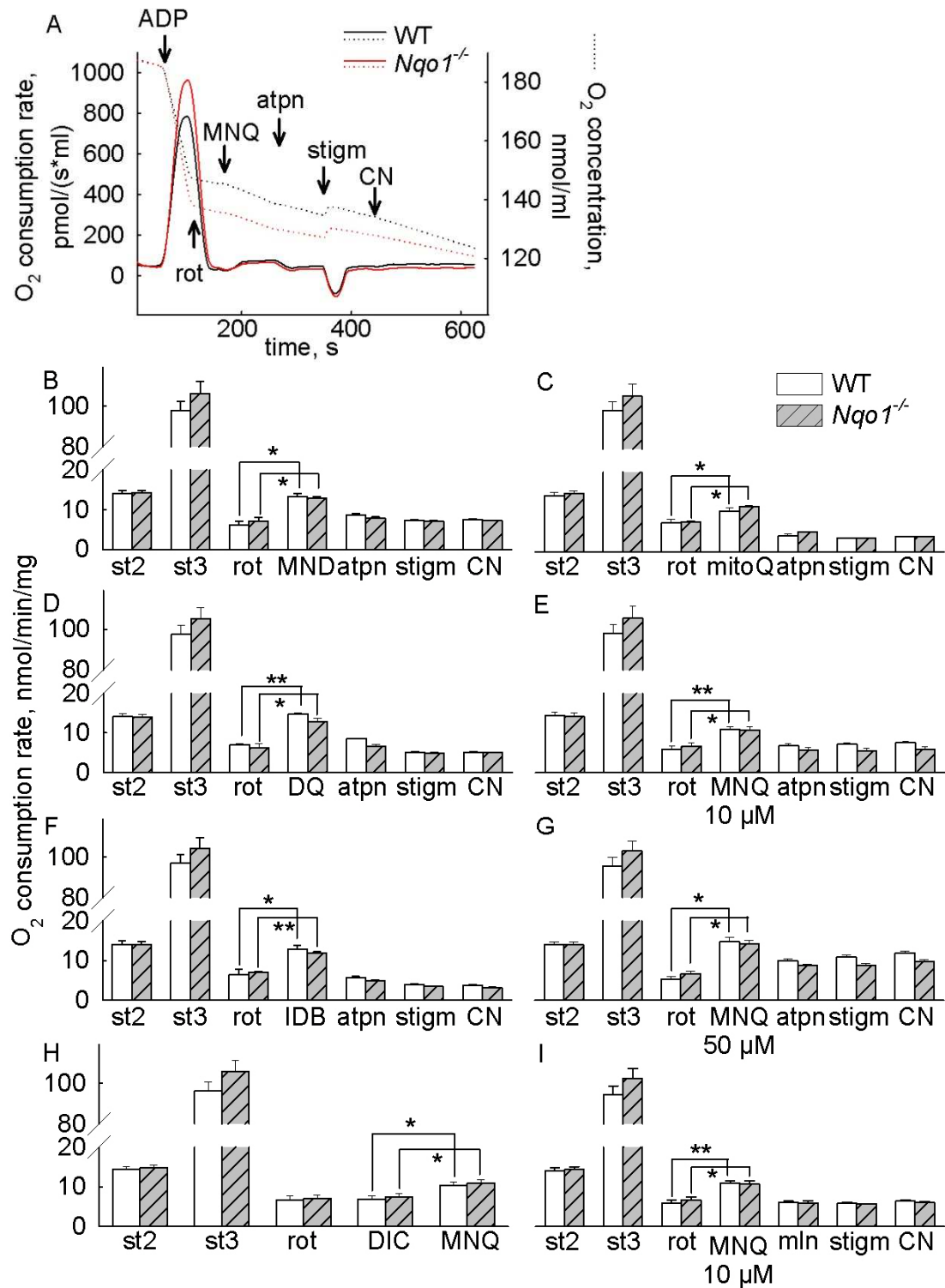


Figure 18. Effect of targeted ETC inhibition on quinone-assisted respiration in intact mitochondria of WT and $Nqo1^{-/-}$ mice. White bars or a black trace signify data from WT mice, grey hatched bars or a red trace from $Nqo1^{-/-}$ mice. Panel A depicts a typical experiment recording oxygen concentration (dotted lines) and calculation of oxygen consumption rate (solid lines). Panels B-G represent cumulated data of experiments performed as shown in panel A. Mitochondrial respiration was supported

by 5 mM glutamate and 5 mM malate. The concentrations of quinones and inhibitors used were: menadione (MND): 10 μ M; mitoquinone (mitoQ): 0.5 μ M; duroquinone (DQ): 50 μ M; 2-methoxy-1,4-napthoquinone (MNQ): 10 or 50 μ M as indicated in the panels; idebenone (IDB): 10 μ M; rotenone (rot): 1 μ M; atpenin A5 (atpn): 1 μ M; stigmatellin (stigm): 1 μ M; KCN (CN): 1 mM; dicoumarol (DIC): 5 μ M; malonate (mln): 5 mM.

4.2.5. The contribution of mitochondrial Nqo1 to quinone-induced gain in $\Delta\Psi_m$ in rotenone-treated mitochondria

To address the extent of contribution of quinones generating $\Delta\Psi_m$ and how much of this is due to Nqo1, we performed the following experiments: as shown in Fig. 19, membrane potential of liver mitochondria from WT (black traces) vs Nqo1^{-/-} (red traces) mice was measured by calibrating safranin O fluorescence signals as described in section 3.3, and the effect of sequential additions of the following compounds was recorded: mitochondria were allowed to fully polarize by using glutamate and malate (present in the medium prior to the addition of mitochondria); then, 2 mM ADP was added that led to a depolarization on the order of 25-30 mV.

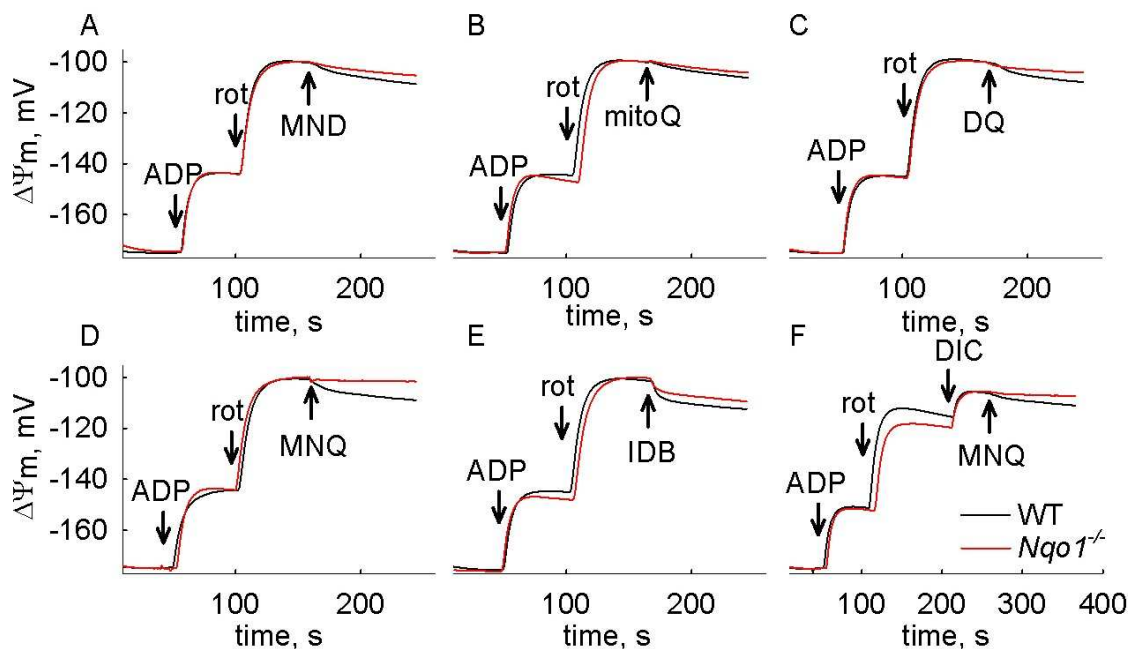


Figure 19. The contribution of mitochondrial Nqo1 on quinone-induced gain in $\Delta\Psi_m$ in rotenone-treated mitochondria. Reconstructed time courses of safranin O signal calibrated to $\Delta\Psi_m$ in isolated liver mitochondria of WT (black traces) vs Nqo1^{-/-} (red traces) mice respiring on 5 mM glutamate and 5 mM malate. ADP (2 mM) and rotenone (rot, 1 μ M) were added where indicated. Quinones were added after rotenone where indicated. The concentrations of quinones used were: menadione (MND): 10 μ M; mitoquinone (mitoQ): 0.5 μ M; duroquinone (DQ): 50 μ M; 2-methoxy-1,4-napthoquinone (MNQ): 10 μ M; idebenone (IDB): 10 μ M; dicoumarol (DIC): 5 μ M.

Subsequently, rotenone was added to inhibit complex I activity which led to a further depolarization, ‘clamping’ $\Delta\Psi_m$ around -100 mV. The subsequent addition of a quinone the identity of which is written in the panels of Fig. 19 led to a small gain in $\Delta\Psi_m$ in mitochondria from WT but not $Nqo1^{-/-}$ mice, except if the quinone was idebenone (Fig. 19E). In Fig. 19F, the effect of dicoumarol is shown, which dampens the effect of MNQ on inducing $\Delta\Psi_m$ gain (compare black traces in Fig. 19D with 19F).

4.2.6. Substrate-level phosphorylation supported by non-Nqo1 dicoumarol-sensitive mitochondrial diaphorases using endogenous quinones

In order to address the extent of contribution of mitochondrial Nqo1 providing NAD^+ to KGDHC yielding succinyl-CoA in turn supporting mitochondrial SLP, we compared the adenine nucleotide translocase directionalities of rotenone- and anoxia-treated mitochondria from WT vs $Nqo1^{-/-}$ mice, using the previously described biosensor test. Mitochondria were energized by four different substrate combinations, which support SLP to varying extents. As shown in Fig. 20A (for rotenone-treatment) and 20B (anoxia), inhibition of the ANT by carboxyatractyloside led to nearly identical changes in $\Delta\Psi_m$ between WT and $Nqo1^{-/-}$ in all cases, implying that mitochondrial Nqo1 is not critical for NAD^+ provision when mitochondria utilize endogenous quinones.

The effect of dicoumarol or other diaphorase inhibitors (chrysin, dihydroxyflavone, phenindione) deteriorating mitochondrial SLP in WT mitochondria was investigated in [45]. However, their presence abolished mitochondrial SLP even in mitochondria obtained from $Nqo1^{-/-}$ mice (green traces in Fig. 20C), implying that the inhibition of some other diaphorase is responsible for this. Exactly as described for WT in [45], diaphorase inhibitors worsened the cATR-induced changes in $\Delta\Psi_m$ in anoxic mitochondria obtained from $Nqo1^{-/-}$ mice (Fig. 20D). Similar to the effect of diaphorase inhibitors on WT mitochondria, these compounds also moderately inhibited state 3 but not state 2 respiration (Fig. 20E), in mitochondria lacking Nqo1 expression.

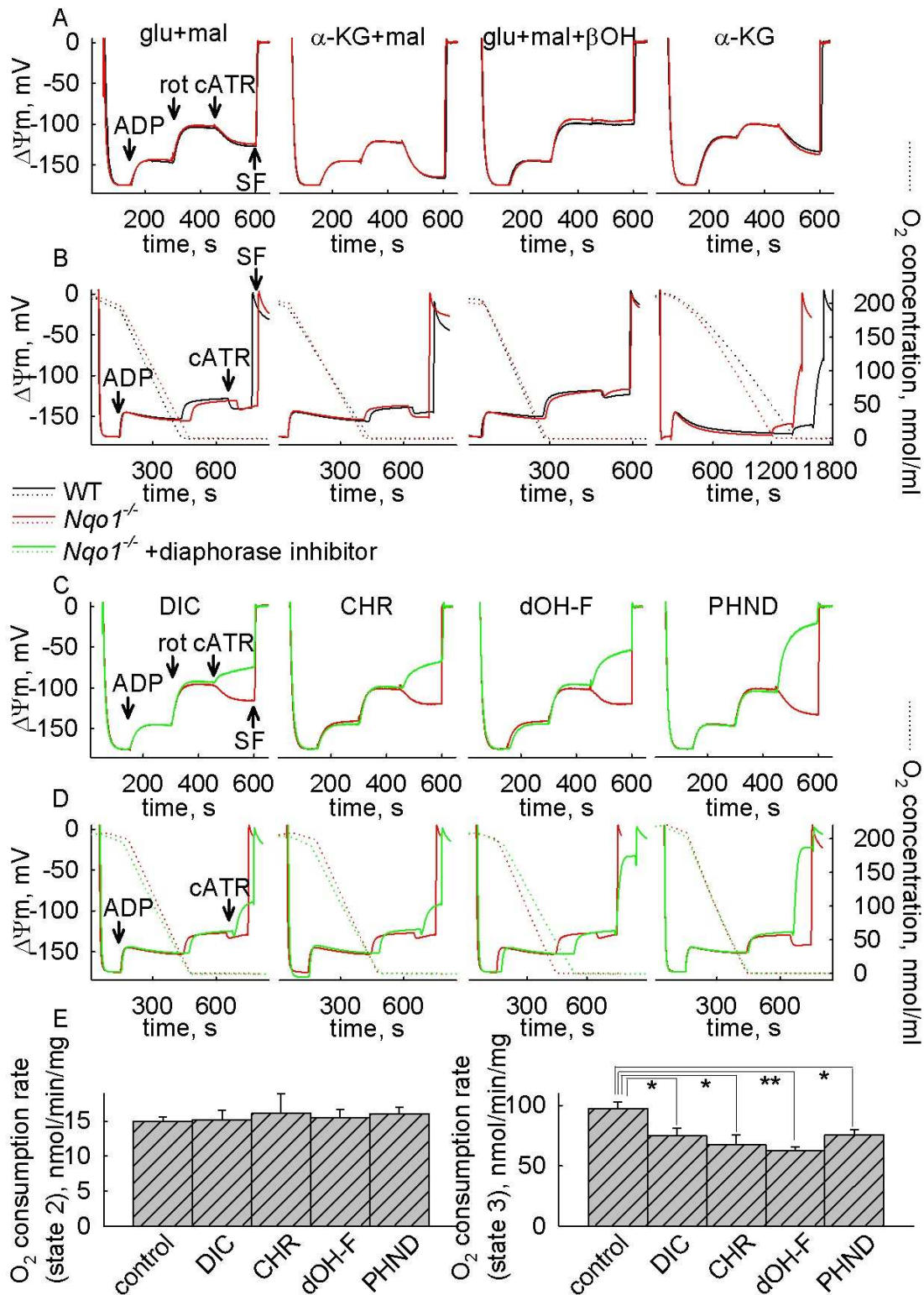


Figure 20. SLP supported by non-Nqo1 mitochondrial diaphorases using endogenous quinones and their sensitivity to diaphorase inhibitors. Panel A shows reconstructed time courses of safranin O signal calibrated to $\Delta\Psi_m$ in isolated liver mitochondria of WT (black traces) vs $Nqo1^{-/-}$ (red traces) mice treated with rotenone. ADP (2 mM) rotenone (rot, 1 μ M) and carboxyatractyloside (cATR, 1 μ M) were added

where indicated on the left-most subpanel, and the same additions were made in all subsequent subpanels. Respiration substrates used are shown in the subpanels. Their concentrations were: glutamate (glu): 5 mM; malate (mal): 5 mM; β -hydroxybutyrate (β OH): 2 mM, α -ketoglutarate (α -Kg): 5 mM. Panel B shows reconstructed time courses of safranin O signal calibrated to $\Delta\Psi_m$ (solid traces) and parallel measurements of oxygen concentration in the medium (dotted traces) in isolated liver mitochondria of WT (black traces) vs $Nqo1^{-/-}$ (red traces) mice, and the effect of anoxia. Substrates were as in corresponding subpanels in panel A. Panels C and D depict the effect of diaphorase inhibitors in reconstructed time courses of safranin O signal calibrated to $\Delta\Psi_m$ (solid traces) in isolated liver mitochondria of $Nqo1^{-/-}$ mice treated with rotenone or during anoxia. In red traces, inhibitors were absent. In green traces, diaphorase inhibitors were present as indicated in the panels, in the following concentrations: Dicoumarol (DIC): 5 μ M; chrysin (CHR): 5 μ M; dihydroxyflavone (dOH-F): 20 μ M; phenindione (PHND): 10 μ M. In panel D and all subpanels parallel measurements of oxygen concentration in the medium (dotted traces) are also shown. At the end of each experiment 1 μ M SF 6847 was added to achieve complete depolarization. In panel E, the effect of diaphorase inhibitors as indicated in the panel (concentrations used as for panels C and D) on state 2 and state 3 respiration of liver mitochondria obtained from $Nqo1^{-/-}$ mice is shown.

4.2.7. MNQ supports mitochondrial SLP preferably through Nqo1

The most important question of the present study was if mitochondrial $Nqo1$ is responsible for provision of NAD^+ to KGDHC yielding succinyl-CoA ultimately supporting mitochondrial SLP as a function of exogenous quinones. To address this, we performed similar experiments as shown for the previous chapter, but mitochondrial substrates were glutamate and malate and β -hydroxybutyrate, a substrate combination in which by titrating β -hydroxybutyrate the mitochondrial $NADH/NAD^+$ ratio can be manipulated: β -hydroxybutyrate is converted to acetoacetate by β -hydroxybutyrate dehydrogenase with the concomitant reduction of NAD^+ , thus less oxidized NAD^+ will be available for KGDHC. As such, it is possible to achieve that by adding cATR after rotenone, no changes in $\Delta\Psi_m$ can be observed because the value of this parameter is nearly identical to that of the reversal potential of the ANT [21; 23]. This strategy was applied in liver mitochondria from WT and $Nqo1^{-/-}$ mice. As shown in Fig. 21A-E, the addition of DQ, IDB and MNQ restored cATR-induced repolarization in the WT samples. From these quinones, only MNQ did not show a rescue of mitochondrial SLP in $Nqo1^{-/-}$ mitochondria (panel 21D, green and black trace). This means, that NAD^+ provision by $Nqo1$ using MNQ as substrate, is preferably used for KGDHC reaction forming succinyl-CoA, in turn supporting mitochondrial SLP.

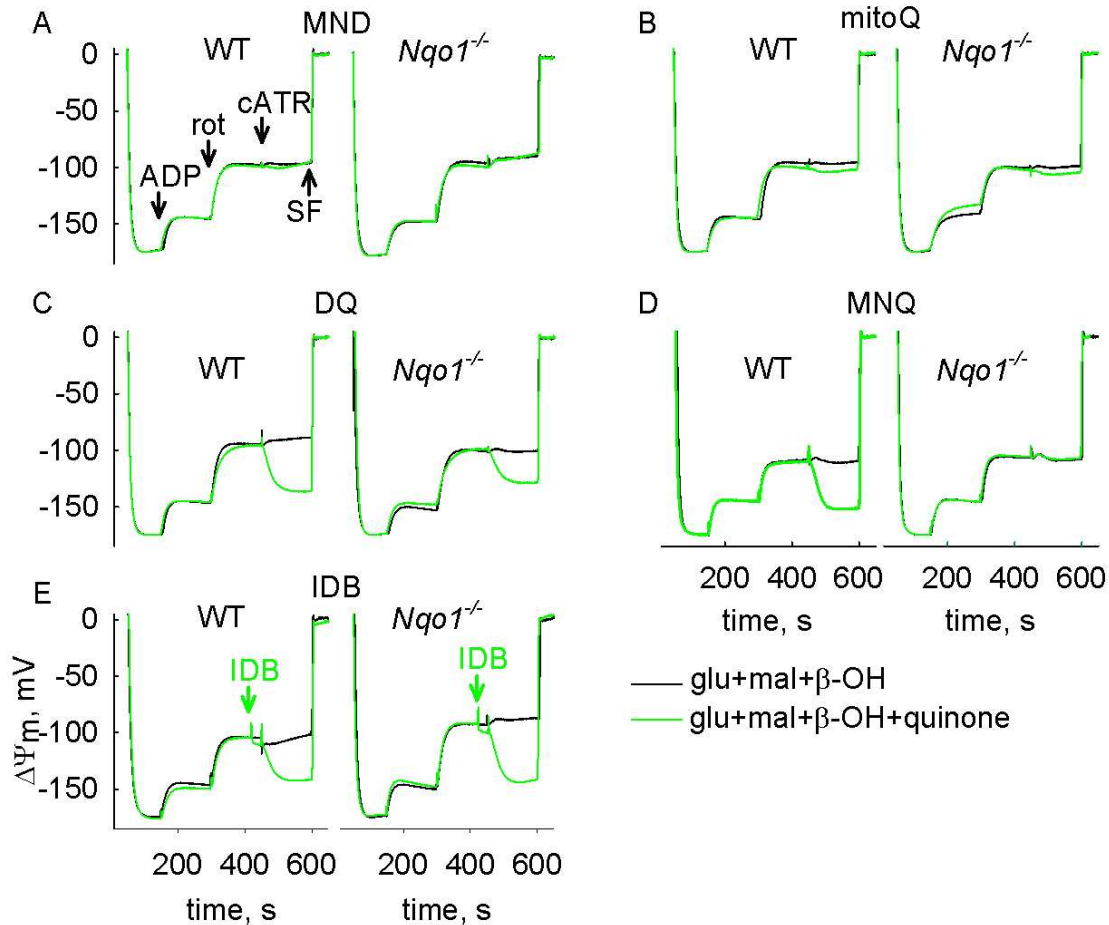


Figure 21. Effect of diaphorase substrates on mitochondrial SLP of liver mitochondria from WT and $Nqo1^{-/-}$ mice, in the presence of rotenone. Panels A-E depict reconstructed time courses of safranin O signal calibrated to $\Delta\Psi_m$ in isolated liver mitochondria of WT vs $Nqo1^{-/-}$ mice as indicated in the panels. ADP (2 mM) rotenone (rot, 1 μ M), carboxyatractyloside (cATR, 1 μ M) and idebenone (IDB, 10 μ M) were added where indicated. Quinones (green traces) were used at the following concentrations: menadione (MND): 10 μ M; mitoquinone (mitoQ): 0.5 μ M; duroquinone (DQ): 50 μ M; 2-methoxy-1,4-naphthoquinone (MNQ): 10 μ M; idebenone (IDB): 10 μ M. Mitochondrial substrates were common for all experiments shown in the panels and were glutamate (glu, 5 mM) and malate (mal, 5 mM) and β -hydroxybutyrate (β OH, 2 mM). At the end of each experiment 1 μ M SF 6847 was added to achieve complete depolarization.

Finally, just like for other diaphorase substrates, the effect of MNQ supporting mitochondrial SLP in WT mitochondria with an inhibited complex I by rotenone was sensitive to inhibition by several compounds tested, shown in Fig. 22A. To avoid trace clutter, in Fig. 22A the black, red, and green traces are identical for all subpanels. Dicoumarol abolished SLP in the presence of MNQ or DQ in $Nqo1^{-/-}$ mitochondria as well (Fig. 22B).

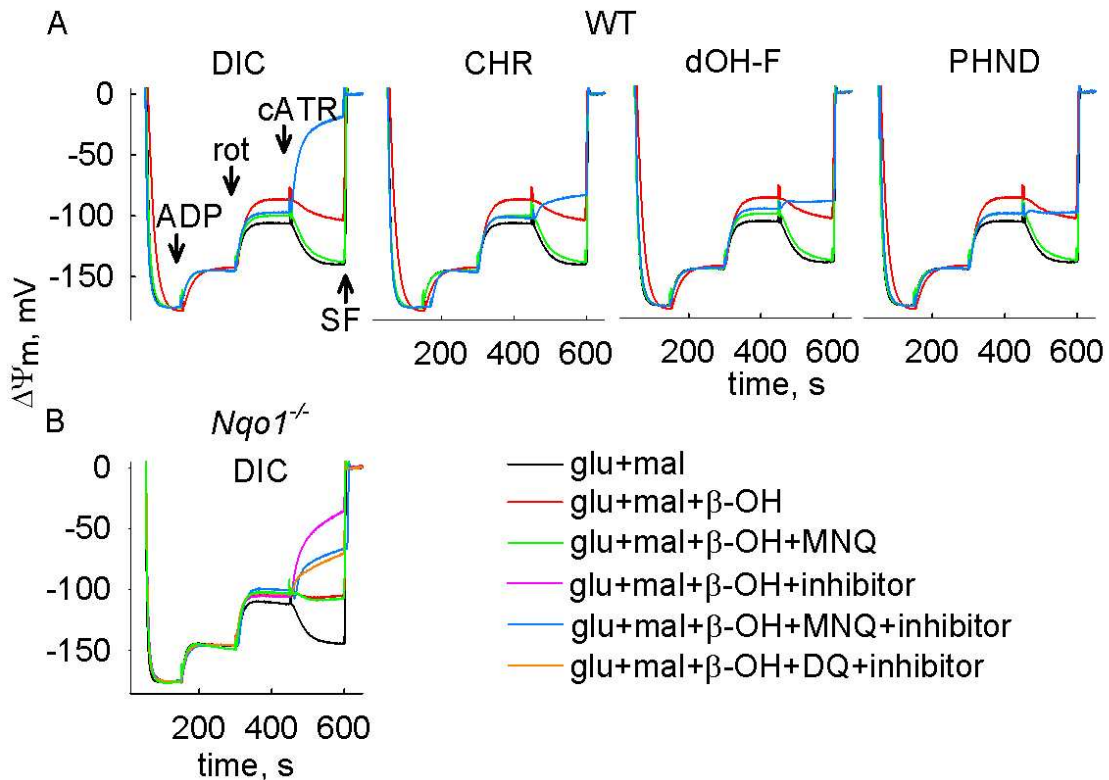


Figure 22. Effect of diaphorase inhibitors on mitochondrial SLP of liver mitochondria from WT and $Nqo1^{-/-}$ mice. Panels A and B depict reconstructed time courses of safranin O signal calibrated to $\Delta\Psi_m$ in isolated liver mitochondria of WT vs $Nqo1^{-/-}$ mice as indicated in the panels. ADP (2 mM) rotenone (rot, 1 μ M) and carboxyatractyloside (cATR, 1 μ M) were added where indicated. Mitochondrial substrates were glutamate (glu, 5 mM) and malate (mal, 5 mM) or glutamate and malate and β -hydroxybutyrate (β -OH, 2 mM), as indicated in the legends. Inhibitors used are indicated in the panels, used in the following concentrations: dicoumarol (DIC): 5 μ M; chrysin (CHR): 5 μ M; dihydroxyflavone (dOH-F): 20 μ M; phenindione (PHND): 10 μ M. When MNQ or DQ were additionally present, their concentrations were 10 μ M. At the end of each experiment 1 μ M SF 6847 was added to achieve complete depolarization.

In a manner similar to that shown in [45], quinones did not rescue mitochondrial SLP when respiratory chain inhibition was achieved by anoxia instead of rotenone, except for DQ (Fig. 23A-E). The presence of DQ restored cATR-induced repolarization in anoxic mitochondria, and there was no difference in this effect between the WT and $Nqo1^{-/-}$ samples (panel 23C).

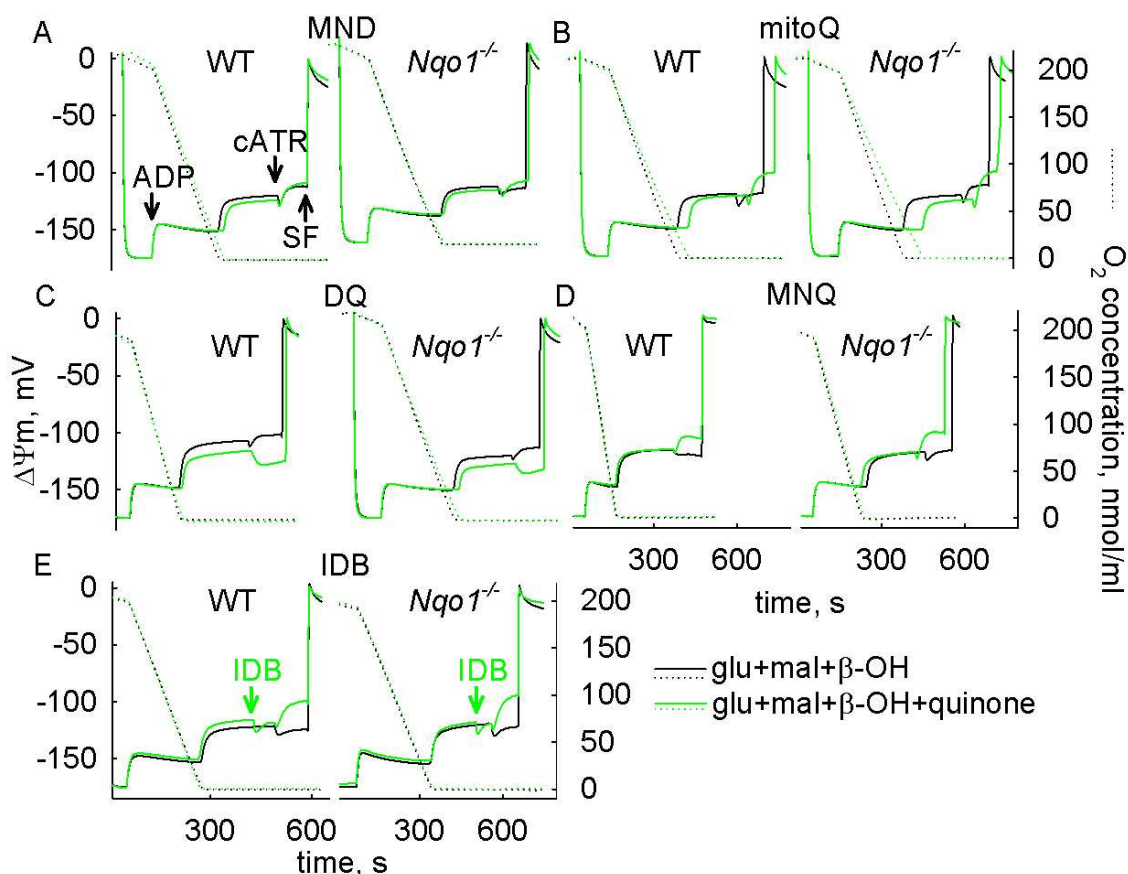


Figure 23. The effect of quinones on mitochondrial SLP of liver mitochondria from WT and *Nqo1*^{-/-} mice, in anoxia. Panels A-E depict reconstructed time courses of safranin O signal calibrated to $\Delta\Psi_m$ (solid lines) and parallel measurements of oxygen concentration in the medium (dotted lines) in isolated liver mitochondria of WT vs *Nqo1*^{-/-} mice as indicated in the panels, and the effect of anoxia. Mitochondrial substrates were common for all experiments shown in the panels and were glutamate (glu, 5 mM) and malate (mal, 5 mM) and β -hydroxybutyrate (β -OH, 2 mM). ADP (2 mM) and carboxyatractyloside (cATR, 1 μ M) were added where indicated. Quinones (green traces) were used at the following concentrations: menadione (MND): 10 μ M; mitoquinone (mitoQ): 0.5 μ M; duroquinone (DQ): 100 μ M; 2-methoxy-1,4-naphthoquinone (MNQ): 10 μ M; idebenone (IDB): 10 μ M. At the end of each experiment 1 μ M SF 6847 was added to achieve complete depolarization.

4.2.8. Investigating the contribution of diaphorases including NQO1 to mitochondrial SLP in HepG2 cells

To examine the extent of contribution of diaphorases including NQO1 to mitochondrial SLP when mitochondria are in their natural environment, we used HepG2 cells. This cell line is known to express NQO1 at high levels [210]. As shown in Fig. 24A, cells were permeabilized as described in [26] and mitochondrial SLP was evaluated by recording safranin O fluorescence signals as described in section 3.8

implying $\Delta\Psi_m$ (converted to percentage) and observing ANT directionality as a function of MNQ. Mitochondria were allowed to polarize by glutamate and malate and α -ketoglutarate (all at 5 mM); subsequently, ADP was added, leading to a physiological depolarization. Then, respiration was halted by rotenone leading to a further loss of $\Delta\Psi_m$. Subsequent inhibition of the ANT by carboxyatractyloside led to unappreciable changes in safranin fluorescence, implying that HepG2 cells in permeabilized mode have lost some endogenous quinone (panel 24A, black circles), and $\Delta\Psi_m$ is near the reversal potential of the translocase. By repeating the experiment but including MNQ (10 μ M) in the media, in situ HepG2 mitochondria exhibited a robust cATR-induced repolarization (panel 24A, green triangles), implying a strong mitochondrial SLP. By replacing cATR with oligomycin (olgm, 10 μ M, panel 24A, red squares), a depolarization was evoked, confirming that the F_o - F_1 ATP synthase operated in reverse as a result of inhibition of complex I by rotenone. The effect of MNQ boosting mitochondrial SLP in HepG2 cells through diaphorases was further supported by the finding that it was sensitive to inhibition by dicoumarol. As shown in Fig. 24B, the presence of 5 μ M dicoumarol (orange circles) or even 0.5 μ M dicoumarol (red squares) abolished the effect of MNQ on boosting mitochondrial SLP, i.e. cATR led to small repolarization or depolarization. The exact same effects were observed by replacing MNQ with duroquinone (50 μ M, panel 24C) or idebenone (10 μ M, panel 24D). Thus, from the experiments shown in Fig. 24A-D we concluded that quinones support mitochondrial SLP in a dicoumarol-sensitive manner, in permeabilized HepG2 cells.

To address the extent of contribution of diaphorase activity attributed to NQO1, we transfected HepG2 cells with siRNA (or scramble RNA, SCR) directed against NQO1. As shown in the scanned western blots in Fig. 24E, by transfecting cells with siRNA against NQO1 we were able to diminish NQO1 expression to a small extent. It is thus not surprising that by reducing NQO1 expression of this magnitude, an impact on mitochondrial SLP supported by MNQ (Fig. 24F) cannot be observed, not even when β -OH is present (4 mM) expected to increase matrix NADH/NAD⁺ ratio (Fig. 24G), potentially weakening the ability of KGDHC to produce succinyl-CoA for succinate-CoA ligase. A similar phenomenon has been observed by the group of Gueven [210] where HepG2 cells transduced with lentivirus encoding NQO1-specific shRNA showed only a moderate reduction in rescuing ATP levels during rotenone treatment.

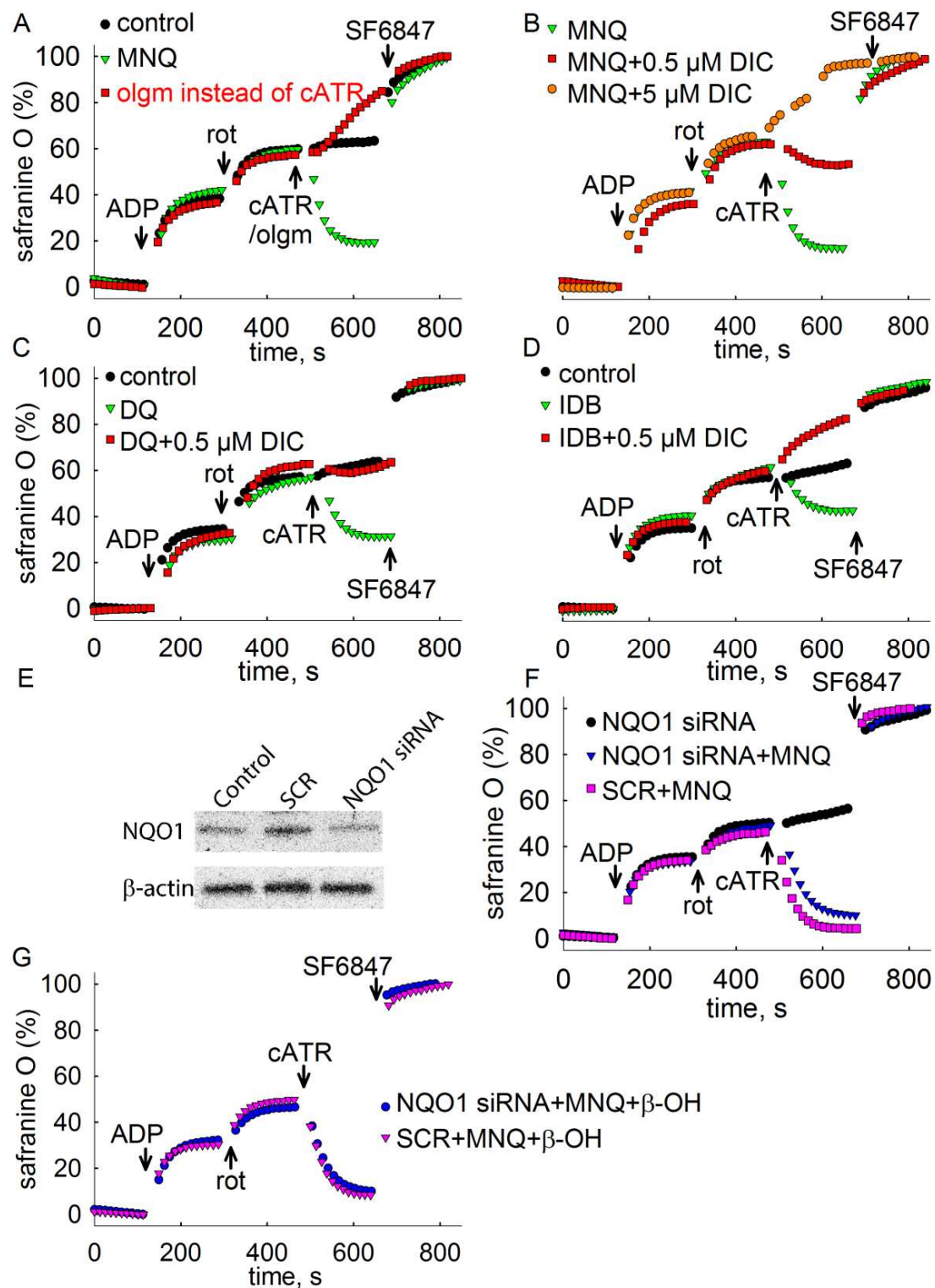


Figure 24. Effect of diaphorase substrates or inhibitors or siRNA directed against NQO1 on mitochondrial SLP in permeabilized HepG2 cells. All panels (except panel E) depict reconstructed time courses of safranin O signal expressed in percentage. ADP (2 mM) rotenone (rot, 5 μM) and carboxyatractylsido (cATR, 1 μM) or oligomycin (olgm, 10 μM) were added where indicated. Mitochondrial substrates were common for all experiments shown in the panels and were glutamate (5 mM) and

malate (5 mM) and α -ketoglutarate (5 mM). β -hydroxybutyrate (β OH, 4 mM) was additionally present in the experiments shown in panel G. Dicoumarol (DIC) was present at 5 or 0.5 μ M concentration, as indicated in the panels. MNQ, DQ and IDB were at 10, 50 and 10 μ M, respectively, present where indicated. Cells transfection with NQO1 siRNA or scramble (SCR) is described in section 3.9. At the end of each experiment 0.5 μ M SF 6847 was added to achieve complete depolarization. In panel E, scanned images of Western blots of anti-NQO1 and β -actin for control, NQO1 siRNA and scramble (SCR)-transfected HepG2 cells is shown.

5. DISCUSSION

In the present work, potential inhibitory and supporting pathways of mitochondrial SLP were investigated.

First, the metabolism of exogenously added GABA, SSA and GHB and their impact on the succinate-CoA ligase catalyzed reaction was addressed in isolated brain and liver mitochondria. Apart from the main observation of these experiments, i.e. that molecules catabolized through the GABA shunt ultimately impair SLP, it is important to dwell on ramifications of these pathways.

The results of the experiments investigating the effect of GABA on $\Delta\Psi_m$ are in agreement with previous studies [88; 97; 194], showing that GABA supports mitochondrial respiration, and its oxidation is sensitive to GABA-T inhibition. An additional observation of this study is the large quantitative difference of GABA-induced polarization between brain and liver mitochondria, indicating a higher metabolizing capacity of the liver. SSA conferred a full $\Delta\Psi_m$ in both types of tissues, whereas GHB was catabolized in the liver only, resulting in moderate mitochondrial polarization.

Based on the observation that SSA was able to build up the maximum $\Delta\Psi_m$, it is unlikely that the variance of GABA consumption in liver and brain mitochondria is due to a differential SSADH activity. We presume that it is due to either a differential expression of the GABA transport mechanism (which is yet to be identified), and/or a difference in GABA-T expression among the two tissues. The observation of Brand and Chapell [88], namely that GABA-T activity is manifold higher in rat brain than in rat liver mitochondria, challenges the latter assumption, however, it is still possible, regarding that in the present study mice tissues were used.

From the NADH-measurements we concluded that SSADH activity in liver is approximately 5 times higher than that in brain mitochondria. This finding is at odds with those reported by Chambliss et al., showing that the liver activity for SSADH was about 2/3 of that in rat brain [211]. Again, perhaps this is due to the different choice of laboratory animal (rat in Chambliss et al., mice in this study).

Also, it makes sense to ponder on the following concept: the reaction catalyzed by SSADH is strongly favored towards succinate formation [212; 213]. However, *in organello*, conditions maybe met where SSA concentration is sufficiently low so that

succinate could get diverted towards SSA formation, oxidizing NADH in the process. This is not an implausible scenario: it is well known that in isolation, the mitochondrial malate dehydrogenase reaction strongly favors NADH oxidation towards formation of malate from oxaloacetate; yet, under physiological conditions within the mitochondrial matrix, oxaloacetate concentration is so low that the reaction is pulled towards NADH formation [214]. Thus, mindful of the possibility that SSADH reaction could operate in reverse, addition of succinate to mitochondria will lead to NADH oxidation by this enzyme. By the same token, any substrate combination that yields succinate would also follow NADH oxidation through the SSADH branch of metabolism. This notion exerts a considerable impact on a large body of work regarding succinate and NADH/NAD⁺ pools addressing the so-called ‘reverse electron transport’, RET. RET is a $\Delta\Psi_m$ - and NADH/NAD⁺ ratio-dependent phenomenon [215], in which succinate-supported mitochondria exhibit electron flow from complex II to complex I involving coenzyme Q [216]. RET is associated with reactive oxygen species formation [217], and thus, it is a putative pharmacological target for many pathological situations involving ROS. On the basis of the results presented in this study, it is at least prudent to consider that NADH oxidation by SSADH, a nearly ubiquitous enzyme, will be confounding in interpreting RET-related experiments in which mitochondria are fueled by succinate, and the NADH/NAD⁺ ratio is a critical determinant of the measured variable. Still on the same line of thought but considering the thermodynamically favored SSADH reaction flow, the consequences on ROS formation by succinate originating from SSA obligatorily connected to an increase in NADH/NAD⁺ ratio can be ‘dissected’ from the status of complex I using rotenone. To put this more simply, the effect(s) of succinate on ROS as a function of an increased level of NADH (by using SSA) could be addressed in the presence of inhibited complex I.

Our finding that GABA inhibits mitochondrial SLP supports the results of Rodichok and Albers [52], who examined the effect of GABA on SLP in isolated rat brain mitochondria respiring on α KG. They found that mitochondrial ATP and GTP production was decreased after 5 minutes of incubation with GABA, and the phosphorylating activity was rescued by AOAA. However, they performed the experiments in the presence of the ATP synthase inhibitor oligomycin and the K⁺ ionophore valinomycin, therefore, mitochondria were unable to produce ATP through

oxidative phosphorylation, but their respiration was still operational. In these circumstances succinate resulting from the GABA shunt could be further oxidized by complex II and was not accumulated, in contrast with our experiments performed in anoxia. Interestingly, when we tested the effect of GABA on SLP under complex I inhibition, it did not lead to reversal of the ANT (not shown). This together with the results of Rodichok and Albers allows us to conclude that in normoxia, flux through the GABA shunt decreases ATP (GTP) production rate by SLP, but as long as SDH is operational, this decrease in the intramitochondrial ATP/ADP ratio is not sufficient to make the organelles ATP consumers under conditions when F_0 - F_1 ATP synthase is in hydrolyzing mode. The authors did not establish the exact mechanism for the inhibitory effect of GABA. They found that the ATP-producing activity of SLP was completely, but the overall ATP concentration was only partially restored by the administration of AOA, which made them suggest that GABA may affect mitochondrial high energy phosphate levels in multiple ways. Our experiments showing that GABA-T inhibitors prevent GABA-induced ANT reversal but not the SSA-induced ANT reversal clearly confirm that the inhibition of SLP is due to metabolism through the GABA shunt.

The relevance of our finding that GABA impairs mitochondrial SLP extends to multiple organs because of the ubiquitous presence of the compound and its metabolizing enzymes. Furthermore, in some cells GABA metabolism is an inducible system [218-220]. Blood GABA level in mammals is in the submicromolar range [221]. The concentration of GABA in the cytosol is not known, but it is estimated that GABAergic neurons could have an intracellular transmitter concentration of at least 2 mM [222], and in the vesicles of nerve endings this may achieve a 1000-fold increase [223]. During neurotransmission the synaptically released GABA can reach transiently 1,5-3 mM concentrations, whereas the extrasynaptic transmitter concentration probably lies in the low micromolar range [223]. Therefore we suppose that the millimolar concentration used in our experiments is not far from the intracellular *in vivo* GABA levels, especially in tissues with the highest GABA concentrations, namely brain and liver. Regarding GHB, its endogenous levels are in the micromolar range, but millimolar concentrations can be achieved after exogenous intake [203]. A flux through the GABA shunt can make cells less capable of maintaining ATP-dependent processes

in anoxia, which may be an additional mechanism contributing to the extreme vulnerability of GABAergic neurons subjected to hypoxia [224-226].

The second main topic of the present thesis was to examine the contribution of Nqo1 to diaphorase activity and mitochondrial SLP, and to test a number of quinone compounds as possible SLP-supporting diaphorase substrates in WT and Nqo1^{-/-} samples. The most important observations can be summarized in the following points:

- i) from the experiments measuring diaphorase activity using DCPIP or cytochrome c as electron acceptor (chapter 4.2.1.), and measuring NADH-oxidizing activity (chapter 4.2.2.) it is obvious that in mouse liver mitochondria the diaphorase activity exerted by Nqo1 is very small compared to the overall diaphorase activity. The main portion of the NAD⁺-regenerating activity can be attributed to some other, dicoumarol-insensitive diaphorase(s). Also MNQ seems to be reduced to a large extent by enzymes other than Nqo1.
- ii) In accordance with these findings, the lack of Nqo1 does not influence mitochondrial respiration (chapter 4.2.3.) or mitochondrial SLP (chapter 4.2.6.), showing that the enzyme is not necessary for the maintenance of matrix NAD⁺-pool in respiratory-inhibited mitochondria.
- iii) Mitochondrial SLP can be inhibited by diaphorase inhibitors in Nqo1^{-/-} samples (chapter 4.2.6.), which suggests that other diaphorases participate in NADH oxidation and these are sensitive to the used inhibitory compounds.
- iv) The five examined quinone molecules can donate electrons to the respiratory chain bypassing complex I, as demonstrated by the generation of $\Delta\Psi_m$ (chapter 4.2.5., however in WT mitochondria only) and a very small but significant increase in oxygen consumption when the quinones were added after rotenone (chapter 4.2.4.). Atpenin A5 decreased this quinone-induced respiration in each case, indicating the involvement of complex II in the pathway of electrons.
- v) From the five quinone substrates, DQ, IDB and MNQ were able to promote SLP in rotenone-treated mitochondria, and from these three, MNQ was ineffective in Nqo1^{-/-} samples (chapter 4.2.7.). This leads to the conclusion

that mitochondrial SLP is supported by MNQ exclusively through the action of Nqo1.

- vi) In anoxia, only DQ was effective in helping SLP (chapter 4.2.7.); the other quinones rather weakened it, for yet not elucidated reasons.
- vii) MNQ, DQ and IDB supported SLP in permeabilized HEPG2 cells as well, and this effect was inhibited by dicoumarol (chapter 4.2.8.).

The results presented above can be visualized in the illustration shown in Fig. 25. As indicated, rotenone (thick red line) prevents the oxidation of NADH to NAD⁺ and the reduction of ubiquinone (Q) to ubiquinol (QH₂) by complex I, implied by dashed grey arrows. The ability of complex II, ETFDH, GPDH and DHODH reducing Q to QH₂ remain intact. Likewise, complex III can still support oxidation of QH₂ to Q. Complexes III and IV are able to pump protons outside the matrix, but the extent of their proton pumping capacity under these conditions is minimal. This is probably because the flux of electron flow in this ETC segment is weak due to a diminished provision of ubiquinol to complex III as mitochondrial diaphorase activity is too small to produce adequate amounts of QH₂. This interpretation is supported by the findings that addition of quinones to rotenone-treated mitochondria led to a very small gain in respiration rates (Fig. 18) and $\Delta\Psi_m$ (Fig. 19). Provision of ubiquinol (QH₂) to complex III may occur by complex II and/or ETFDH and/or DHODH and/or GPDH and/or Nqo1 and/or other mitochondrial diaphorases. It is not known if provision of more water-soluble quinols (QH₂') could occur through ETFDH and/or DHODH and/or GPDH. If through Nqo1, then there is concomitant oxidation of NADH to NAD⁺. If other diaphorases provided QH₂', these could either use NADH or some other electron donor (e⁻D). In any case, QH₂ and QH₂' can be re-oxidized to Q and Q' respectively, by complex III [227-230]. Alternatively, oxidation of QH₂' to Q' may be redox-coupled to Q/QH₂, implied by the double line brown arrow. The possibility of complex III reducing cytochrome c or some other cytosolic oxidant has been addressed in [45] and [231]. In either case, when a suitable Q' and a mitochondrial diaphorase are concomitantly present, regeneration of NAD⁺ can occur allowing for the KGDHC reaction to proceed yielding succinyl-CoA. In turn, succinyl-CoA and ADP (or GDP) can be converted to succinate and ATP (or GTP) by SUCL. If MNQ is Q', NAD⁺ provision for

KGDHC occurs through Nqo1. If idebenone, menadione, mitoquinone or duroquinone is Q', mostly other diaphorases can perform this catalysis that are coupled to either NADH or eD oxidation. Overall, bypassing an inhibited complex I with a suitable quinone leads to generation of high-energy phosphates in the mitochondrial matrix through mitochondrial SLP.

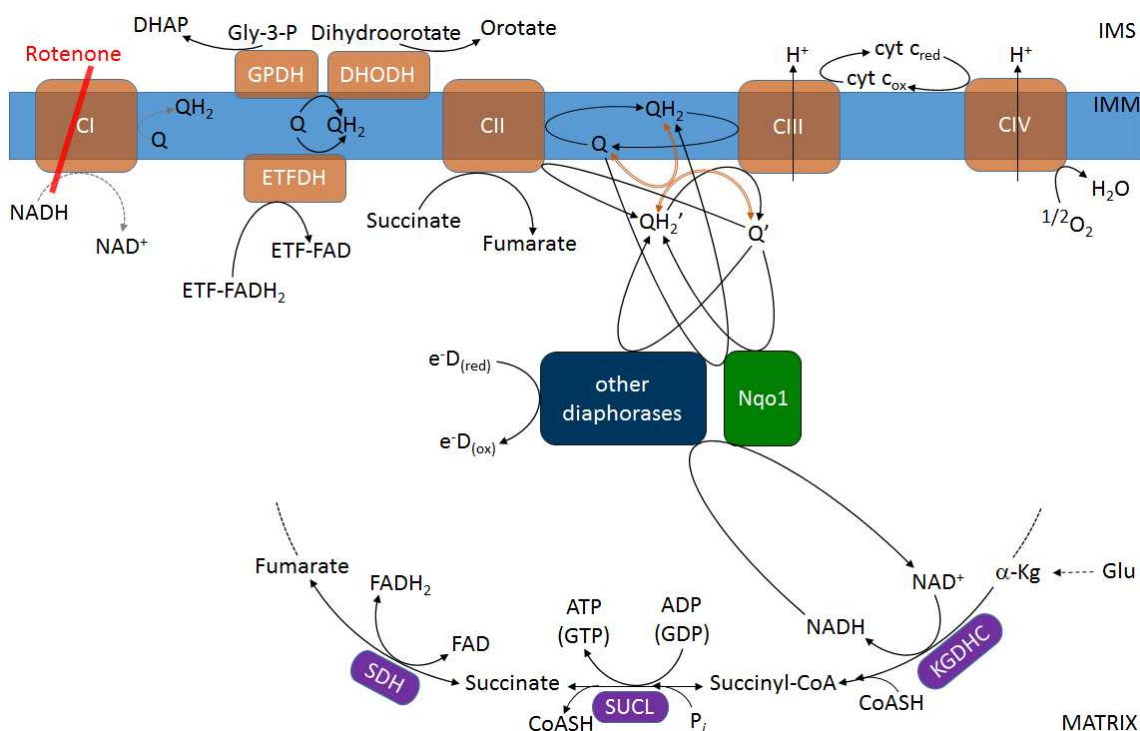


Figure 25. Illustration of the pathways linking electron transport chain components with Nqo1 and other intramitochondrial diaphorases and the segment of the citric acid cycle performing mitochondrial SLP, when complex I is inhibited by rotenone. Q and QH₂ indicate a lipophilic quinone and quinol (hydroquinone), respectively. Q' and QH₂' indicate a hydrophilic quinone and quinol (hydroquinone), respectively. eD_(red) and eD_(ox) indicate an electron donor in the reduced or oxidized state, respectively. α-Kg: α-ketoglutarate; DHAP: dihydroxyacetone phosphate; DHODH: dihydroorotate dehydrogenase; ETFDH: electron-transferring flavoprotein dehydrogenase; Gly-3-P: glycerol-3-phosphate; GPDH: glycerol-3-phosphate dehydrogenase; IMM: inner mitochondrial membrane; IMS: intermembrane space; Glu: glutamate; KGDHC: α-ketoglutarate dehydrogenase complex; SDH: succinate dehydrogenase; SUCL: succinate-CoA ligase. The FAD cofactor of GPDH has been omitted, for clarity.

Regarding MNQ, this is a naturally occurring naphthoquinone found in garden balsam, *Impatiens Balsamina* L [232] but has also been synthesized several years ago [233]. MNQ has been recently added to a list of “complex I bypass factors” as a result

of an effort to explore tool compounds for investigating tissues with an impaired complex I [184]. Complex I deficiency can be due to several mutations in structural subunits or assembly factors [29; 234] or Parkinson's disease [27], for which a number of mouse models exist [235]. "Complex I bypass" is a strategy followed for treating complex I deficiency in an attempt to rescue oxidative phosphorylation by recruiting complex I-independent pathways. Several redox-active quinones are known to possess such an activity, namely idebenone and its analogues, menadione (vitamin K3), mitoquinone and duroquinone [183; 236-239], and recently an idebenone metabolite, 6-(9-carboxynonyl)-2,3-dimethoxy-5-methyl-1,4-benzoquinone (QS10) was added to this list [240]. Among these, idebenone has been extensively researched and is approved for the treatment of Leber's Hereditary Optic Neuropathy (LHON), a genetic disorder most commonly attributed to mutations in mitochondrial DNA encoding complex I subunits [241]. Idebenone is more hydrophilic than ubiquinone [183; 242], and it is a substrate for NQO1 [243], GPDH, complexes II and III, but not complex I [209; 244]. Current consensus is that complex II, mitochondrial GPDH and cytosolic NQO1 reduce idebenone to idebenol which is subsequently oxidized by complex III [209; 243; 244]. However, this consensus ignores the possibility that idebenone - and in all likelihood - other quinones are reduced by mitochondrial NQO1 and/or other matrix diaphorases. Our results unequivocally showed that idebenone and duroquinone supported mitochondrial SLP from glutamate implying that there was NAD^+ regeneration in the matrix of intact, isolated mouse liver mitochondria; this occurred in the absence of exogenous pyridine nucleotides and a cytosolic diaphorase, and it was due to a dicoumarol-sensitive mitochondrial diaphorase activity; furthermore, MNQ was preferentially reduced by Nqo1, yielding matrix NAD^+ . Regeneration of NAD^+ in the matrix of mitochondria with an inhibited complex I allowed KGDHC reaction to occur, eventually providing high-energy phosphates through mitochondrial SLP [21; 40]. This can at least partly explain why short-chain quinones exhibit ATP rescue abilities under conditions of a defective complex I [210]. At this junction it is important to consider that the potential benefit of quinones protecting mitochondria and the cells that harbor them may not be solely due to mitochondrial SLP, but also from acting as ROS scavengers. Indeed, it has been reported that in rat liver cells, CoQ1H_2 formation from

CoQ1 by NQO1 was acting as a ROS scavenger at sufficiently high concentrations, affording cytoprotection independent from restoring ATP levels [245].

Regarding mitochondrial diaphorases responsible for NAD^+ regeneration not being Nqo1, these cannot be Nqo2 either because this isoform uses dihydronicotinamide riboside (NRH) and not NAD(P)H as an electron donor [246; 247]. They could still be responsible though for quinone oxidation driving complex III and IV activity supporting respiration and mitochondrial membrane potential. As already pointed out by Ernster and colleagues, the mitochondrial DT-diaphorase and complex III exhibit different preferences and affinities for quinones and corresponding quinols, respectively [148; 152]. Thus, it is important to consider not only which diaphorase oxidizes NADH, but also which quinone is reduced. As we have shown previously, addition of an exogenous redox-active quinone to isolated, respiration-inhibited mitochondria is not a requirement for demonstrating KGDHC-mediated provision of succinyl-CoA to succinate-CoA ligase, and the presence of a diaphorase inhibitor abolishes mitochondrial SLP [45]. This means that endogenous quinones are available and sufficient to sustain diaphorase activity. It is standard practice to include menadione or other vitamin K analogues in the chow of laboratory mice; it may well be possible that these or some other quinones that interconverted in the mouse liver mitochondria accounted for the redundancy of adding quinones exogenously. Perhaps this is why HepG2 cells did not exhibit an appreciable mitochondrial SLP, since standard cell growth media do not contain vitamin K analogues or other quinones. In rodent mitochondria only CoQ1, CoQ9 and CoQ10 have been identified [248; 249]. Nqo1 is able to reduce CoQ1, but CoQ9 and CoQ10 are very poor diaphorase substrates [168; 243; 245; 250]. Thus, CoQ1 could be a candidate quinone for matrix diaphorases. On the other hand, CoQ1 concentration is much lower than that of CoQ9 and CoQ10; it cannot be excluded that there is some other, yet to be identified quinone in mitochondria with a sufficiently high hydrophilicity rendering it a suitable substrate for matrix diaphorases. Alternatively, endogenous quinones may participate in coupled redox reactions leading to a sequential reduction from the less concentrated, hydrophilic quinone utilized by the matrix-soluble diaphorases to the more concentrated, lipophilic quinone embedded in the inner mitochondrial membrane. The possibility of a yet to be identified mitochondrial quinone and the concept of coupled redox reactions of endogenous quinones (enzymatic or non-enzymatic) are non-

mutually exclusive postulations. It is also important to emphasize that matrix diaphorases reducing quinones are responsible for oxidizing only a fraction of matrix NADH pools [45]; thus, other, non-diaphorase mediated, perhaps quinone-independent reactions are responsible for providing NAD^+ to KGDHC when complex I is inhibited. Relevant to this, the group of Mootha have recently assembled a compendium of reactions producing or consuming NAD(P)H or NA(D)H, or using them as a redox co-factor in liver cells [251]. Because several of those localize to the mitochondrial matrix, it would be interesting to explore if they contribute - and to what extent - to NAD^+ provision for KGDHC when complex I is inhibited.

Our results contribute to the understanding of the dynamic regulation of nicotinamide adenine dinucleotide metabolism in mitochondria [252]. NAD^+ -boosting strategies in particular, are rapidly becoming intense areas of research involving a wide spectrum of diseases, ranging from diabetes to cancer [253; 254]. More specifically and in the field of cancer, NQO1 has been implicated in cancer therapy [177]: inhibition of the enzyme may divert quinones towards a one-electron transfer by the cytochrome P450 system forming free radicals [255; 256] that oxidatively damage NQO1-expressing cancer cells [257]. On the other hand, NQO1 converts certain quinones to cytotoxic agents, thus, its induction could be beneficial for cancer treatment. To this list of processes, inhibition of NQO1 and other mitochondrial diaphorases as a chemotherapeutic strategy could be added because it abolishes mitochondrial SLP, a process by which cancer cells are likely to rely upon in order to harness energy during adverse conditions of the tumor microenvironment [258].

6. CONCLUSION

Our results show that GABA, SSA and GHB are metabolized through the GABA shunt, and SSA is an extremely efficient substrate energizing mitochondria in normoxia. In anoxia, the conversion of the molecules through the GABA shunt results in a build-up of succinate and impairs mitochondrial SLP. This leads to the reverse operation of the ANT associated with a consequent consumption of extramitochondrial ATP. An important exception is the lack of effect of GHB in brain, most likely due to the very low HOT expression, the enzyme responsible for GHB catabolism towards the citric acid cycle. Otherwise, the implications of the results presented in this work extend to a multitude of tissues, because the expression of enzymes participating in the GABA shunt appears to be widespread [58-60; 82], and not limited to the central nervous system. It is therefore, reasonable to assume that in those cells where GABA shunt is active, mitochondrial SLP is impaired, making these cells more vulnerable to hypoxic injuries.

The present work also confirms that mitochondrial diaphorases are important in regenerating NAD^+ for KGDHC when complex I is inhibited, thus supporting mitochondrial SLP substantiated by succinate-CoA ligase. The most important observations of our experiments investigating the role of Nqo1 in this process are: i) provision of mitochondrial NAD^+ during complex I inhibition was preferentially supported by Nqo1 diaphorase activity when MNQ was the substrate supporting mitochondrial SLP, and ii) mouse liver mitochondria harbor other than Nqo1 dicoumarol-sensitive diaphorases capable of oxidizing NADH or other electron donors, when suitable quinones are available. Our work corroborates that complex I bypass can occur by quinones reduced by intramitochondrial diaphorases oxidizing NADH, ultimately supporting mitochondrial SLP. Finally, it may help to elucidate structure-activity relationships of redox-active quinones with diaphorase enzymes, which could have relevance in the treatment of complex I deficiencies and certain cancer types.

7. SUMMARY

Mitochondrial substrate-level phosphorylation is catalyzed by succinate-CoA ligase. In the reversible reaction succinyl-CoA and ADP (or GDP) is converted to succinate, CoASH and ATP (GTP). The enzyme is capable of producing high energy phosphates independently from the oxidative phosphorylation, thus it plays a significant role in preventing mitochondria from becoming ATP-consuming organelles when their respiratory chain is inhibited. For the operation of succinate-CoA ligase an adequate succinyl-CoA provision by the α -ketoglutarate dehydrogenase complex (KGDHC) is needed. When complex I is inhibited (due to the presence of rotenone or in anoxia), NAD^+ that is required for the reaction catalyzed by KGDHC can be provided by mitochondrial diaphorases.

In the present work metabolic pathways affecting mitochondrial substrate-level phosphorylation are described. GABA is a neurotransmitter which is metabolized via the GABA shunt to succinic semialdehyde, and finally to succinate which is able to enter the citric acid cycle. γ -Hydroxybutyrate (GHB) is a neurotransmitter and a psychoactive drug which is also converted to succinate during its degradation. Our results support the hypothesis that succinate produced through the metabolism of GABA, succinic semialdehyde or GHB shifts the equilibrium of the reversible reaction catalyzed by succinate-CoA ligase towards ATP (or GTP) hydrolysis. Thus, operation of the GABA shunt inhibits mitochondrial substrate-level phosphorylation.

NAD(P)H quinone oxidoreductase 1 (NQO1) is an enzyme exhibiting diaphorase activity; it is able to provide oxidized NAD^+ for the operation of substrate-level phosphorylation when suitable quinones are available. Our experiments performed on mitochondria isolated from $\text{Nqo1}^{-/-}$ and wild type mice show that Nqo1 is dispensable for the reaction catalyzed by succinate-CoA ligase. Conversely, other, yet unidentified dicoumarol-sensitive diaphorases are necessary for the suitable NAD^+ -provision during respiratory chain inhibition. Among the quinone substrates examined in the present thesis 2-methoxy-1,4-naphthoquinone, duroquinone and idebenone support diaphorase function and consequently substrate-level phosphorylation when complex I is inhibited. From these, 2-methoxy-1,4-naphthoquinone exerts its beneficial effect as a substrate for Nqo1 .

8. ÖSSZEFOGLALÁS

A mitokondriális szubsztrátszintű foszforilációt a szukcinil-CoA-szintetáz katalizálja. A reverzibilis reakcióban szukcinil-CoA és ADP (vagy GDP) alakul át a szukcináttá, CoASH-vá és ATP-vé (GTP-vé). Mivel az enzim az oxidatív foszforilációtól függetlenül képes magas energiájú foszfátok előállítására, kitüntetett szerepet játszik abban, hogy a mitokondrium ne váljon ATP-fogyasztó organellemé gátolt légzési lánc esetén. A szukcinil-CoA-szintetáz működéséhez szükség van az α -ketoglutarát-dehidrogenáz komplex (KGDHC) általi szukcinil-CoA ellátásra. A KGDHC által katalizált reakcióhoz szükséges NAD^+ -ot a komplex-I gátoltsága esetén (rotenon mellett vagy anoxiában) a mitokondriális diaforázok képesek biztosítani.

Jelen munkában a mitokondriális szubsztrátszintű foszforilációt befolyásoló metabolikus utakat írtunk le. A GABA egy neurotranszmitter, mely a GABA-shunt folyamatában szukcinát-szemialdehiddé metabolizálódik, végül szukcinát formájában lép be a citromsavciklusba. A γ -hidroxi-butirát (GHB) egy neurotranszmitter és egy pszichoaktív szer, mely lebontása során szintén szukcináttá alakul. Eredményeink alátámasztják feltevésünket, miszerint a GABA, a szukcinát-szemialdehid és a GHB metabolizmusa során keletkező szukcinát anoxiában eltolja a szukcinil-CoA-szintetáz által katalizált reverzibilis reakciót ATP (GTP) hidrolízis irányába. Így a GABA-shunt működése a mitokondriális szubsztrátszintű foszforilációt gátolja.

A NAD(P)H kinon oxidoreduktáz 1 (NQO1) egy diaforáz aktivitással bíró enzim, amely képes oxidált NAD^+ -ot szolgáltatni a szubsztrátszintű foszforiláció működéséhez, amennyiben megfelelő kinon szubsztrátok vannak jelen. $\text{Nqo1}^{-/-}$ és vad típusú egerekből izolált mitokondriumokon végzett méréseink azt mutatták, hogy az Nqo1 működése nélkülözhető a szukcinil-CoA-szintetáz által katalizált reakció végbemeneteléhez. Ellenben más, jelenleg még azonosítatlan dikumarol-szenzitív diaforáz enzimek hozzájárulása elengedhetetlen a szükséges NAD^+ -ellátás biztosításához gátolt légzési lánc esetén. A jelen tézisben vizsgált kinon szubsztrátok közül a 2-metoxi-1,4-naftokinon, a durokinon és az idebenon támogatja a diaforáz működést és így a szubsztrátszintű foszforilációt gátolt komplex-I mellett. Ezek közül a 2-metoxi-1,4-naftokinon jótékony hatását az Nqo1 szubsztrátjaként fejt ki.

9. BIBLIOGRAPHY

1. Ernster L, Schatz G. (1981) Mitochondria: a historical review. *J Cell Biol*, 91: 227s-255s.
2. Duchen MR. (2004) Mitochondria in health and disease: perspectives on a new mitochondrial biology. *Mol Aspects Med*, 25: 365-451.
3. Nunnari J, Suomalainen A. (2012) Mitochondria: in sickness and in health. *Cell*, 148: 1145-1159.
4. Nelson DL, Cox MM. *Lehninger Principles of Biochemistry* (6th ed.). W.H. Freeman and Company, New York, 2013: 690-716.
5. Fang J, Uchiumi T, Yagi M, Matsumoto S, Amamoto R, Takazaki S, Yamaza H, Nonaka K, Kang D. (2013) Dihydro-orotate dehydrogenase is physically associated with the respiratory complex and its loss leads to mitochondrial dysfunction. *Biosci Rep*, 33: e00021.
6. Mitchell P. (1961) Coupling of phosphorylation to electron and hydrogen transfer by a chemi-osmotic type of mechanism. *Nature*, 191: 144-148.
7. Watt IN, Montgomery MG, Runswick MJ, Leslie AG, Walker JE. (2010) Bioenergetic cost of making an adenosine triphosphate molecule in animal mitochondria. *Proc Natl Acad Sci U S A*, 107: 16823-16827.
8. Klingenberg M. (2008) The ADP and ATP transport in mitochondria and its carrier. *Biochim Biophys Acta*, 1778: 1978-2021.
9. Klingenberg M. (1980) The ADP-ATP translocation in mitochondria, a membrane potential controlled transport. *J Membr Biol*, 56: 97-105.
10. Brenner C, Subramaniam K, Pertuiset C, Pervaiz S. (2011) Adenine nucleotide translocase family: four isoforms for apoptosis modulation in cancer. *Oncogene*, 30: 883-895.
11. Kokoszka JE, Waymire KG, Levy SE, Sligh JE, Cai J, Jones DP, MacGregor GR, Wallace DC. (2004) The ADP/ATP translocator is not essential for the mitochondrial permeability transition pore. *Nature*, 427: 461-465.
12. Doczi J, Torocsik B, Echaniz-Laguna A, Mousson de Camaret B, Starkov A, Starkova N, Gal A, Molnar MJ, Kawamata H, Manfredi G, Adam-Vizi V,

- Chinopoulos C. (2016) Alterations in voltage-sensing of the mitochondrial permeability transition pore in ANT1-deficient cells. *Sci Rep*, 6: 26700.
13. Kramer R. (1980) Influence of divalent cations on the reconstituted ADP, ATP exchange. *Biochim Biophys Acta*, 592: 615-620.
 14. Chance B, Williams GR. (1955) Respiratory enzymes in oxidative phosphorylation. III. The steady state. *J Biol Chem*, 217: 409-427.
 15. Estabrook RW. Mitochondrial respiratory control and the polarographic measurement of ADP : O ratios. In: Estabrook RW, Pullman ME (eds.), *Methods in Enzymology* (Vol. 10). Academic Press, New York, 1967: 41-47.
 16. Nicholls DG, Ferguson SSJ. *Bioenergetics 3* (3rd ed.). Academic Press, London, 2002: 69-73.
 17. Brand MD, Pakay JL, Ocloo A, Kokoszka J, Wallace DC, Brookes PS, Cornwall EJ. (2005) The basal proton conductance of mitochondria depends on adenine nucleotide translocase content. *Biochem J*, 392: 353-362.
 18. Korzeniewski B. (2002) Effect of enzyme deficiencies on oxidative phosphorylation: from isolated mitochondria to intact tissues. Theoretical studies. *Mol Biol Rep*, 29: 197-202.
 19. Feniouk BA, Yoshida M. (2008) Regulatory mechanisms of proton-translocating F(O)F (1)-ATP synthase. *Results Probl Cell Differ*, 45: 279-308.
 20. Klingenberg M, Rottenberg H. (1977) Relation between the gradient of the ATP/ADP ratio and the membrane potential across the mitochondrial membrane. *Eur J Biochem*, 73: 125-130.
 21. Chinopoulos C, Gerencser AA, Mandi M, Mathe K, Torocsik B, Doczi J, Turiak L, Kiss G, Konrad C, Vajda S, Vereczki V, Oh RJ, Adam-Vizi V. (2010) Forward operation of adenine nucleotide translocase during FOF1-ATPase reversal: critical role of matrix substrate-level phosphorylation. *Faseb j*, 24: 2405-2416.
 22. Martell AE, Smith RM. *Critical Stability Constants* (Vol. 2). Plenum Press, New York, 1975: 281-284.
 23. Chinopoulos C. (2011) Mitochondrial consumption of cytosolic ATP: not so fast. *FEBS Lett*, 585: 1255-1259.

24. Chinopoulos C, Vajda S, Csanady L, Mandi M, Mathe K, Adam-Vizi V. (2009) A novel kinetic assay of mitochondrial ATP-ADP exchange rate mediated by the ANT. *Biophys J*, 96: 2490-2504.
25. Chinopoulos C, Adam-Vizi V. (2010) Mitochondrial Ca²⁺ sequestration and precipitation revisited. *Febs j*, 277: 3637-3651.
26. Kawamata H, Starkov AA, Manfredi G, Chinopoulos C. (2010) A kinetic assay of mitochondrial ADP-ATP exchange rate in permeabilized cells. *Anal Biochem*, 407: 52-57.
27. Greenamyre JT, Sherer TB, Betarbet R, Panov AV. (2001) Complex I and Parkinson's disease. *IUBMB Life*, 52: 135-141.
28. Cadonic C, Sabbir MG, Albensi BC. (2016) Mechanisms of Mitochondrial Dysfunction in Alzheimer's Disease. *Mol Neurobiol*, 53: 6078-6090.
29. Vafai SB, Mootha VK. (2012) Mitochondrial disorders as windows into an ancient organelle. *Nature*, 491: 374-383.
30. Kalogeris T, Baines CP, Krenz M, Korthuis RJ. (2012) Cell biology of ischemia/reperfusion injury. *Int Rev Cell Mol Biol*, 298: 229-317.
31. Chinopoulos C, Adam-Vizi V. (2010) Mitochondria as ATP consumers in cellular pathology. *Biochim Biophys Acta*, 1802: 221-227.
32. Lambeth DO, Tews KN, Adkins S, Frohlich D, Milavetz BI. (2004) Expression of two succinyl-CoA synthetases with different nucleotide specificities in mammalian tissues. *J Biol Chem*, 279: 36621-36624.
33. Johnson JD, Mehus JG, Tews K, Milavetz BI, Lambeth DO. (1998) Genetic evidence for the expression of ATP- and GTP-specific succinyl-CoA synthetases in multicellular eucaryotes. *J Biol Chem*, 273: 27580-27586.
34. Dobolyi A, Ostergaard E, Bago AG, Doczi T, Palkovits M, Gal A, Molnar MJ, Adam-Vizi V, Chinopoulos C. (2015) Exclusive neuronal expression of SUCLA2 in the human brain. *Brain Struct Funct*, 220: 135-151.
35. Dobolyi A, Bago AG, Gal A, Molnar MJ, Palkovits M, Adam-Vizi V, Chinopoulos C. (2015) Localization of SUCLA2 and SUCLG2 subunits of succinyl CoA ligase within the cerebral cortex suggests the absence of matrix substrate-level phosphorylation in glial cells of the human brain. *J Bioenerg Biomembr*, 47: 33-41.

36. Kadrmas EF, Ray PD, Lambeth DO. (1991) Apparent ATP-linked succinate thiokinase activity and its relation to nucleoside diphosphate kinase in mitochondrial matrix preparations from rabbit. *Biochim Biophys Acta*, 1074: 339-346.
37. Kowluru A, Tannous M, Chen HQ. (2002) Localization and characterization of the mitochondrial isoform of the nucleoside diphosphate kinase in the pancreatic beta cell: evidence for its complexation with mitochondrial succinyl-CoA synthetase. *Arch Biochem Biophys*, 398: 160-169.
38. Chinopoulos C. (2013) Which way does the citric acid cycle turn during hypoxia? The critical role of alpha-ketoglutarate dehydrogenase complex. *J Neurosci Res*, 91: 1030-1043.
39. Sheu KF, Blass JP. (1999) The alpha-ketoglutarate dehydrogenase complex. *Ann N Y Acad Sci*, 893: 61-78.
40. Kiss G, Konrad C, Doczi J, Starkov AA, Kawamata H, Manfredi G, Zhang SF, Gibson GE, Beal MF, Adam-Vizi V, Chinopoulos C. (2013) The negative impact of alpha-ketoglutarate dehydrogenase complex deficiency on matrix substrate-level phosphorylation. *Faseb j*, 27: 2392-2406.
41. Kacso G, Ravasz D, Doczi J, Nemeth B, Madgar O, Saada A, Ilin P, Miller C, Ostergaard E, Iordanov I, Adams D, Vargedo Z, Araki M, Araki K, Nakahara M, Ito H, Gal A, Molnar MJ, Nagy Z, Patocs A, Adam-Vizi V, Chinopoulos C. (2016) Two transgenic mouse models for beta-subunit components of succinate-CoA ligase yielding pleiotropic metabolic alterations. *Biochem J*, 473: 3463-3485.
42. Phillips D, Aponte AM, French SA, Chess DJ, Balaban RS. (2009) Succinyl-CoA synthetase is a phosphate target for the activation of mitochondrial metabolism. *Biochemistry*, 48: 7140-7149.
43. Komlodi T, Tretter L. (2017) Methylene blue stimulates substrate-level phosphorylation catalysed by succinyl-CoA ligase in the citric acid cycle. *Neuropharmacology*, 123: 287-298.
44. Li X, Wu F, Beard DA. (2013) Identification of the kinetic mechanism of succinyl-CoA synthetase. *Biosci Rep*, 33: 145-163.

45. Kiss G, Konrad C, Pour-Ghaz I, Mansour JJ, Nemeth B, Starkov AA, Adam-Vizi V, Chinopoulos C. (2014) Mitochondrial diaphorases as NAD(+) donors to segments of the citric acid cycle that support substrate-level phosphorylation yielding ATP during respiratory inhibition. *Faseb j*, 28: 1682-1697.
46. Ostergaard E. (2008) Disorders caused by deficiency of succinate-CoA ligase. *J Inherit Metab Dis*, 31: 226-229.
47. Labbe RF, Kurumada T, Onisawa J. (1965) The role of succinyl-CoA synthetase in the control of heme biosynthesis. *Biochim Biophys Acta*, 111: 403-415.
48. Stern JR, Coon MJ, Del Campillo A. (1956) Enzymes of fatty acid metabolism. III. Breakdown and synthesis of beta-keto fatty acids. *J Biol Chem*, 221: 1-14.
49. Nemeth B, Doczi J, Csete D, Kacso G, Ravasz D, Adams D, Kiss G, Nagy AM, Horvath G, Tretter L, Mocsai A, Csepanyi-Komi R, Iordanov I, Adam-Vizi V, Chinopoulos C. (2016) Abolition of mitochondrial substrate-level phosphorylation by itaconic acid produced by LPS-induced Irg1 expression in cells of murine macrophage lineage. *Faseb j*, 30: 286-300.
50. Machiyama Y, Balazs R, Hammond BJ, Julian T, Richter D. (1970) The metabolism of gamma-aminobutyrate and glucose in potassium ion-stimulated brain tissue in vitro. *Biochem J*, 116: 469-481.
51. Balazs R, Machiyama Y, Hammond BJ, Julian T, Richter D. (1970) The operation of the gamma-aminobutyrate bypath of the tricarboxylic acid cycle in brain tissue in vitro. *Biochem J*, 116: 445-461.
52. Rodichok LD, Albers RW. (1980) The effect of gamma-aminobutyric acid on substrate-level phosphorylation in brain mitochondria. *J Neurochem*, 34: 808-812.
53. Maitre M. (1997) The gamma-hydroxybutyrate signalling system in brain: organization and functional implications. *Prog Neurobiol*, 51: 337-361.
54. McCormick DA. (1989) GABA as an inhibitory neurotransmitter in human cerebral cortex. *J Neurophysiol*, 62: 1018-1027.
55. Udenfriend S. (1950) Identification of gamma-aminobutyric acid in brain by the isotope derivative method. *J Biol Chem*, 187: 65-69.
56. Roberts E, Frankel S. (1950) gamma-Aminobutyric acid in brain: its formation from glutamic acid. *J Biol Chem*, 187: 55-63.

57. Awapara J, Landua AJ, Fuerst R, Seale B. (1950) Free gamma-aminobutyric acid in brain. *J Biol Chem*, 187: 35-39.
58. Gladkevich A, Korf J, Hakobyan VP, Melkonyan KV. (2006) The peripheral GABAergic system as a target in endocrine disorders. *Auton Neurosci*, 124: 1-8.
59. Garry DJ, Coulter HD, McIntee TJ, Wu JY, Sorenson RL. (1987) Immunoreactive GABA transaminase within the pancreatic islet is localized in mitochondria of the B-cell. *J Histochem Cytochem*, 35: 831-836.
60. Minuk GY. (1993) Gamma-aminobutyric acid and the liver. *Dig Dis*, 11: 45-54.
61. Krnjevic K, Schwartz S. (1967) The action of gamma-aminobutyric acid on cortical neurones. *Exp Brain Res*, 3: 320-336.
62. Olsen RW, Sieghart W. (2008) International Union of Pharmacology. LXX. Subtypes of gamma-aminobutyric acid(A) receptors: classification on the basis of subunit composition, pharmacology, and function. Update. *Pharmacol Rev*, 60: 243-260.
63. Bowery NG. (1993) GABAB receptor pharmacology. *Annu Rev Pharmacol Toxicol*, 33: 109-147.
64. Cherubini E, Gaiarsa JL, Ben-Ari Y. (1991) GABA: an excitatory transmitter in early postnatal life. *Trends Neurosci*, 14: 515-519.
65. Yoon BE, Lee CJ. (2014) GABA as a rising gliotransmitter. *Front Neural Circuits*, 8: 141.
66. Angulo MC, Le Meur K, Kozlov AS, Charpak S, Audinat E. (2008) GABA, a forgotten gliotransmitter. *Prog Neurobiol*, 86: 297-303.
67. Bazargani N, Attwell D. (2016) Astrocyte calcium signaling: the third wave. 19: 182-189.
68. Schafer DF, Jones EA. (1982) Hepatic encephalopathy and the gamma-aminobutyric-acid neurotransmitter system. *Lancet*, 1: 18-20.
69. Wan Y, Wang Q, Prud'homme GJ. (2015) GABAergic system in the endocrine pancreas: a new target for diabetes treatment. *Diabetes Metab Syndr Obes*, 8: 79-87.
70. Davies SL, Roussa E, Le Rouzic P, Thevenod F, Alper SL, Best L, Brown PD. (2004) Expression of K⁺-Cl⁻ cotransporters in the alpha-cells of rat endocrine pancreas. *Biochim Biophys Acta*, 1667: 7-14.

71. Ong J, Kerr DI. (1982) GABAA- and GABAB-receptor-mediated modification of intestinal motility. *Eur J Pharmacol*, 86: 9-17.
72. Kataoka Y, Gutman Y, Guidotti A, Panula P, Wroblewski J, Cosenza-Murphy D, Wu JY, Costa E. (1984) Intrinsic GABAergic system of adrenal chromaffin cells. *Proc Natl Acad Sci U S A*, 81: 3218-3222.
73. Geigerseder C, Doepner R, Thalhammer A, Frungieri MB, Gamel-Didelon K, Calandra RS, Kohn FM, Mayerhofer A. (2003) Evidence for a GABAergic system in rodent and human testis: local GABA production and GABA receptors. *Neuroendocrinology*, 77: 314-323.
74. Persson H, Pelto-Huikko M, Metsis M, Soder O, Brene S, Skog S, Hokfelt T, Ritzen EM. (1990) Expression of the neurotransmitter-synthesizing enzyme glutamic acid decarboxylase in male germ cells. *Mol Cell Biol*, 10: 4701-4711.
75. Jin Z, Mendu SK, Birnir B. (2013) GABA is an effective immunomodulatory molecule. *Amino Acids*, 45: 87-94.
76. Owens DF, Kriegstein AR. (2002) Is there more to GABA than synaptic inhibition? *Nat Rev Neurosci*, 3: 715-727.
77. Lakhani R, Vogel KR, Till A, Liu J, Burnett SF, Gibson KM, Subramani S. (2014) Defects in GABA metabolism affect selective autophagy pathways and are alleviated by mTOR inhibition. *EMBO Mol Med*, 6: 551-566.
78. Gilliam M, Tyerman SD. (2016) Linking Metabolism to Membrane Signaling: The GABA-Malate Connection. *Trends Plant Sci*, 21: 295-301.
79. Wong CG, Bottiglieri T, Snead OC, 3rd. (2003) GABA, gamma-hydroxybutyric acid, and neurological disease. *Ann Neurol*, 54 Suppl 6: S3-12.
80. Gajcy K, Lochynski S, Librowski T. (2010) A role of GABA analogues in the treatment of neurological diseases. *Curr Med Chem*, 17: 2338-2347.
81. Tillakaratne NJ, Medina-Kauwe L, Gibson KM. (1995) gamma-Aminobutyric acid (GABA) metabolism in mammalian neural and nonneural tissues. *Comp Biochem Physiol A Physiol*, 112: 247-263.
82. White HL, Sato TL. (1978) GABA-transaminases of human brain and peripheral tissues--kinetic and molecular properties. *J Neurochem*, 31: 41-47.
83. Soghomonian JJ, Martin DL. (1998) Two isoforms of glutamate decarboxylase: why? *Trends Pharmacol Sci*, 19: 500-505.

84. Sluse FE. (1996) Mitochondrial metabolite carrier family, topology, structure and functional properties: an overview. *Acta Biochim Pol*, 43: 349-360.
85. Monne M, Palmieri F. (2014) Antiporters of the mitochondrial carrier family. *Curr Top Membr*, 73: 289-320.
86. Sequerra EB, Gardino P, Hedin-Pereira C, de Mello FG. (2007) Putrescine as an important source of GABA in the postnatal rat subventricular zone. *Neuroscience*, 146: 489-493.
87. Pisano JJ, Wilson JD, Cohen L, Abraham D, Udenfriend S. (1961) Isolation of gamma-aminobutyrylhistidine (homocarnosine) from brain. *J Biol Chem*, 236: 499-502.
88. Brand MD, Chappell JB. (1974) Permeability of mitochondria from rat brain and rat liver to GABA. *J Neurochem*, 22: 47-51.
89. Michaeli S, Fait A, Lagor K, Nunes-Nesi A, Grillich N, Yellin A, Bar D, Khan M, Fernie AR, Turano FJ, Fromm H. (2011) A mitochondrial GABA permease connects the GABA shunt and the TCA cycle, and is essential for normal carbon metabolism. *Plant J*, 67: 485-498.
90. Zhou Y, Danbolt NC. (2013) GABA and Glutamate Transporters in Brain. *Front Endocrinol (Lausanne)*, 4: 165.
91. Pin JP, Bockaert J. (1989) Two distinct mechanisms, differentially affected by excitatory amino acids, trigger GABA release from fetal mouse striatal neurons in primary culture. *J Neurosci*, 9: 648-656.
92. Bernath S. (1992) Calcium-independent release of amino acid neurotransmitters: fact or artifact? *Prog Neurobiol*, 38: 57-91.
93. Belhage B, Hansen GH, Schousboe A. (1993) Depolarization by K⁺ and glutamate activates different neurotransmitter release mechanisms in GABAergic neurons: vesicular versus non-vesicular release of GABA. *Neuroscience*, 54: 1019-1034.
94. Minchin MC, Iversen LL. (1974) Release of (3H)gamma-aminobutyric acid from glial cells in rat dorsal root ganglia. *J Neurochem*, 23: 533-540.
95. Salganicoff L, De Robertis E. (1963) Subcellular distribution of glutamic decarboxylase and gamma-aminobutyric alpha-ketoglutaric transaminase. *Life Sci (1962)*, 2: 85-91.

96. Malaspina P, Picklo MJ, Jakobs C, Snead OC, Gibson KM. (2009) Comparative genomics of aldehyde dehydrogenase 5a1 (succinate semialdehyde dehydrogenase) and accumulation of gamma-hydroxybutyrate associated with its deficiency. *Hum Genomics*, 3: 106-120.
97. Wallach DP. (1961) Studies on the GABA pathway. I. The inhibition of gamma-aminobutyric acid-alpha-ketoglutaric acid transaminase in vitro and in vivo by U-7524 (amino-oxyacetic acid). *Biochem Pharmacol*, 5: 323-331.
98. Kauppinen RA, Sihra TS, Nicholls DG. (1987) Aminooxyacetic acid inhibits the malate-aspartate shuttle in isolated nerve terminals and prevents the mitochondria from utilizing glycolytic substrates. *Biochim Biophys Acta*, 930: 173-178.
99. Wu JY, Roberts E. (1974) Properties of brain L-glutamate decarboxylase: inhibition studies. *J Neurochem*, 23: 759-767.
100. Kim KJ, Pearl PL, Jensen K, Snead OC, Malaspina P, Jakobs C, Gibson KM. (2011) Succinic semialdehyde dehydrogenase: biochemical-molecular-clinical disease mechanisms, redox regulation, and functional significance. *Antioxid Redox Signal*, 15: 691-718.
101. Kaufman EE, Nelson T, Goochee C, Sokoloff L. (1979) Purification and characterization of an NADP⁺-linked alcohol oxido-reductase which catalyzes the interconversion of gamma-hydroxybutyrate and succinic semialdehyde. *J Neurochem*, 32: 699-712.
102. Hearl WG, Churchich JE. (1985) A mitochondrial NADP⁺-dependent reductase related to the 4-aminobutyrate shunt. Purification, characterization, and mechanism. *J Biol Chem*, 260: 16361-16366.
103. Hoffman PL, Wermuth B, von Wartburg JP. (1980) Human brain aldehyde reductases: relationship to succinic semialdehyde reductase and aldose reductase. *J Neurochem*, 35: 354-366.
104. Picklo MJ, Sr., Olson SJ, Hayes JD, Markesbery WR, Montine TJ. (2001) Elevation of AKR7A2 (succinic semialdehyde reductase) in neurodegenerative disease. *Brain Res*, 916: 229-238.

105. Kaufman EE, Nelson T, Miller D, Stadlan N. (1988) Oxidation of gamma-hydroxybutyrate to succinic semialdehyde by a mitochondrial pyridine nucleotide-independent enzyme. *J Neurochem*, 51: 1079-1084.
106. Kaufman EE, Nelson T, Fales HM, Levin DM. (1988) Isolation and characterization of a hydroxyacid-oxoacid transhydrogenase from rat kidney mitochondria. *J Biol Chem*, 263: 16872-16879.
107. Kardon T, Noel G, Vertommen D, Schaftingen EV. (2006) Identification of the gene encoding hydroxyacid-oxoacid transhydrogenase, an enzyme that metabolizes 4-hydroxybutyrate. *FEBS Lett*, 580: 2347-2350.
108. Struys EA, Salomons GS, Achouri Y, Van Schaftingen E, Grosso S, Craigen WJ, Verhoeven NM, Jakobs C. (2005) Mutations in the D-2-hydroxyglutarate dehydrogenase gene cause D-2-hydroxyglutaric aciduria. *Am J Hum Genet*, 76: 358-360.
109. Struys EA, Verhoeven NM, Ten Brink HJ, Wickenhagen WV, Gibson KM, Jakobs C. (2005) Kinetic characterization of human hydroxyacid-oxoacid transhydrogenase: relevance to D-2-hydroxyglutaric and gamma-hydroxybutyric acidurias. *J Inherit Metab Dis*, 28: 921-930.
110. Wanders RJ, Mooyer P. (1995) D-2-hydroxyglutaric acidemia: identification of a new enzyme, D-2-hydroxyglutarate dehydrogenase, localized in mitochondria. *J Inherit Metab Dis*, 18: 194-196.
111. Achouri Y, Noel G, Vertommen D, Rider MH, Veiga-Da-Cunha M, Van Schaftingen E. (2004) Identification of a dehydrogenase acting on D-2-hydroxyglutarate. *Biochem J*, 381: 35-42.
112. Lindahl G, Lindstedt G, Lindstedt S. (1967) Metabolism of 2-amino-5-hydroxyadipic acid in the rat. *Arch Biochem Biophys*, 119: 347-352.
113. Chalmers RA, Lawson AM, Watts RW, Tavill AS, Kamerling JP, Hey E, Ogilvie D. (1980) D-2-hydroxyglutaric aciduria: case report and biochemical studies. *J Inherit Metab Dis*, 3: 11-15.
114. Dang L, White DW, Gross S, Bennett BD, Bittinger MA, Driggers EM, Fantin VR, Jang HG, Jin S, Keenan MC, Marks KM, Prins RM, Ward PS, Yen KE, Liao LM, Rabinowitz JD, Cantley LC, Thompson CB, Vander Heiden MG, Su

- SM. (2009) Cancer-associated IDH1 mutations produce 2-hydroxyglutarate. *Nature*, 462: 739-744.
115. Pietrak B, Zhao H, Qi H, Quinn C, Gao E, Boyer JG, Concha N, Brown K, Duraiswami C, Wooster R, Sweitzer S, Schwartz B. (2011) A tale of two subunits: how the neomorphic R132H IDH1 mutation enhances production of alphaHG. *Biochemistry*, 50: 4804-4812.
116. Losman JA, Kaelin WG, Jr. (2013) What a difference a hydroxyl makes: mutant IDH, (R)-2-hydroxyglutarate, and cancer. *Genes Dev*, 27: 836-852.
117. Struys EA. (2006) D-2-Hydroxyglutaric aciduria: unravelling the biochemical pathway and the genetic defect. *J Inherit Metab Dis*, 29: 21-29.
118. Hagos Y, Krick W, Braulke T, Muhlhausen C, Burckhardt G, Burckhardt BC. (2008) Organic anion transporters OAT1 and OAT4 mediate the high affinity transport of glutarate derivatives accumulating in patients with glutaric acidurias. *Pflugers Arch*, 457: 223-231.
119. Kugler P. (1993) In situ measurements of enzyme activities in the brain. *Histochem J*, 25: 329-338.
120. De Boer T, Bruinvels J. (1977) Assay and properties of 4-aminobutyric-2-oxoglutaric acid transaminase and succinic semialdehyde dehydrogenase in rat brain tissue. *J Neurochem*, 28: 471-478.
121. Nelson T, Kaufman E, Kline J, Sokoloff L. (1981) The extraneural distribution of gamma-hydroxybutyrate. *J Neurochem*, 37: 1345-1348.
122. Laborit H. (1964) SODIUM 4-HYDROXYBUTYRATE. *Int J Neuropharmacol*, 3: 433-451.
123. Leone MA, Vigna-Taglianti F, Avanzi G, Brambilla R, Faggiano F. (2010) Gamma-hydroxybutyrate (GHB) for treatment of alcohol withdrawal and prevention of relapses. *Cochrane Database Syst Rev*: Cd006266.
124. Boscolo-Berto R, Viel G, Montagnese S, Raduazzo DI, Ferrara SD, Dauvilliers Y. (2012) Narcolepsy and effectiveness of gamma-hydroxybutyrate (GHB): a systematic review and meta-analysis of randomized controlled trials. *Sleep Med Rev*, 16: 431-443.
125. Kam PC, Yoong FF. (1998) Gamma-hydroxybutyric acid: an emerging recreational drug. *Anaesthesia*, 53: 1195-1198.

126. Andresen H, Aydin BE, Mueller A, Iwersen-Bergmann S. (2011) An overview of gamma-hydroxybutyric acid: pharmacodynamics, pharmacokinetics, toxic effects, addiction, analytical methods, and interpretation of results. *Drug Test Anal*, 3: 560-568.
127. Benavides J, Rumigny JF, Bourguignon JJ, Cash C, Wermuth CG, Mandel P, Vincendon G, Maitre M. (1982) High affinity binding sites for gamma-hydroxybutyric acid in rat brain. *Life Sci*, 30: 953-961.
128. Ratomponirina C, Hode Y, Hechler V, Maitre M. (1995) gamma-Hydroxybutyrate receptor binding in rat brain is inhibited by guanyl nucleotides and pertussis toxin. *Neurosci Lett*, 189: 51-53.
129. Xie X, Smart TG. (1992) Gamma-hydroxybutyrate hyperpolarizes hippocampal neurones by activating GABAB receptors. *Eur J Pharmacol*, 212: 291-294.
130. Emri Z, Antal K, Crunelli V. (1996) Gamma-hydroxybutyric acid decreases thalamic sensory excitatory postsynaptic potentials by an action on presynaptic GABAB receptors. *Neurosci Lett*, 216: 121-124.
131. Snead OC, 3rd, Gibson KM. (2005) Gamma-hydroxybutyric acid. *N Engl J Med*, 352: 2721-2732.
132. Giarman NJ, Schmidt KF. (1963) Some neurochemical aspects of the depressant action of gamma-butyrolactone on the central nervous system. *Br J Pharmacol Chemother*, 20: 563-568.
133. Feigenbaum JJ, Howard SG. (1996) Does gamma-hydroxybutyrate inhibit or stimulate central DA release? *Int J Neurosci*, 88: 53-69.
134. Hechler V, Gobaille S, Bourguignon JJ, Maitre M. (1991) Extracellular events induced by gamma-hydroxybutyrate in striatum: a microdialysis study. *J Neurochem*, 56: 938-944.
135. Takahara J, Yunoki S, Yakushiji W, Yamauchi J, Yamane Y. (1977) Stimulatory effects of gamma-hydroxybutyric acid on growth hormone and prolactin release in humans. *J Clin Endocrinol Metab*, 44: 1014-1017.
136. Mamelak M, Escriu JM, Stokan O. (1977) The effects of gamma-hydroxybutyrate on sleep. *Biol Psychiatry*, 12: 273-288.
137. Cui D, Morris ME. (2009) The drug of abuse gamma-hydroxybutyrate is a substrate for sodium-coupled monocarboxylate transporter (SMCT) 1

- (SLC5A8): characterization of SMCT-mediated uptake and inhibition. *Drug Metab Dispos*, 37: 1404-1410.
138. Wang Q, Darling IM, Morris ME. (2006) Transport of gamma-hydroxybutyrate in rat kidney membrane vesicles: Role of monocarboxylate transporters. *J Pharmacol Exp Ther*, 318: 751-761.
 139. Halestrap AP. (2013) Monocarboxylic acid transport. *Compr Physiol*, 3: 1611-1643.
 140. Perez-Escuredo J, Van Hee VF, Sboarina M, Falces J, Payen VL, Pellerin L, Sonveaux P. (2016) Monocarboxylate transporters in the brain and in cancer. *Biochim Biophys Acta*, 1863: 2481-2497.
 141. Hussien R, Brooks GA. (2011) Mitochondrial and plasma membrane lactate transporter and lactate dehydrogenase isoform expression in breast cancer cell lines. *Physiol Genomics*, 43: 255-264.
 142. Alzeer S, Ellis EM. (2014) Metabolism of gamma hydroxybutyrate in human hepatoma HepG2 cells by the aldo-keto reductase AKR1A1. *Biochem Pharmacol*, 92: 499-505.
 143. Straub FB. (1939) Isolation and properties of a flavoprotein from heart muscle tissue. *Biochem J*, 33: 787-792.
 144. Massey V. (1960) The identity of diaphorase and lipoyl dehydrogenase. *Biochim Biophys Acta*, 37: 314-322.
 145. Ernster L. (1987) DT diaphorase: a historical review. *Chem. Scripta*, 27A: 1-13.
 146. Ernster L, Navazio L. (1958) Soluble diaphorase in animal tissues. *Acta Chem Scand*, 12: 595-602.
 147. Ernster L. (1958) Diaphorase activities in liver cytoplasmic fractions. *Federation Proc.*, 17: 216.
 148. Conover TE, Ernster L. (1962) DT diaphorase. II. Relation to respiratory chain of intact mitochondria. *Biochim Biophys Acta*, 58: 189-200.
 149. Ernster L, Danielson L, Ljunggren M. (1960) Purification and some properties of a highly dicoumarol-sensitive liver diaphorase. *Biochem Biophys Res Commun*, 2: 88-92.
 150. Danielson L, Ernster L, Ljunggren M. (1960) Selective extraction of DT diaphorase from mitochondria and microsomes. *Acta Chem Scand*, 14.

151. Stein AM, Kaplan NO. (1958) The diaphorases of rat-liver mitochondria. *Biochim Biophys Acta*, 29: 452-453.
152. Ernster L, Danielson L, Ljunggren M. (1962) DT diaphorase. I. Purification from the soluble fraction of rat-liver cytoplasm, and properties. *Biochim Biophys Acta*, 58: 171-188.
153. Williams CH, Jr., Gibbs RH, Kamin H. (1959) A microsomal TPNH-neotetrazolium diaphorase. *Biochim Biophys Acta*, 32: 568-569.
154. Conover TE, Danielson L, Ernster L. (1963) DT diaphorase. III. Separation of mitochondrial DT diaphorase and respiratory chain. *Biochim Biophys Acta*, 67: 254-267.
155. Conover TE, Ernster L. (1963) DT diaphorase. IV. Coupling of extramitochondrial reduced pyridine nucleotide oxidation to mitochondrial respiratory chain. *Biochim Biophys Acta*, 67: 268-280.
156. Dong H, Shertzer HG, Genter MB, Gonzalez FJ, Vasiliou V, Jefcoate C, Nebert DW. (2013) Mitochondrial targeting of mouse NQO1 and CYP1B1 proteins. *Biochem Biophys Res Commun*, 435: 727-732.
157. Bianchet MA, Faig M, Amzel LM. Structure and mechanism of NAD[P]H:quinone acceptor oxidoreductases (NQO). In: Sies H, Packer L (eds.), *Methods in Enzymology* (Vol. 382). Academic Press, San Diego, 2004: 144-174.
158. Winski SL, Koutalos Y, Bentley DL, Ross D. (2002) Subcellular localization of NAD(P)H:quinone oxidoreductase 1 in human cancer cells. *Cancer Res*, 62: 1420-1424.
159. Hosoda S, Nakamura W, Hayashi K. (1974) Properties and reaction mechanism of DT diaphorase from rat liver. *J Biol Chem*, 249: 6416-6423.
160. Gong X, Gutala R, Jaiswal AK. (2008) Quinone oxidoreductases and vitamin K metabolism. *Vitam Horm*, 78: 85-101.
161. Tie JK, Jin DY, Straight DL, Stafford DW. (2011) Functional study of the vitamin K cycle in mammalian cells. *Blood*, 117: 2967-2974.
162. Ingram BO, Turbyfill JL, Bledsoe PJ, Jaiswal AK, Stafford DW. (2013) Assessment of the contribution of NAD(P)H-dependent quinone oxidoreductase

- 1 (NQO1) to the reduction of vitamin K in wild-type and NQO1-deficient mice. *Biochem J*, 456: 47-54.
163. Gaikwad A, Long DJ, 2nd, Stringer JL, Jaiswal AK. (2001) In vivo role of NAD(P)H:quinone oxidoreductase 1 (NQO1) in the regulation of intracellular redox state and accumulation of abdominal adipose tissue. *J Biol Chem*, 276: 22559-22564.
164. Iyanagi T, Yamazaki I. (1970) One-electron-transfer reactions in biochemical systems. V. Difference in the mechanism of quinone reduction by the NADH dehydrogenase and the NAD(P)H dehydrogenase (DT-diaphorase). *Biochim Biophys Acta*, 216: 282-294.
165. Siegel D, Gustafson DL, Dehn DL, Han JY, Boonchoong P, Berliner LJ, Ross D. (2004) NAD(P)H:quinone oxidoreductase 1: role as a superoxide scavenger. *Mol Pharmacol.*, 65: 1238-1247.
166. Zhu H, Jia Z, Mahaney JE, Ross D, Misra HP, Trush MA, Li Y. (2007) The highly expressed and inducible endogenous NAD(P)H:quinone oxidoreductase 1 in cardiovascular cells acts as a potential superoxide scavenger. *Cardiovasc Toxicol*, 7: 202-211.
167. Siegel D, Bolton EM, Burr JA, Liebler DC, Ross D. (1997) The reduction of alpha-tocopherolquinone by human NAD(P)H: quinone oxidoreductase: the role of alpha-tocopherolhydroquinone as a cellular antioxidant. *Mol Pharmacol*, 52: 300-305.
168. Beyer RE, Segura-Aguilar J, Di Bernardo S, Cavazzoni M, Fato R, Fiorentini D, Galli MC, Setti M, Landi L, Lenaz G. (1996) The role of DT-diaphorase in the maintenance of the reduced antioxidant form of coenzyme Q in membrane systems. *Proc Natl Acad Sci U S A*, 93: 2528-2532.
169. Asher G, Lotem J, Kama R, Sachs L, Shaul Y. (2002) NQO1 stabilizes p53 through a distinct pathway. *Proc Natl Acad Sci U S A*, 99: 3099-3104.
170. Garate M, Wong RP, Campos EI, Wang Y, Li G. (2008) NAD(P)H quinone oxidoreductase 1 inhibits the proteasomal degradation of the tumour suppressor p33(ING1b). *EMBO Rep*, 9: 576-581.

171. Radjendirane V, Joseph P, Lee YH, Kimura S, Klein-Szanto AJ, Gonzalez FJ, Jaiswal AK. (1998) Disruption of the DT diaphorase (NQO1) gene in mice leads to increased menadione toxicity. *J Biol Chem*, 273: 7382-7389.
172. Bauer AK, Faiola B, Abernethy DJ, Marchan R, Pluta LJ, Wong VA, Roberts K, Jaiswal AK, Gonzalez FJ, Butterworth BE, Borghoff S, Parkinson H, Everitt J, Recio L. (2003) Genetic susceptibility to benzene-induced toxicity: role of NADPH:quinone oxidoreductase-1. *Cancer Res*, 63: 929-935.
173. Long DJ, 2nd, Waikel RL, Wang XJ, Perlaky L, Roop DR, Jaiswal AK. (2000) NAD(P)H:quinone oxidoreductase 1 deficiency increases susceptibility to benzo(a)pyrene-induced mouse skin carcinogenesis. *Cancer Res*, 60: 5913-5915.
174. Long DJ, 2nd, Waikel RL, Wang XJ, Roop DR, Jaiswal AK. (2001) NAD(P)H:quinone oxidoreductase 1 deficiency and increased susceptibility to 7,12-dimethylbenz[a]-anthracene-induced carcinogenesis in mouse skin. *J Natl Cancer Inst*, 93: 1166-1170.
175. Long DJ, 2nd, Gaikwad A, Multani A, Pathak S, Montgomery CA, Gonzalez FJ, Jaiswal AK. (2002) Disruption of the NAD(P)H:quinone oxidoreductase 1 (NQO1) gene in mice causes myelogenous hyperplasia. *Cancer Res*, 62: 3030-3036.
176. Rothman N, Smith MT, Hayes RB, Traver RD, Hoener B, Campleman S, Li GL, Dosemeci M, Linet M, Zhang L, Xi L, Wacholder S, Lu W, Meyer KB, Titenko-Holland N, Stewart JT, Yin S, Ross D. (1997) Benzene poisoning, a risk factor for hematological malignancy, is associated with the NQO1 609C-->T mutation and rapid fractional excretion of chlorzoxazone. *Cancer Res*, 57: 2839-2842.
177. Oh ET, Park HJ. (2015) Implications of NQO1 in cancer therapy. *BMB Rep*, 48: 609-617.
178. Siegel D, Ross D. (2000) Immunodetection of NAD(P)H:quinone oxidoreductase 1 (NQO1) in human tissues. *Free Radic Biol Med*, 29: 246-253.
179. Jaiswal AK. (2004) Nrf2 signaling in coordinated activation of antioxidant gene expression. *Free Radic Biol Med*, 36: 1199-1207.
180. Menegon S, Columbano A, Giordano S. (2016) The Dual Roles of NRF2 in Cancer. *Trends Mol Med*, 22: 578-593.

181. Sporn MB, Liby KT. (2012) NRF2 and cancer: the good, the bad and the importance of context. *Nat Rev Cancer*, 12: 564-571.
182. De Flora S, Bannicelli C, D'Agostini F, Izzotti A, Camoirano A. (1994) Cytosolic activation of aromatic and heterocyclic amines. Inhibition by dicoumarol and enhancement in viral hepatitis B. *Environ Health Perspect*, 102 Suppl 6: 69-74.
183. Jaber S, Polster BM. (2015) Idebenone and neuroprotection: antioxidant, pro-oxidant, or electron carrier? *J Bioenerg Biomembr*, 47: 111-118.
184. Vafai SB, Mevers E, Higgins KW, Fomina Y, Zhang J, Mandinova A, Newman D, Shaw SY, Clardy J, Mootha VK. (2016) Natural Product Screening Reveals Naphthoquinone Complex I Bypass Factors. *PLoS One*, 11: e0162686.
185. Haefeli RH, Erb M, Gemperli AC, Robay D, Courdier Fruh I, Anklin C, Dallmann R, Gueven N. (2011) NQO1-dependent redox cycling of idebenone: effects on cellular redox potential and energy levels. *PLoS One*, 6: e17963.
186. Tyler DD, Gonze J. The preparation of heart mitochondria from laboratory animals. In: Estabrook RW, Pullman ME (eds.), *Methods in Enzymology* (Vol. 10). Academic Press, New York, 1967: 75-77.
187. Sims NR. (1990) Rapid isolation of metabolically active mitochondria from rat brain and subregions using Percoll density gradient centrifugation. *J Neurochem*, 55: 698-707.
188. Chinopoulos C, Starkov AA, Fiskum G. (2003) Cyclosporin A-insensitive permeability transition in brain mitochondria: inhibition by 2-aminoethoxydiphenyl borate. *J Biol Chem*, 278: 27382-27389.
189. Akerman KE, Wikstrom MK. (1976) Safranin as a probe of the mitochondrial membrane potential. *FEBS Lett*, 68: 191-197.
190. Prochaska HJ, Talalay P. (1986) Purification and characterization of two isofunctional forms of NAD(P)H: quinone reductase from mouse liver. *J Biol Chem*, 261: 1372-1378.
191. Shaw PM, Reiss A, Adesnik M, Nebert DW, Schembri J, Jaiswal AK. (1991) The human dioxin-inducible NAD(P)H: quinone oxidoreductase cDNA-encoded protein expressed in COS-1 cells is identical to diaphorase 4. *Eur J Biochem*, 195: 171-176.

192. Lind C, Cadenas E, Hochstein P, Ernster L. DT-diaphorase: purification, properties, and function. In: Packer L, Glazer AN (eds.), *Methods in Enzymology* (Vol. 186). Academic Press, New York, 1990: 287-301.
193. Walsh JM, Clark JB. (1976) Studies on the control of 4-aminobutyrate metabolism in 'synaptosomal' and free rat brain mitochondria. *Biochem J*, 160: 147-157.
194. Cunningham J, Clarke DD, Nicklas WJ. (1980) Oxidative metabolism of 4-aminobutyrate by rat brain mitochondria: inhibition by branched-chain fatty acid. *J Neurochem*, 34: 197-202.
195. Tunnicliff G, Ngo TT, Rojo-Ortega JM, Barbeau A. (1977) The inhibition by substrate analogues of gamma-aminobutyrate aminotransferase from mitochondria of different subcellular fractions of rat brain. *Can J Biochem*, 55: 479-484.
196. Loscher W, Honack D, Gramer M. (1989) Use of inhibitors of gamma-aminobutyric acid (GABA) transaminase for the estimation of GABA turnover in various brain regions of rats: a reevaluation of aminooxyacetic acid. *J Neurochem*, 53: 1737-1750.
197. Schousboe A, Waagepetersen HS. (2006) Glial modulation of GABAergic and glutamate ergic neurotransmission. *Curr Top Med Chem*, 6: 929-934.
198. Schousboe A, Waagepetersen HS. (2007) GABA: homeostatic and pharmacological aspects. *Prog Brain Res*, 160: 9-19.
199. Cash CD, Maitre M, Ossola L, Mandel P. (1978) Purification and properties of two succinate semialdehyde dehydrogenases from human brain. *Biochim Biophys Acta*, 524: 26-36.
200. Ryzlak MT, Pietruszko R. (1988) Human brain "high Km" aldehyde dehydrogenase: purification, characterization, and identification as NAD⁺ - dependent succinic semialdehyde dehydrogenase. *Arch Biochem Biophys*, 266: 386-396.
201. Gibson KM, Nyhan WL. (1989) Metabolism of [U-14C]-4-hydroxybutyric acid to intermediates of the tricarboxylic acid cycle in extracts of rat liver and kidney mitochondria. *Eur J Drug Metab Pharmacokinet*, 14: 61-70.

202. Kim JY, Tillison KS, Zhou S, Lee JH, Smas CM. (2007) Differentiation-dependent expression of Adhfe1 in adipogenesis. *Arch Biochem Biophys*, 464: 100-111.
203. Bay T, Eghorn LF, Klein AB, Wellendorph P. (2014) GHB receptor targets in the CNS: focus on high-affinity binding sites. *Biochem Pharmacol*, 87: 220-228.
204. Alexandre A, Reynafarje B, Lehninger AL. (1978) Stoichiometry of vectorial H⁺ movements coupled to electron transport and to ATP synthesis in mitochondria. *Proc Natl Acad Sci U S A*, 75: 5296-5300.
205. Schousboe A, Wu JY, Roberts E. (1974) Subunit structure and kinetic properties of 4-aminobutyrate-2-ketoglutarate transaminase purified from mouse brain. *J Neurochem*, 23: 1189-1195.
206. Iskander K, Gaikwad A, Paquet M, Long DJ, 2nd, Brayton C, Barrios R, Jaiswal AK. (2005) Lower induction of p53 and decreased apoptosis in NQO1-null mice lead to increased sensitivity to chemical-induced skin carcinogenesis. *Cancer Res*, 65: 2054-2058.
207. Asher G, Lotem J, Cohen B, Sachs L, Shaul Y. (2001) Regulation of p53 stability and p53-dependent apoptosis by NADH quinone oxidoreductase 1. *Proc Natl Acad Sci U S A*, 98: 1188-1193.
208. Giorgio V, Petronilli V, Ghelli A, Carelli V, Rugolo M, Lenaz G, Bernardi P. (2012) The effects of idebenone on mitochondrial bioenergetics. *Biochim Biophys Acta*, 1817: 363-369.
209. James AM, Cocheme HM, Smith RA, Murphy MP. (2005) Interactions of mitochondria-targeted and untargeted ubiquinones with the mitochondrial respiratory chain and reactive oxygen species. Implications for the use of exogenous ubiquinones as therapies and experimental tools. *J Biol Chem*, 280: 21295-21312.
210. Erb M, Hoffmann-Enger B, Deppe H, Soeberdt M, Haefeli RH, Rummey C, Feurer A, Gueven N. (2012) Features of idebenone and related short-chain quinones that rescue ATP levels under conditions of impaired mitochondrial complex I. *PLoS One*, 7: e36153.
211. Chambliss KL, Zhang YA, Rossier E, Vollmer B, Gibson KM. (1995) Enzymatic and immunologic identification of succinic semialdehyde

- dehydrogenase in rat and human neural and nonneural tissues. *J Neurochem*, 65: 851-855.
212. Cash C, Ciesielski L, Maitre M, Mandel P. (1977) Purification and properties of rat brain succinic semialdehyde dehydrogenase. *Biochimie*, 59: 257-268.
 213. Blaner WS, Churchich J. (1979) Succinic semialdehyde dehydrogenase. Reactivity of lysyl residues. *J Biol Chem*, 254: 1794-1798.
 214. Li X, Wu F, Qi F, Beard DA. (2011) A database of thermodynamic properties of the reactions of glycolysis, the tricarboxylic acid cycle, and the pentose phosphate pathway. *Database (Oxford)*, 2011: bar005.
 215. Murphy MP. (2009) How mitochondria produce reactive oxygen species. *Biochem J*, 417: 1-13.
 216. Hinkle PC, Butow RA, Racker E, Chance B. (1967) Partial resolution of the enzymes catalyzing oxidative phosphorylation. XV. Reverse electron transfer in the flavin-cytochrome beta region of the respiratory chain of beef heart submitochondrial particles. *J Biol Chem*, 242: 5169-5173.
 217. Tretter L, Adam-Vizi V. (2007) Moderate dependence of ROS formation on DeltaPsim in isolated brain mitochondria supported by NADH-linked substrates. *Neurochem Res*, 32: 569-575.
 218. Stuckey DJ, Anthony DC, Lowe JP, Miller J, Palm WM, Styles P, Perry VH, Blamire AM, Sibson NR. (2005) Detection of the inhibitory neurotransmitter GABA in macrophages by magnetic resonance spectroscopy. *J Leukoc Biol*, 78: 393-400.
 219. Bhat R, Axtell R, Mitra A, Miranda M, Lock C, Tsien RW, Steinman L. (2010) Inhibitory role for GABA in autoimmune inflammation. *Proc Natl Acad Sci U S A*, 107: 2580-2585.
 220. Tannahill GM, Curtis AM, Adamik J, Palsson-McDermott EM, McGettrick AF, Goel G, Frezza C, Bernard NJ, Kelly B, Foley NH, Zheng L, Gardet A, Tong Z, Jany SS, Corr SC, Haneklaus M, Caffrey BE, Pierce K, Walmsley S, Beasley FC, Cummins E, Nizet V, Whyte M, Taylor CT, Lin H, Masters SL, Gottlieb E, Kelly VP, Clish C, Auron PE, Xavier RJ, O'Neill LA. (2013) Succinate is an inflammatory signal that induces IL-1beta through HIF-1alpha. *Nature*, 496: 238-242.

221. Ferkany JW, Smith LA, Seifert WE, Caprioli RM, Enna SJ. (1978) Measurement of gamma-aminobutyric acid (GABA) in blood. *Life Sci*, 22: 2121-2128.
222. Wu Y, Wang W, Diez-Sampedro A, Richerson GB. (2007) Nonvesicular inhibitory neurotransmission via reversal of the GABA transporter GAT-1. *Neuron*, 56: 851-865.
223. Roth FC, Draguhn A. (2012) GABA metabolism and transport: effects on synaptic efficacy. *Neural Plast*, 2012: 805830.
224. Francis A, Pulsinelli W. (1982) The response of GABAergic and cholinergic neurons to transient cerebral ischemia. *Brain Res*, 243: 271-278.
225. Romijn HJ, Ruijter JM, Wolters PS. (1988) Hypoxia preferentially destroys GABAergic neurons in developing rat neocortex explants in culture. *Exp Neurol*, 100: 332-340.
226. Sloper JJ, Johnson P, Powell TP. (1980) Selective degeneration of interneurons in the motor cortex of infant monkeys following controlled hypoxia: a possible cause of epilepsy. *Brain Res*, 198: 204-209.
227. Kolesova GM, Karnaukhova LV, Iaguzhinskii LS. (1991) [Interaction of menadione and duroquinone with Q-cycle during DT-diaphorase function]. *Biokhimiia.*, 56: 1779-1786.
228. Kolesova GM, Karnaukhova LV, Segal NK, Iaguzhinskii LS. (1993) [The effect of inhibitors of the Q-cycle on cyano-resistant oxidation of malate by rat liver mitochondria in the presence of menadione]. *Biokhimiia.*, 58: 1630-1640.
229. Kolesova GM, Kapitanova NG, Iaguzhinskii LS. (1987) [Stimulation by quinones of cyanide-resistant respiration in rat liver and heart mitochondria]. *Biokhimiia.*, 52: 715-719.
230. Kolesova GM, Vishnivetskii SA, Iaguzhinskii LS. (1989) [A study of the mechanism of cyanide resistant oxidation of succinate from rat liver mitochondria in the presence of menadione]. *Biokhimiia.*, 54: 103-111.
231. Giorgio M, Migliaccio E, Orsini F, Paolucci D, Moroni M, Contursi C, Pelliccia G, Luzi L, Minucci S, Marcaccio M, Pinton P, Rizzuto R, Bernardi P, Paolucci F, Pelicci PG. (2005) Electron transfer between cytochrome c and p66Shc

- generates reactive oxygen species that trigger mitochondrial apoptosis. *Cell*, 122: 221-233.
232. Little JE, Sproston TJ, Foote MW. (1948) Isolation and antifungal action of naturally occurring 2-methoxy-1,4-naphthoquinone. *J Biol Chem*, 174: 335-342.
233. Fieser LF, Martin EL. Organic syntheses (Vol. 21). Organic Syntheses, Inc., New York, 1941: 56.
234. Rodenburg RJ. (2016) Mitochondrial complex I-linked disease. *Biochim Biophys Acta*, 1857: 938-945.
235. Irwin MH, Parameshwaran K, Pinkert CA. (2013) Mouse models of mitochondrial complex I dysfunction. *Int J Biochem Cell Biol*, 45: 34-40.
236. Shneyvays V, Leshem D, Shmist Y, Zinman T, Shainberg A. (2005) Effects of menadione and its derivative on cultured cardiomyocytes with mitochondrial disorders. *J Mol Cell Cardiol*, 39: 149-158.
237. Isaev NK, Stelmashook EV, Ruscher K, Andreeva NA, Zorov DB. (2004) Menadione reduces rotenone-induced cell death in cerebellar granule neurons. *Neuroreport*, 15: 2227-2231.
238. Kelso GF, Porteous CM, Coulter CV, Hughes G, Porteous WK, Ledgerwood EC, Smith RA, Murphy MP. (2001) Selective targeting of a redox-active ubiquinone to mitochondria within cells: antioxidant and antiapoptotic properties. *J Biol Chem*, 276: 4588-4596.
239. Ghosh A, Bera S, Ghosal S, Ray S, Basu A, Ray M. (2011) Differential inhibition/inactivation of mitochondrial complex I implicates its alteration in malignant cells. *Biochemistry (Mosc)*, 76: 1051-1060.
240. Giorgio V, Schiavone M, Galber C, Carini M, Da Ros T, Petronilli V, Argenton F, Carelli V, Acosta Lopez MJ, Salviati L, Prato M, Bernardi P. (2018) The idebenone metabolite QS10 restores electron transfer in complex I and coenzyme Q defects. *Biochim Biophys Acta Bioenerg*, 1859: 901-908.
241. La Morgia C, Carbonelli M, Barboni P, Sadun AA, Carelli V. (2014) Medical management of hereditary optic neuropathies. *Front Neurol*, 5: 141.
242. Suno M, Nagaoka A. (1984) Inhibition of lipid peroxidation by a novel compound, idebenone (CV-2619). *Jpn J Pharmacol*, 35: 196-198.

243. Haefeli RH, Erb M, Gemperli AC, Robay D, Courdier FI, Anklin C, Dallmann R, Gueven N. (2011) NQO1-dependent redox cycling of idebenone: effects on cellular redox potential and energy levels. *PLoS.ONE.*, 6: e17963.
244. Esposti MD, Ngo A, Ghelli A, Benelli B, Carelli V, McLennan H, Linnane AW. (1996) The interaction of Q analogs, particularly hydroxydecyl benzoquinone (idebenone), with the respiratory complexes of heart mitochondria. *Arch Biochem Biophys*, 330: 395-400.
245. Chan TS, Teng S, Wilson JX, Galati G, Khan S, O'Brien PJ. (2002) Coenzyme Q cytoprotective mechanisms for mitochondrial complex I cytopathies involves NAD(P)H: quinone oxidoreductase 1(NQO1). *Free Radic Res*, 36: 421-427.
246. Wu K, Knox R, Sun XZ, Joseph P, Jaiswal AK, Zhang D, Deng PS, Chen S. (1997) Catalytic properties of NAD(P)H:quinone oxidoreductase-2 (NQO2), a dihydronicotinamide riboside dependent oxidoreductase. *Arch.Biochem.Biophys.*, 347: 221-228.
247. Zhao Q, Yang XL, Holtzclaw WD, Talalay P. (1997) Unexpected genetic and structural relationships of a long-forgotten flavoenzyme to NAD(P)H:quinone reductase (DT-diaphorase). *Proc.Natl.Acad.Sci.U.S.A*, 94: 1669-1674.
248. Albano CB, Muralikrishnan D, Ebadi M. (2002) Distribution of coenzyme Q homologues in brain. *Neurochem Res*, 27: 359-368.
249. Tang PH, Miles MV, Miles L, Quinlan J, Wong B, Wenisch A, Bove K. (2004) Measurement of reduced and oxidized coenzyme Q9 and coenzyme Q10 levels in mouse tissues by HPLC with coulometric detection. *Clin Chim Acta*, 341: 173-184.
250. Dragan M, Dixon SJ, Jaworski E, Chan TS, O'Brien P J, Wilson JX. (2006) Coenzyme Q(1) depletes NAD(P)H and impairs recycling of ascorbate in astrocytes. *Brain Res*, 1078: 9-18.
251. Goodman RP, Calvo SE, Mootha VK. (2018) Spatiotemporal compartmentalization of hepatic NADH and NADPH metabolism. *J Biol Chem*, 293: 7508-7516.
252. Stein LR, Imai S. (2012) The dynamic regulation of NAD metabolism in mitochondria. *Trends Endocrinol Metab*, 23: 420-428.

253. Canto C, Menzies KJ, Auwerx J. (2015) NAD(+) Metabolism and the Control of Energy Homeostasis: A Balancing Act between Mitochondria and the Nucleus. *Cell Metab*, 22: 31-53.
254. Yang Y, Sauve AA. (2016) NAD(+) metabolism: Bioenergetics, signaling and manipulation for therapy. *Biochim Biophys Acta*, 1864: 1787-1800.
255. Bachur NR, Gordon SL, Gee MV, Kon H. (1979) NADPH cytochrome P-450 reductase activation of quinone anticancer agents to free radicals. *Proc Natl Acad Sci U S A*, 76: 954-957.
256. Manoj KM, Gade SK, Mathew L. (2010) Cytochrome P450 reductase: a harbinger of diffusible reduced oxygen species. *PLoS One*, 5: e13272.
257. Fiorillo M, Sotgia F, Sisci D, Cappello AR, Lisanti MP. (2017) Mitochondrial "power" drives tamoxifen resistance: NQO1 and GCLC are new therapeutic targets in breast cancer. *Oncotarget*, 8: 20309-20327.
258. Seyfried TN, Shelton LM. (2010) Cancer as a metabolic disease. *Nutr Metab (Lond)*, 7: 7.

10. BIBLIOGRAPHY OF THE CANDIDATE'S PUBLICATIONS

10.1. Publications related to the PhD thesis

Nemeth B, Doczi J, Csete D, Kacso G, **Ravasz D**, Adams D, Kiss G, Nagy AM, Horvath G, Tretter L, Mocsai A, Csepanyi-Komi R, Iordanov I, Adam-Vizi V, Chinopoulos C. (2016) Abolition of mitochondrial substrate-level phosphorylation by itaconic acid produced by LPS-induced Irg1 expression in cells of murine macrophage lineage. *Faseb j*, 30: 286-300.

IF: 5.498

Kacso G, **Ravasz D**, Doczi J, Nemeth B, Madgar O, Saada A, Ilin P, Miller C, Ostergaard E, Iordanov I, Adams D, Vargedo Z, Araki M, Araki K, Nakahara M, Ito H, Gal A, Molnar MJ, Nagy Z, Patocs A, Adam-Vizi V, Chinopoulos C. (2016) Two transgenic mouse models for beta-subunit components of succinate-CoA ligase yielding pleiotropic metabolic alterations. *Biochem J*, 473: 3463-3485.

IF.: 3.797

Ravasz D, Kacso G, Fodor V, Horvath K, Adam-Vizi V, Chinopoulos C. (2017) Catabolism of GABA, succinic semialdehyde or gamma-hydroxybutyrate through the GABA shunt impair mitochondrial substrate-level phosphorylation. *Neurochem Int*, 109: 41-53.

IF.: 3.603

Ravasz D, Kacso G, Fodor V, Horvath K, Adam-Vizi V, Chinopoulos C. (2018) Reduction of 2-methoxy-1,4-naphthoquinone by mitochondrially-localized Nqo1 yielding NAD⁺ supports substrate-level phosphorylation during respiratory inhibition. *Biochim Biophys Acta*, 1859: 909-924.

IF.: 4.280

10.2. Publications not related to the PhD thesis

Chen E, Kiebish MA, McDaniel J, Gao F, Narain NR, Sarangarajan R, Kacso G, **Ravasz D**, Seyfried TN, Adam-Vizi V, Chinopoulos C. (2016) The total and mitochondrial lipidome of *Artemia franciscana* encysted embryos. *Biochim Biophys Acta*, 1861: 1727-1735.
IF.: 5.547

Chen E, Kiebish MA, McDaniel J, Niedzwiecka K, Kucharczyk R, **Ravasz D**, Gao F, Narain NR, Sarangarajan R, Seyfried TN, Adam-Vizi V, Chinopoulos C. (2018) Perturbation of the yeast mitochondrial lipidome and associated membrane proteins following heterologous expression of *Artemia*-ANT. *Sci Rep*, 8: 5915.
IF.:4.122

11. ACKNOWLEDGEMENTS

First I would like to express my gratitude to my supervisor, Dr. Christos Chinopoulos who guided me throughout this research with great patience and expertise, and who was never tired of answering my questions. I wish to thank Prof. Veronika Ádám-Vizi and Prof. László Tretter for providing me the opportunity to work at the Department of Medical Biochemistry at Semmelweis University. I would also like to thank Dr. Gergely Kacsó, with whom I performed and discussed many experiments described in this thesis, for the large contribution he made to this work and for the inspiring conversations we had. My thanks go to Dr. Viktória Fodor and Dr. Kata Horváth as well for their sustained and reliable work in this project. I am grateful for the guidance and assistance provided by Dr. Judit Dóczy in cell culturing. My thanks are also extended to all my colleagues in the department for their helpfulness and encouragement. Finally, I wish to thank my family and my friends for their endless support during these years.